CELL DEATH MECHANISMS AT THE ENDOPLASMIC RETICULUM

CELL DEATH MECHANISMS AT THE ENDOPLASMIC RETICULUM

By FEI GENG, M.Sc.

A Thesis Submitted to the School of Graduate Studies in Partial Fulfillment of the Requirements for the Degree Doctor of Philosophy

DOCTOR OF PHILOSOPHY (2012) McMaster University
(Biochemistry and Biomedical Sciences) Hamilton, Ontario

TITLE: Cell death mechanisms at the endoplasmic reticulum

AUTHOR: Fei Geng, M.Sc. (Fudan University)

SUPERVISOR: Professor David W. Andrews

NUMBER OF PAGES: xi, 143

ABSTRACT

In the recent years considerable progress has been made to understand how the protein Bcl-2 regulates apoptosis at the mitochondria. By comparison, the cell death mechanisms at the endoplasmic reticulum remain unclear. In response to the agents that cause endoplasmic reticulum stress in breast cancer cells, the cell-cell adhesion molecule E-cadherin is modified by two independent modifications comprising pro-region retention and O-glycosylation. Both the modifications on E-cadherin inhibit its cell surface transport and the resultant loss of E-cadherin on the plasma membrane sensitizes cells to apoptosis. During this process binding of E-cadherin to type I gamma phosphatidylinositol phosphate kinase (PIPKIγ), a protein required for E-cadherin trafficking to the plasma membrane is prevented by O-glycosylation. E-cadherin deletion mutants that cannot be O-GlcNAcylated continue to bind PIPKIγ, traffick to the cell surface and delay apoptosis, confirming the biological significance of the modifications and PIPKIγ binding in the cell death regulation. These results also led me to determine whether there is a cell death pathway in which commitment to cell death is mediated by proteins primarily located at the endoplasmic reticulum. The studies show that the growth of estrogen receptor-positive breast cancer cells in charcoal stripped bovine serum leads to a form of programmed cell death which is protected by Bcl-2 exclusively localized at the endoplasmic reticulum instead of the mitochondria. Interestingly, the BH3 mimetic ABT-737 can abolish the protection mediated by Bcl-2 localized at the endoplasmic reticulum. Taken together, these studies suggest the novel role of the endoplasmic reticulum in programmed cell death through the identification and elucidation of the mechanisms that regulate the cell death pathway at this organelle.

ACKNOWLEDGEMENTS

I wish to thank the following people for specific contributions to this thesis:

In Chaper 3,

Weijia Zhu for the preliminary research work on E-cadherin O-glycosylation

In Chaper 4,

Hetal Brahmbhatt and Frank Chan for their involvement in the optimization of charcoal stripped bovine serum conditions

In Chaper 5,

Tony Collins for Figure 5.2, Figure 5.3C and Figure 5.4C

Sudeepa Dixit for the classification analysis and feature extraction

TABLE OF CONTENTS

LIST OF FIGURES

LIST OF TABLES

LIST OF ABBREVIATIONS AND SYMBOLS

ActD	Actinomycin D
AJ	Adherens junction
AP	Adaptor Protein
ATF6	Activating transcription factor 6
Bap31	B-cell receptor-associated protein 31
BCA	Bicinchoninic assay
Bcl-2	B-cell lymphoma 2
BFA	Brefeldin A
BIK	Bcl-2-interacting killer
BH	Bcl-2 homology
Bp	Base pair
BSA	Bovine serum albumin
CD	Cytoplasmic domain
CER	Ceramide
CHOP	C/EBP homologous protein
CL	Cardiolipin
CpG	Cytosine-phosphate-guanine
CSBS	Charcoal stripped bovine serum
D5	DRAQ5
DNA	Deoxyribonucleic acid
DTT	Dithiothreitol
EC	Extracellular cadherin domain
EMT	Epithelial-mesenchymal transition
Endo H	Endoglycosidase H
FBS	Fetal bovine serum
FI	Furin inhibitor

FITC	Fluorescein isothiocyanate
GlcNAc	N-acetylglucosamine
GRP78	Glucose-regulated protein 78
HA	Hemagglutinin
HER2	Human epidermal growth factor receptor 2
IB	Immunoblot
IP	Immunoprecipitation
IP3	Inositol 1,4,5-trisphosphate
IRE1	Inositol-requiring enzyme 1
LC3	Light chain 3
kDa	Kilodalton
mAb	Monoclonal antibody
MDCK	Madin-Darby Canine Kidney
MOMP	Mitochondrial outer membrane permeabilization
mRNA	Messenger RNA
MUT	Mutant
NAF-1	Nutrient-deprivation autophagy factor-1
NAO	Acridine Orange 10-nonyl bromide (10-N-nonyl acridine orange)
O-GlcNAc	O-linked N-acetylglucosamine
OGT	O-GlcNAc transferase
PARP	Poly (ADP-ribose) polymerase
PBS	Phosphate buffered saline
PERK	PKR-like endoplasmic reticulum kinase
PI	Propidium iodide
PIPKIγ	Type I gamma phosphatidylinositol phosphate kinase
PNGase F	Peptide:N-glycosidase F
PR	Progesterone receptor
PS	Phosphatidylserine

pSer	Polyserine
PtdIns(4,5)P2	Phosphatidylinositol(4,5)-bisphosphate
RNA	Ribonucleic acid
SDS	Sodium dodecyl sulfate
Ser	Serine
SERCA	Sarcoplasmic/ endoplasmic reticulum calcium ATPase
shRNA	Short hairpin RNA
siRNA	Small interfering RNA
STS	Staurosporine
SVM	Support Vector Machines
TAM	Tamoxifen
TCA	Trichloroacetic acid
TG	Thapsigargin
TGN	Trans Golgi Network
TM	Transmembrane domain
TMRE	Tetramethylrhodamine, Ethyl Ester
TRAIL	TNF-related apoptosis-inducing ligand
TN	Tunicamycin
TNF-α	Tumor necrosis factor-α
Tyr	Tyrosine
UPR	Unfolded protein response
WGA	Wheat germ agglutinin
WT	Wild type
XBP-1	X-box-binding protein 1
$\Delta\psi_m$	Mitochondrial membrane potential

Chapter 1 : General Introduction

1.1 E-cadherin mediated cell adhesion

Cells do not simply "stick" together to form tissues. Cell adhesion is crucial for the assembly of individual cells into the three-dimensional tissues of animals. The ability of cells to form cell contacts, adhere to the extracellular matrix, change morphology, and migrate is essential for development, wound healing, metastasis, cell survival and the immune response (Ling, Doughman, Firestone, Bunce, & Anderson, 2002). It is therefore important to understand how cell-cell adhesion mechanisms evolved and how they have contributed to the generation of diversity among animal species. A variety of cell adhesion mechanisms are responsible for assembling cells together and along with their connections to the internal cytoskeleton, determine the overall architecture of the tissue. Epithelia in the vertebrates typically have a junctional complex comprising tight junctions, adherens junctions (AJ), and desmosomes; these junctional types are located in this order starting from the apical end of the lateral cell-cell contacts (Oda & Takeichi, 2011).

Cell-cell adhesion at adherens junctions is predominantly mediated by cadherins, a superfamily of transmembrane glycoprotein adhesion molecules. Cadherins are divided into different sub-classes (such as E-cadherin, N-cadherin, P-cadherin) characterized by their distinct tissue distributions.

E-cadherin, a type-I single-span transmembrane protein, is an endogenous adhesion molecule of epithelial cells. It is generally considered to be the prototype of all cadherins because of its early identification and its thorough characterization, both in normal and pathological conditions. As early as 1977, Takeichi (Pagano & Takeichi, 1977) proposed that the adhesive properties of the V79 Chinese hamster lung cell line could be divided into Ca^{2+} -independent agglutination, and a more physiological Ca^{2+} -dependent cell-cell adhesion. By iodinating surface proteins, Takeichi discovered that a surface protein of about 150 Kilodalton (kDa) was protected by Ca^{2+} against iodination and trypsinization. This was probably the first report on E-cadherin and its Ca^{2+} -

dependent adhesion potential. However, at that time this interesting adhesion molecule of 120 kDa was called uvomorulin. In 1984, Yoshida-Noro and Takeichi (Kanno, Sasaki, Shiba, Yoshida-Noro, & Takeichi, 1984) introduced the name “cadherins” as a more generic name for this important class of cell-cell adhesion molecules, and over time this name became generally adopted. E-cadherin obtained its prefix E (for epithelial) when new antibodies produced by Takeichi’s group revealed the existence of other related cadherins, like N- (neural) and P- (placental) cadherins, which have distinct spatiotemporal expression patterns throughout development (van Roy & Berx, 2008).

Mature E-cadherin, with molecular mass of 120 kDa, is composed of a highly conserved carboxy-terminal cytoplasmic domain, a single-pass transmembrane domain and an extracellular domain that consists of five tandemly repeated cadherin-motif subdomains (EC1-EC5), each harbouring two conserved regions representing the putative calcium binding sites (Beavon, 2000).

The widely accepted model on E-cadherin mediated cell-cell adhesion is the 'linear zipper' model. This model is based on the crystal structure of the extracellular cadherin domain (EC) and two dimerization interfaces which were observed in EC (Shapiro, et al., 1995). One was thought to mediate cis-dimerization formed by binding of the extracellular domains of two cadherins on the same cell surface (Figure 1.1A), in which the tryptophan residue of each subunit inserts into a hydrophobic pocket on the other EC1 subunit (Shapiro, et al., 1995). The second putative adhesion dimer interface is trans-dimerization (Gumbiner, 2005; Takeichi, 2007) formed by binding of extracellular domains of two cadherins between the EC1 domains on opposing cell surfaces (Figure 1.1A).

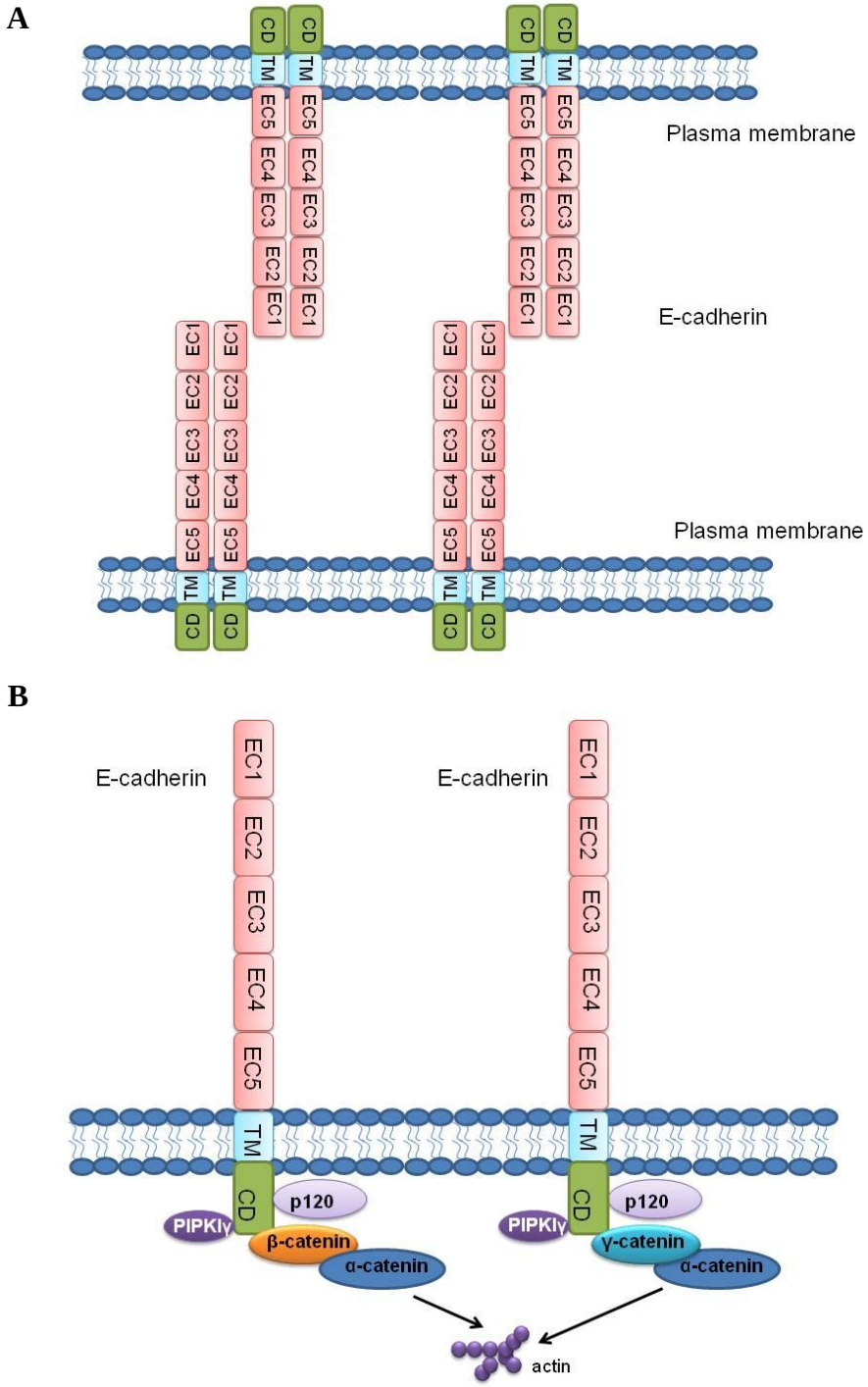

Figure 1.1 E-cadherin mediated cell adhesion. Legend see next page.

(**A**) A cartoon model of the dimerization of E-cadherin in Adherens Junctions. Cis-dimerization and trans-dimerization were observed in the X-ray crystal structure of the N-terminal extracellular cadherin domain (EC) (van Roy & Berx, 2008) (TM: transmembrane domain**;** CD: cytoplasmic domain). A tight parallel strand dimer (cis-dimer) orients two cadherin adhesion binding interfaces outward from the cell surface. An antiparallel dimer between adhesion binding interfaces of EC1 domains (trans-dimer) is proposed to represent a homophilic binding interface, leading to the interaction of adhesive elements from the neighboring cells. (**B**) The cadherin-catenin protein complex. The extracellular region of classic cadherins consists of five cadherin-type repeats. The core universal-catenin complex consists of type I phosphatidylinositol phosphate kinase type Iγ (PIPKIγ) and p120 catenin, bound to the juxtamembrane region, and β-catenin/ γ-catenin, bound to the distal region, which in turn binds α-catenin. In a less well-understood way, α-catenin binds to actin.

The cytoplasmic domain of E-cadherin is the site of interaction with its main binding partners that consists of α-catenin, β-catenin/γ-catenin, p120ctn and type I gamma phosphatidylinositol phosphate kinase (PIPKIγ) (Figure 1.1B). E-cadherin binds to either β-catenin or γ-catenin, while α-catenin also binds β-catenin or γ-catenin but not to E-cadherin (Beavon, 2000; Gumbiner, 2005; Zhurinsky, Shtutman, & Ben-Ze'ev, 2000).

The main binding partners of E-cadherin are the catenins. The catenin complex consists of α-catenin (102 kDa), β-catenin (92 kDa) and p120ctn (120 kDa) (Figure 1.1B). During the trafficking to and from the cell surface, cadherin-catenin complexes are dynamically assembled and disassembled. β-catenin binds to the cytoplasmic domain of E-cadherin shortly after E-cadherin synthesis and the two proteins are trafficked and sorted as a complex for delivery to the epithelial cell surface. By contrast, α-catenin and p120ctn do not join the complex until it is near or at the basolateral cell surface (Bryant & Stow, 2004; Y. T. Chen, Stewart, & Nelson, 1999; Delva & Kowalczyk, 2009).

γ-catenin and β-catenin are closely related by sharing 80% sequence identity within their arm repeat domains (A. H. Huber & Weis, 2001). In desmosomes, γ-catenin interacts with the cytoplasmic domains of desmosomal cadherins (Bierkamp, Schwarz, Huber, & Kemler, 1999). Although γ-catenin is primarily a desmosomal protein, it is also

found in adherens junctions to a limited extent (Troyanovsky, Chitaev, & Troyanovsky, 1996).

Phosphatidylinositol(4,5)-bisphosphate [PtdIns(4,5)P2] controls the dynamic turnover of the actin cytoskeleton and focal adhesions, which are crucial to a migrating cell (Ling, Schill, Wagoner, Sun, & Anderson, 2006). Most PtdIns(4,5)P2 is synthesized by the type I PIPKs (PIPKIs) in vivo (Stephens, Hughes, & Irvine, 1991). PIPKIγ, the newest member of the family, was found to be targeted to focal adhesions by an association with talin. It acts as a signaling scaffold that links Adaptor Protein (AP) complexes to E-cadherin (Ling, et al., 2007; Ling, et al., 2002). PIPKIγ directly binds to E-cadherin and modulates E-cadherin trafficking. Thus, depletion of PIPKIγ or disruption of PIPKIγ binding to either E-cadherin or AP complexes results in defects in E-cadherin transport and blocks AJ assembly (Ling, et al., 2007).

1.1.1 E-cadherin expression in cancer

Intercellular interactions are critical for the dynamic differentiation processes activated periodically in normal human breast epithelium throughout life, as well as for the induction and maintenance of differentiated tissues in adults (Berx & Van Roy, 2001). Changes in the normal expression pattern of the E-cadherin complex have been found in various human cancers. In breast cancer, partial or total loss of E-cadherin expression correlates with loss of markers of differentiated breast tissue, acquisition of invasiveness, increased tumor grade, metastatic behavior and poor prognoses (Lombaerts, et al., 2006).

E-cadherin mediates cell-cell adhesion by calcium-dependent homotypic interactions between E-cadherin extracellular domains on opposing membranes of contacting cells. The 5-10-hour half-life for E-cadherin in confluent epithelial cells make cell contacts or junctions susceptible to alterations or remodeling by a number of regulatory mechanisms (Oda & Takeichi, 2011). These mechanisms include: changes in gene expression; control of the biogenesis, transport or turnover of cell junctions; AJ formation associated with major changes in cell states, such as the epithelial-

mesenchymal transition (EMT). Numerous phenotypic changes occur through the process of EMT (Savagner, 2001). EMT involving down-regulation of E-cadherin plays a fundamental role during early steps of invasion and metastasis of carcinoma cells. Upon downregulation of E-cadherin, epithelial cells acquire a fibroblastic phenotype, which allows them to dissociate from the epithelium and migrate. This process is essential for cancer metastasis.

1.1.2 Transcriptional and epigenetic regulation of E-cadherin

E-cadherin dysfunction is a major contributor to the development and progression of cancers involving epithelial cell types. Such dysfunction can occur through several molecular mechanisms including mutations of the E-cadherin gene *CDH1* (Berx, Becker, Hofler, & van Roy, 1998); epigenetic silencing through promoter hypermethylation (Graziano, Humar, & Guilford, 2003), or transcriptional silencing through a variety of transcriptional repressors that target the *CDH1* promoter (Batlle, et al., 2000; Bolos, et al., 2003; M. A. Huber, Kraut, & Beug, 2005), and by microRNAs, which have been shown to indirectly regulate the expression of E-cadherin (Pinho, et al., 2011).

Mutational inactivation of *CDH1* has been found in 56% of lobular breast carcinomas (Berx, et al., 1996). Genetic screens identified at least 122 *CDH1* germline mutations (Corso, Marrelli, Pascale, Vindigni, & Roviello, 2012). In addition to a few missense mutations, the majority of mutations were splice site mutations and truncation mutations caused by insertions, deletions, and nonsense mutations (Berx, et al., 1998; Corso, et al., 2012; Schrader, et al., 2011).

Other than mutational inactivation, epigenetic silencing of the *CDH1* gene by aberrant hypermethylation of a promoter-associated cytosine-phosphate-guanine (CpG) island, a GC-rich sequence of about 1500 base pair (bp) in intron 1 of the human E-cadherin gene has been identified (Berx, et al., 1995; Graff, Gabrielson, Fujii, Baylin, & Herman, 2000; Tamura, et al., 2000; Zou, et al., 2009). The mechanistic association between aberrant CpG island methylation and transcriptional silencing is complicated

(Baylin, Herman, Graff, Vertino, & Issa, 1998; Jones, 1996). In normal cells, the promoter region CpG islands of E-cadherin are unmethylated and maintain a transcriptionally favorable local chromatin configuration (Graff, et al., 2000). Aberrant methylation of these normally unmethylated CpG islands is associated with underacetylated histones and a shift to a transcriptionally repressive chromatin structure (Graff, et al., 2000).

The transcription of E-cadherin is controlled by both positive- and negative-regulatory elements located in the 5' proximal sequences of its promoter region (Behrens, Lowrick, Klein-Hitpass, & Birchmeier, 1991; Cano, et al., 2000; Ringwald, Baribault, Schmidt, & Kemler, 1991). Zinc-finger transcription repressors of E-cadherin acting through interaction with specific E-boxes of the proximal promoter, Snail/Slug, E12/47, ZEB-1, SIP-1 and Twist have been characterized (Cano, et al., 2000; M. A. Huber, et al., 2005).

MicroRNAs are small non-coding Ribonucleic acid (RNA) molecules that suppress gene expression mostly by interacting with the 3’ untranslated regions of target messenger RNAs, which are increasingly implicated in regulating the malignant progression of cancer. MiR-9, a microRNA which is upregulated in breast cancer cells, directly targets the E-cadherin-encoding messenger RNA (mRNA) and leads to increased cell motility and invasiveness (Ma, et al., 2010).

1.1.3 E-cadherin pro-region processing

Newly synthesized E-cadherin is trafficked from the trans Golgi network (TGN) to the cell surface for incorporation, together with catenins, into AJ complexes. Surface E-cadherin can be endocytosed. During this process it encounters a variety of trafficking steps that either recycle it back to the cell surface or target it for degradation (Bryant & Stow, 2004).

In the E-cadherin trafficking route, the TGN is the first major site for differential regulation or sorting of newly synthesized E-cadherin. E-cadherin is synthesized as a 140

kDa precursor that undergoes transportation from the endoplasmic reticulum to the Golgi complex followed by cleavage of the pro-region mediated by the proprotein convertase family at the TGN. The cleavage of the pro-region results in the formation of the extracellular N-terminal end of the mature molecule (Beavon, 2000). E-cadherin precursor resulting from the inhibition of pro-region cleavage do not mediate adhesive function as the extracellular N-terminal end of E-cadherin is essential for the homotypic calcium-dependent cell-cell adhesion (Ozawa & Kemler, 1990).

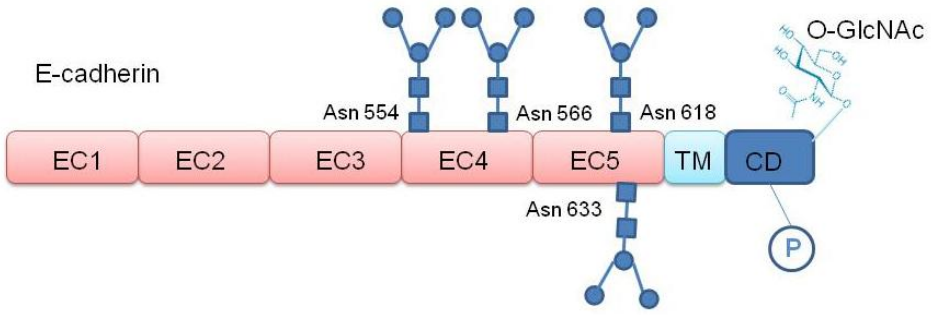

Figure 1.2 Post-translational regulation of E-cadherin.
E-cadherin can be post-translationally modified through phosphorylation, N-glycosylation and O-glycosylation. The phosphorylation of E-cadherin by casein kinase II can occur in a short stretch of 30 amino acids in the cytoplasmic domain (CD), which contains a cluster of 8 Serine (Ser) residues. The extracellular domain (EC) of human E-cadherin contains four potential N-glycosylation sites, which are located in EC4 and EC5. The modification of O-linked N-acetylglucosamine (O-GlcNAc) in the cytoplasmic domain has been reported to regulate E-cadherin transport (Zhu, Leber, & Andrews, 2001). These modifications can modulate E-cadherin mediated cell-cell adhesion at a post-translational level (Pinho, et al., 2011).

1.1.4 Post-translational regulation of E-cadherin

Beyond the modes of regulation mentioned above, E-cadherin function is tightly regulated by post-translational modifications including phosphorylation and glycosylation

in response to cellular context and signaling (Lilien & Balsamo, 2005; Liwosz, Lei, & Kukuruzinska, 2006).

The structural integrity of the cadherin-catenin complex is positively and negatively regulated by kinases that are often up-regulated during dynamic cell movements in development and in cancer (Daniel & Reynolds, 1997). Tyrosine (Tyr) phosphorylation of β-catenin at Tyr489 or Tyr654 disrupts binding to cadherin, and tyrosine phosphorylation of β-catenin at Tyr142 disrupts binding to α-catenin (Rosivatz, et al., 2002). Three serine residues in the cadherin cytoplasmic domain (Ser684, Ser686 and Ser692) are phosphorylated by the protein kinases casein kinase II and glycogen synthase kinase 3β, which create additional interactions with β-catenin resulting in a large increase in the affinity of the interaction. Specifically, in vitro phosphorylation of cadherin serine residues 834, 836, and 842 enhances the affinity with which β-catenin binds E-cadherin by 300-fold (Daugherty & Gottardi, 2007)

Glycosylation is an important and common form of post-translational modification of proteins and involves the enzymatic attachment of glycans to asparagine (N-linked glycans) and serine or threonine (O-linked glycans) (Nwosu, et al., 2011).

Regarding N-glycosylation, the resulting structures are generally classified into three principal categories: (1) high-mannose-type, in which only α-mannose residues are attached to the core structure. The total number of mannose residues is often five to nine. (2) complex-type, in which N-acetylglucosamine (GlcNAc) residues are linked to the two α-mannose residues of the core. (3) hybrid- type oligosaccharides have structures composed of elements characteristic of both high-mannose and complex-type glycans.

The extracellular domain of E-cadherin undergoes extensive N-glycosylation and contains four potential N-glycosylation sites at asparagine residues 554, 566, 618 and 633 (Liwosz, et al., 2006). Two of the putative N-glycosylation sites of human E-cadherin are located in extracellular domain 4 (EC4) whereas the other two sites are in EC5 (Figure 1.2).

The glycosyltransferases including N-acetylglucosaminyltransferase III, N-acetylglucosaminyltransferase V, and the α1,6 fucosyltransferase enzyme are involved in the remodeling of N-glycans on E-cadherin (Geng, Shi, Yuan, & Wu, 2004). The N-glycan products of these enzymes are bisecting GlcNAc structures, β1,6 Glc-NAc branched structures and α1,6 fucose N-glycan structure (Geng, et al., 2004; Liwosz, et al., 2006). N-glycans on E-cadherin destabilize AJ by affecting their molecular organization (Liwosz, et al., 2006; Pinho, et al., 2011). E-cadherin N-glycosylation variant lacking the major complex N-glycan exhibits increased association with the actin cytoskeleton and greater interaction with vinculin, an important component of cell-matrix adhesions (Peng, Cuff, Lawton, & DeMali, 2010). Likewise, a variant missing both complex and high mannose/hybrid N-glycans displays an enhanced association with γ-catenin and vinculin compared with either the wild type or endogenous E-cadherin (Liwosz, et al., 2006). Thus N-glycans influence the stability of AJs by affecting their molecular organization. Extensive modification of E-cadherin with complex N-glycans renders the formation of dynamic but weak AJs, whereas diminished N-glycosylation of E-cadherin promotes the establishment of stable AJs (Liwosz, et al., 2006).

However, in comparison with glycosylation of the extracellular domains of the protein, the regulation and consequences of O-glycosylation of the cytoplasmic domain of E-cadherin have been studied less extensively. O-glycosylation comprises extracellular O-glycosylation (mucin-type glycosylation) and intracellular O-GlcNAc (O-linked β-N-acetylglucosamine) modification (Julenius, Molgaard, Gupta, & Brunak, 2005)

O-GlcNAc is a monosaccharide modification abundant on serine and threonine residues of a multitude of nucleocytoplasmic proteins (Hart, Housley, & Slawson, 2007). O-GlcNAcylation has been found in almost every intracellular compartment and is especially abundant on proteins involved in stress responses and energy metabolism (Hart, et al., 2007). The enzymes responsible for O-GlcNAc addition and removal are OGT (O-GlcNAc transferase) and O-GlcNAcase (neutral β-N-acetylglucosaminidase), respectively.

The cytoplasmic region of E-cadherin is post-translationally modified by O-GlcNAc in response to treatment of cells with thapsigargin (TG) an irreversible inhibitor of the sarcoplasmic/endoplasmic reticulum calcium ATPase (SERCA) (Zhu, et al., 2001). TG is a well-established inducer of endoplasmic reticulum stress (Lytton, Westlin, & Hanley, 1991) and it decreases E-cadherin-mediated intercellular adhesion by preventing transport to the plasma membrane by an unidentified mechanism (Zhu, et al., 2001). In addition to O-GlcNAcylation, TG was suggested to mediate other post-translational modification(s), as treatment of cells resulted in the apparent molecular weight of E-cadherin increasing by 20 kDa an increase much larger than the molecular weight of O-GlcNAc added to serine and threonine residues by OGT (Vosseller, Wells, & Hart, 2001). The significance and relationship of other modification(s) to O-GlcNAcylation is unknown. In this thesis I extend these findings by characterizing two independent modifications of E-cadherin and addressing the relevant biological significance.

1.2 E-cadherin mediated cell survival signaling

E-cadherin mediated cell anchorage not only provides structural anchorage for a cell but also mediates pivotal cell survival signals (Grossmann, 2002). The disturbance of cell anchorage will frequently lead to the immediate initiation of a suicide program called anoikis. This form of programmed cell death is a special form of apoptosis triggered by the loss of cell anchorage between cells. In chimeric mice, the disruption of cadherin function in vivo leads to increased prevalence of apoptosis in intestinal epithelial cells. In primary mouse mammary gland epithelial cells, anoikis is inhibited by preservation of cell-cell anchorage despite loss of cell-matrix anchorage (Grossmann, 2002).

Upon examination of mammary epithelial cell lines in suspension, Overholtzer et al. revealed that detachment of mammary epithelial cells from the extracellular matrix initiates a new pathway of non-apoptotic cell death called entosis in which one cell invades into another (Overholtzer, et al., 2007; White, 2007). Similar to anoikis, entosis is E-cadherin dependent and can be inhibited by cadherin-blocking antibodies in MCF-7

cells (Overholtzer, et al., 2007), which indicates that E-cadherin mediated cell-cell adhesion is involved in the regulation of programmed cell death pathways.

1.3 Programmed cell death

Cell death plays an essential role in the development of tissues and organisms (Danial & Korsmeyer, 2004). Dysregulated cell death is a common feature of many human diseases, including cancer, stroke and neurodegeneration, and modulation of this cellular response has proved to be an effective therapeutic strategy. For example, imatinib, which inhibits the Abl tyrosine kinase that is activated by the Philadelphia translocations is shown to induce cancer cell death and to be highly effective in the treatment of all stages of chronic myelogenous leukemia (Capdeville, Buchdunger, Zimmermann, & Matter, 2002; Gerl & Vaux, 2005). Cell death responses including apoptosis, endoplasmic reticulum stress and autophagy will be introduced in the following section.

1.3.1 Apoptosis

Apoptotic cells are characterized by the condensation of the nucleus, a decrease in cell size and plasma membrane blebbing (Kerr, Wyllie, & Currie, 1972; Wyllie, Kerr, & Currie, 1980). At the molecular level, several common features are often associated with apoptosis: loss of mitochondrial membrane potential, cytochrome c release, activation of a family of cysteine proteases called caspases and exposure of phosphatidylserine (PS) to the extracellular space. The initiation of apoptosis can occur through a variety of both external and internal cues that are integrated somewhat differently, and hence these events have been broadly divided into extrinsic and intrinsic pathways (Leber, Geng, Kale, & Andrews, 2010; Shamas-Din, Brahmbhatt, Leber, & Andrews, 2011).

1.3.1.1 Extrinsic cell death pathway

Extrinsic apoptotic pathways are initiated by the binding of extracellular "death" ligands such as tumour necrosis factor-α (TNF-α), TNF-related apoptosis-inducing ligand (TRAIL) or Fas ligand to their respective "death" receptors on the plasma membrane. The binding of "death" ligands to their receptors results in receptor trimerization and the recruitment of a variety of adaptor proteins on the cytoplasmic side of the plasma membrane (Baud & Karin, 2001). Ultimately, for this complex to induce apoptosis, the recruitment of multiple procaspase-8 molecules is required (Muzio, Stockwell, Stennicke, Salvesen, & Dixit, 1998). In certain cells, designated as type I cells, activation of caspase-8 directly leads to the activation of broad spectrum effector caspases such as caspase-3 or caspase-7, effectively bypassing the decision stage of apoptosis and initiating the execution stage (Scaffidi, et al., 1998). However, in the majority of cells the activation of effector caspases by caspase-8 requires the cleavage of Bid, a member of the B-cell lymphoma 2 (Bcl-2) family of proteins (S. Li, et al., 2002; Yin, et al., 1999), which inserts into the outer mitochondrial membrane and engages the mitochondrial pathway (H. Li, Zhu, Xu, & Yuan, 1998; Luo, Budihardjo, Zou, Slaughter, & Wang, 1998).

The extrinsic or "death receptor" pathway of apoptosis is a highly regulated pathway, and the activation of caspase-8 can be inhibited by a variety of mechanisms, most of which rely on the transcriptional activity of NF-κB which is also activated during "death receptor" signaling by TNF-α and TRAIL (L. Wang, Du, & Wang, 2008).

1.3.1.2 Intrinsic apoptosis pathway

While the initiation of the extrinsic pathway of apoptosis occurs on the plasma membrane through the actions of "death" ligands, the intrinsic pathway can be initiated by a variety of mechanisms that disrupt or alter cellular processes at various locations throughout the cell and is executed through the interactions between the Bcl-2 family proteins (H. L. Wang, et al., 2007).

The mitochondria are of central importance in the apoptotic process. The embedded together model proposes that antiapoptotic proteins are able to sequester both

activated Bax and Bcl-2 homology 3 (BH3)-only activators on the mitochondria. BH3-only sensitizers displace Bax and BH3-only activators from the antiapoptotic proteins. The 'freed' Bax can oligomerise whereas the BH3-only activators can bind and recruit additional Bax, which also oligomerises, resulting in pore formation and mitochondrial outer membrane permeabilization (MOMP) (Leber, Lin, & Andrews, 2007). Cytochrome c binds to an adaptor molecule called Apaf-1, which results in the activation of caspases (Green & Reed, 1998). Smac/Diablo induces apoptosis by de-repressing the inhibitor of apoptosis proteins, leading to the activation of caspases, which regulate the induction and execution of apoptosis (van Loo, et al., 2002). Caspases exist as zymogens until they are cleaved into their active form. They can be divided into two different categories: the initiator caspases and the executioner caspases. The initiator caspases are activated by a variety of molecular cues, and the executioner caspases cleave substrates that catalyze the dismantling of the cell. Caspase-3 and caspase-7, typical executioner caspases, cleave multiple downstream targets, among which are ICAD, an inhibitor of a nuclease that assists in nuclear condensation (Enari, et al., 1998) and poly (ADP-ribose) polymerase (PARP) (Distelhorst & Shore, 2004). Breast cancer MCF-7 cells lack caspase-3 but undergo mitochondrial-dependent apoptosis via caspase-7 activation (Twiddy, Cohen, Macfarlane, & Cain, 2006). In MCF-7 cells procaspase-7 is directly cleaved and activated by the apoptosome complex (Twiddy, et al., 2006). Upon disruption of the outer mitochondrial membrane, a set of proteins normally found in the space between the inner and outer mitochondrial membranes is released, including cytochrome c, Smac/DIABLO, Omi/HtrA2 and endonuclease G (Saelens, et al., 2004). Once in the cytosol, these apoptogenic proteins trigger the execution of cell death by promoting caspase activation or by acting as caspase-independent death effectors (Saelens, et al., 2004).

These mechanisms also include cytotoxic drugs that exert stresses on particular subcellular locations or organelles such as the endoplasmic reticulum. In this respect, the induction of apoptosis arises through the activation of a characteristic set of BH3-only

proteins that relay apoptotic signals to the mitochondrial pathway to induce outer mitochondrial membrane permeabilization (Fulda & Debatin, 2006).

1.3.2 Endoplasmic reticulum stress

The endoplasmic reticulum has become key player in a variety of apoptotic signaling pathways (Heath-Engel, Chang, & Shore, 2008). This organelle represents the primary site for intracellular Ca^{2+} storage and is the location for the folding and some post-translational modification of transmembrane and secreted proteins. Disruption of these functions of the endoplasmic reticulum can be induced pharmacologically through agents that selectively disturb calcium homeostasis (thapsigargin, TG) (Booth & Koch, 1989) or redox balance (dithiotreitol, DTT) (Jamsa, Simonen, & Makarow, 1994), inhibit protein modifications (tunicamycin, TN) (Feige & Scheffler, 1987) or disrupt protein trafficking (brefeldin A, BFA) (Brostrom, Prostko, Gmitter, & Brostrom, 1995). All of these signals induce protein misfolding and activation of an adaptive stress response termed the unfolded protein response (UPR). The UPR attempts to increase the folding capacity of the endoplasmic reticulum through the induction of key proteins involved in chaperoning, protein folding, and degradation pathways.

Transduction of the UPR pathway occurs through three endoplasmic reticulum resident proteins that function as primary sensors of endoplasmic reticulum stress: PKR-like endoplasmic reticulum kinase (PERK) (Harding, Zhang, & Ron, 1999), inositol-requiring enzyme 1 (IRE1) (Shen, et al., 2001), and activating transcription factor 6 (ATF6) (Haze, Yoshida, Yanagi, Yura, & Mori, 1999). All three of the stress sensors are transmembrane proteins containing luminal domains that sense the accumulation of unfolded proteins within the endoplasmic reticulum lumen. In the absence of stress, glucose-regulated protein 78 (GRP78) is bound to all three, maintaining the sensors in an inactive configuration (Bertolotti, Zhang, Hendershot, Harding, & Ron, 2000). Accumulation of unfolded proteins and the altered redox status within the endoplasmic

reticulum lumen up-regulate the expression of GRP78 and trigger its dissociation from all three sensors, leading to the initiation of UPR signal transduction pathways.

IRE1α is a serine-threonine protein kinase and endoribonuclease that, on activation, initiates the unconventional splicing of the mRNA encoding X-box-binding protein 1 (XBP-1) (Calfon, et al., 2002). Spliced XBP-1 is a potent transcriptional activator that increases the expression of a subset of UPR-related genes and thus XBP-1 splicing is an important marker for UPR (Yoshida, 2007). As one of the target gene of spliced XBP-1, $P58^{IPK}$ binds and inhibits PERK, thereby providing a negative feedback loop that relieves a PERK-mediated translational block (Yan et al, 2002).

If the UPR has been successful at this point, the endoplasmic reticulum returns to normal functioning and the cell survives; however, if the stress persists, relieving the translational block by $P58^{IPK}$ might allow the synthesis of pro-apoptotic proteins. Signaling through PERK, ATF6 and IRE1 can trigger pro-apoptotic signals during prolonged endoplasmic reticulum stress. However, they do not directly cause cell death but rather initiate the activation of downstream transcription factor C/EBP homologous protein (CHOP) by up-regulating its transcription, which further push the cell down the path of death (Szegezdi, Logue, Gorman, & Samali, 2006).

Activated PERK directly phosphorylates and inhibits the translation initiation factor eIF2α (thus decreasing protein loading into the endoplasmic reticulum) and induces expression of the transcription factor ATF4, which increases expression of UPR genes CHOP and GRP78 (Su & Kilberg, 2008).

1.3.3 Autophagy

Similar to endoplasmic reticulum stress, autophagy is another cellular response mainly regulated at the endoplasmic reticulum (Heath-Engel, et al., 2008). As a major intracellular process for the degradation and recycling of proteins and cytoplasmic damaged organelles, autophagy is essential for maintaining cell survival following a variety of extracellular and intracellular stimuli including starvation. During autophagy

cells form autophagosomes that sequester organelles, proteins or portions of the cytoplasm for delivery to the lysosome (He and Klionsky, 2009). The sequestered contents are degraded in the lysosome, allowing cells to eliminate damaged or harmful components through catabolism and recycling them to maintain nutrient and energy homeostasis. Autophagy constitutes a major protective mechanism that allows cells to survive in response to multiple stressors. It also helps organisms defend against degenerative, inflammatory, infectious and neoplastic diseases (Kroemer, Marino, & Levine, 2010).

While autophagy is often induced as part of an adaptive response, induction of autophagy may also lead to cell death (Kundu & Thompson, 2005). Unlike apoptosis, which is characterized by nuclear condensation and fragmentation without major structural changes in cytoplasmic organelles, autophagic cell death is a caspase-independent process characterized by the accumulation of autophagic vacuoles in the cytoplasm, with extensive degradation of the Golgi complex and the endoplasmic reticulum preceding destruction of the nucleus (Klionsky & Emr, 2000). The final effector phase involves the fusion of the autophagosome-enclosed cargo with lysosomes for catabolism by intralysosomal enzymes (Maiuri, Zalckvar, Kimchi, & Kroemer, 2007).

1.4 Bcl-2 family proteins localized on the endoplasmic reticulum

As a critical regulator of cellular responses including apoptosis, endoplasmic reticulum stress and autophagy, the Bcl-2 family is classified into the antiapoptotic and the proapoptotic groups based upon their functions. The antiapoptotic proteins possess four BH domains and include Bcl-2, Bcl-XL, Bcl-w, Mcl-1 and A1, while the proapoptotic proteins are divided into two distinct subgroups—the multi-BH region proteins containing BH regions 1-3 (e.g. Bax, Bak and Bid) (Billen, Shamas-Din, & Andrews, 2008) and the BH3-only proteins (e.g. Bad, BIK, Bim, Noxa and Puma) which contain only the BH3 region (Shamas-Din, et al., 2011).

The endoplasmic reticulum has emerged as a central player in many cell death pathways, and evidence of an essential role for Bcl-2 family members at this location is becoming increasingly apparent (Hetz, 2007; Oakes, Lin, & Bassik, 2006). Interestingly each class of Bcl-2 family member has its representatives on the endoplasmic reticulum (antiapoptotic protein Bcl-2 and Bcl-XL, proapoptotic protein Bax and Bak, BH3-only protein BIK and Puma) and their related functions are listed in Table 1.1.

Bcl-2 family	**Effect on ER Ca^{2+}**	**Effect on UPR signaling**	**Effect on autophagy**
Bcl-2, Bcl-XL	Attenuates ER Ca^{2+} release	No known function	Suppress induction of autophagy via interacting with Beclin 1
Bax, Bak	Increase ER Ca^{2+} load and enhance Ca^{2+} release	Modulate the UPR by direct interaction with IRE1α	May promote autophagy
BIK	Promote Ca^{2+} release from the ER	No known function	No known function
Bad	No known function	No known function	Promote autophagy by inhibiting Bcl-2
Puma	Promotes ER Ca^{2+} depletion	Initiate apoptosis in neuronal cells	No known function
Nix	Increase resting ER Ca^{2+} load	No known function	Required for autophagic maturation
BI-1	Lower resting ER Ca^{2+} load	Attenuates UPR by inhibition of IRE-1 and PERK signaling	No known function

Table 1.1 Proposed functions of known endoplasmic reticulum localized Bcl-2 family proteins. ER: endoplasmic reticulum

1.4.1 Antiapoptotic protein Bcl-2

The founding member of the Bcl-2 protein family, Bcl-2, was discovered during molecular analysis of the t14-18 chromosomal translocation in B cell lymphoma (Tsujimoto, Finger, Yunis, Nowell, & Croce, 1984). Bcl-2 contains four BH regions (BH1-4) and a carboxyl-terminal hydrophobic sequence called a tail-anchor. Unlike many other tail-anchor proteins which are targeted to a single subcellular location, Bcl-2 is localized to the endoplasmic reticulum, and the outer mitochondrial membrane in mammalian cells (Zhu, et al., 1996). Over the past several years, extensive work has been done to elucidate the process whereby members of the Bcl-2 protein family at the mitochondrial outer membrane regulate the decision phase that commits cells to apoptosis (Leber & Andrews, 2010). In comparison, the molecular mechanisms of Bcl-2 localized at the endoplasmic reticulum are less studied.

To target Bcl-2 specifically to the outer mitochondrial membrane, a mutant Bcl-2 in which the carboxy terminal hydrophobic tail of Bcl-2 has been replaced by that from ActA was generated (Zhu, et al., 1996). To target Bcl-2 specifically to the endoplasmic reticulum membrane, a mutant Bcl-2 (Bcl2-cb5) in which the 21 C-terminal residues of Bcl-2 were replaced with the C-terminus of rat cytochrome B5 was generated (Zhu, et al., 1996). To determine whether apoptosis can be inhibited by Bcl-cb5, two spatially distinct pathways for apoptosis were found to be present in Rat-1 cells (Annis, et al., 2001). Apoptosis elicited by stimuli that led to a decrease in mitochondrial membrane potential ($\Delta\psi_m$), that precedes cytochrome c release is effectively inhibited by Bcl-cb5. By contrast, in the same cell type, Bcl-cb5 is not effective at inhibiting apoptosis induced by stimuli that cause mitochondrial translocation of Bax and redistribution of cytochrome c at a time when decreased $\Delta\psi_m$ is not yet apparent (Annis, et al., 2001).

1.4.2 Bcl-2 binding partners at the endoplasmic reticulum

At the endoplasmic reticulum Bcl-2 is a constituent of several distinct complexes with binding partners including Beclin 1, B-cell receptor-associated protein 31 (Bap31), Bcl-2-interacting killer (BIK), the inositol 1,4,5-trisphosphate (IP3) receptor (IP3R) and sarcoplasmic/endoplasmic reticulum Ca^{2+} -ATPase (SERCA) (Leber, et al., 2010). The functions of Bcl-2 binding partners at the endoplasmic reticulum membrane are summarized in Table 1.2.

Bcl-2 binding partners on the endoplasmic reticulum	**Function**
BIK	Induce ER Ca^{2+} release, caspase activation and autophagy
Beclin 1	Required for the initiation of the formation of the autophagosome during autophagy
NAF1	Displaced by BIK and causes Beclin 1 dependent autophagy
IP3R	Induce ER Ca^{2+} release
Bap31	Induce mitochondrial fission through ER Ca^{2+} signaling
SERCA	Pump cytosolic Ca^{2+} back into the ER

Table 1.2 Bcl-2 binding partners on the endoplasmic reticulum and their corresponding function. ER: endoplasmic reticulum

1.4.2.1 BIK

As a BH3-only protein, BIK contains a transmembrane domain in addition to the BH3 region and it is predominantly localized in the endoplasmic reticulum. BIK induces apoptosis through the mitochondrial pathway by mobilizing calcium from the endoplasmic reticulum to the mitochondria and remodeling the mitochondrial cristae (Chinnadurai, Vijayalingam, & Rashmi, 2008). BIK is induced in human breast cancer

MCF-7 cells in the absence of estrogen signaling and plays a critical role in the antiestrogen-provoked breast cancer cell apoptosis (Hur, et al., 2004). BIK-mediated apoptosis is mediated by selective activation of Bax and enhanced expression of BIK leads to cell death with autophagic features (Chinnadurai, et al., 2008).

1.4.2.2 Beclin 1

As an essential trigger of autophagy, Beclin 1 was first identified as a binding partner for Bcl-2 located at the endoplasmic reticulum (Aita, et al., 1999). It has recently been identified as a BH3-only protein. The overall structure of Beclin 1, as well as its essential role in autophagosome formation, is evolutionarily conserved throughout all eukaryotic phyla (Levine, Sinha, & Kroemer, 2008). During nutrient deprivation as a physiological stimulus of autophagy, Bcl-2 is known to function through inhibition of the autophagy effector and tumor suppressor Beclin 1 (Pattingre, et al., 2005). The nutrient-deprivation autophagy factor-1 (NAF-1) was recently demonstrated to be required for Bcl-2 to antagonize the autophagy regulatory protein Beclin 1 (Chang, Nguyen, Germain, & Shore, 2010). BH3-only proteins such as Bad, which are known to be induced during starvation, have been shown to displace Beclin 1 from Bcl-2, leading to the proposal that a signaling cascade analogous to the release of BH3-only activator proteins by BH3-only sensitizers to initiate the apoptosis pathway by Bax/Bak activation also extends to autophagy (Levine, et al., 2008; Maiuri, Criollo, et al., 2007). This suggests BH3 mimetics such as ABT-737 may also be used to probe the mechanisms occurring on the endoplasmic reticulum.

1.4.2.3 IP3R and SERCA

The cytosolic Ca^{2+} concentration in resting cells is maintained at low levels by enzymes that translocate Ca^{2+} across the plasma membrane or into intracellular stores (Hanson, Bootman, & Roderick, 2004). The sarcoplasmic/endoplasmic reticulum is the

major organelle involved in intracellular Ca^{2+} homeostasis and signaling. Ca^{2+} is sequestered in the sarcoplasmic/endoplasmic reticulum through the action of SERCA pumps which maintain the luminal Ca^{2+} concentration at much higher levels than in the surrounding cytoplasm. Ca^{2+} signals are generated when Ca^{2+} is released from the endoplasmic reticulum via IP3R activation (Rong & Distelhorst, 2008).

IP3R are large tetrameric proteins, each subunit of which projects an amino-terminal domain into the cytoplasm whereas their membrane spanning carboxy-terminal regions form an integral Ca^{2+} channel. IP3 binding by the amino-terminal domains causes a conformational change that promotes channel opening (Hanson, et al., 2004). Recent studies have demonstrated that IP3R can also be activated during apoptosis independently of the production of IP3. This may occur following proteolysis by activated caspase-3 (Hirota, Furuichi, & Mikoshiba, 1999) or caspase-7 (Elkoreh, Blais, Beliveau, Guillemette, & Denault, 2012). Truncation of IP3R by caspase-3/caspase-7 removes a large portion of the protein, including the amino-terminal IP3-binding region and other regulatory domains. The part that remains in the endoplasmic reticulum membrane is a constitutively active channel that continuously leaks Ca^{2+} (Hanson, et al., 2004). Bcl-2 has been shown to interact with IP3R and this suppresses Ca^{2+} release through IP3R and inhibits Ca^{2+} uptake by mitochondria without affecting endoplasmic reticulum Ca^{2+} stores (Grimm, 2012; Hanson, Bootman, Distelhorst, Wojcikiewicz, & Roderick, 2008).

Bcl-2 preserves endoplasmic reticulum Ca^{2+} stores by upregulating SERCA gene expression and by interacting with this pump directly (Dremina, et al., 2004; Kuo, et al., 1998). The interaction of Bcl-2 with SERCA was further reported to be involved in the regulation of apoptotic processes through modulation of cytoplasmic and/or endoplasmic reticulum Ca^{2+} levels required for the execution of apoptosis (Dremina, et al., 2004).

1.4.2.4 Bap31

Bap31 is a 28-kDa polytopic integral protein of the endoplasmic reticulum membrane, and like BID, is a preferred substrate of caspase-8 in vitro (Ng, et al., 1997).

Upon Fas/CD95 stimulation, Bap31 is cleaved within its cytosolic domain, generating proapoptotic p20 Bap31 (Nguyen, Breckenridge, Ducret, & Shore, 2000). The p20 caspase cleavage fragment of Bap31 induces Ca^{2+} release from the endoplasmic reticulum concomitant with increased Ca^{2+} uptake by mitochondria. TNF-α stimulation of MCF-7 cells has been shown to result in procaspase-8 processing, which correlated with weak cleavage of Bap31 (B. Wang, et al., 2003). Bcl2 at the endoplasmic reticulum protects against a Bax/Bak-independent paraptosis-like cell death pathway initiated via p20Bap31 (Abe, Van Prooyen, Ladasky, & Edidin, 2009; Heath-Engel, Wang, & Shore, 2012).

1.4.2.5 NAF-1

Crosslinking and subsequent mass spectrometry were used to identify proteins that both bound to Bcl2-cb5 and were displaced by Bik at the endoplasmic reticulum (Chang, et al., 2010). The most abundant protein found in this search was a previously recognized type 1 transmembrane protein containing a cytosolic iron-sulfur binding cluster designated NAF-1. NAF-1 is displaced from Bcl-2 by the endoplasmic reticulum-restricted BH3-only protein BIK and contributes to regulation of BIK-initiated autophagy, but not BIK-dependent activation of caspases (Chang, et al., 2010). In co-immunoprecipitation assays, NAF-1 was also shown to be present in a complex containing Bcl-2 and IP3R (Chang, et al., 2010) and required for Bcl-2 mediated maintenance of endoplasmic reticulum Ca^{2+} homeostasis (Chang, et al., 2012; He, Lam, McCormick, & Distelhorst, 1997). The presence of NAF-1 in Bcl-2-IP3R complexes has intriguing implications for both the composition of the Bcl-2 complex at the endoplasmic reticulum and the potential involvement of NAF-1 in regulating autophagy via IP3R. As mentioned above, NAF-1 was demonstrated to be required for Bcl-2 to antagonize the autophagy regulatory protein Beclin 1. Thus, NAF-1 is a Bcl2-associated co-factor that targets Bcl-2 for antagonism of the autophagy pathway at the endoplasmic reticulum and may also act as a switch between autophagy and apoptosis at the endoplasmic reticulum (Leber & Andrews, 2010).

1.5 Investigations presented in this thesis

The antiapoptotic function of Bcl-2 at the endoplasmic reticulum confers resistance to cell death initiated by a variety of stimuli (Annis, et al., 2001; Pattingre, et al., 2005; X. Wang, Olberding, White, & Li, 2011). The relevant mechanisms however, have remained elusive and controversial.

Chapter 3 of this thesis reveals the mechanism of two independent modifications of E-cadherin in response to treatments that cause endoplasmic reticulum stress in breast cancer cells. Firstly, O-GlcNAc modification of the cytoplasmic domain retains E-cadherin in the endoplasmic reticulum. Secondly, incomplete processing by proprotein convertases arrests E-cadherin transport late in the secretory pathway. O-GlyNAcylation of E-cadherin accelerated apoptosis. Cell stress-induced inactivation of proprotein convertases inhibited E-cadherin maturation further exacerbating apoptosis. The modifications of E-cadherin by O-GlcNAcylation and lack of pro-region processing represent novel mechanisms for the rapid regulation of cell surface transport of E-cadherin in response to toxic stress.

In the past, the apoptotic cell death that is prevented by Bcl-2 localized at the mitochondria (Bcl2-ActA) rather than Bcl-2 localized at the endoplasmic reticulum (Bcl2-cb5) was shown by our lab (Fiebig, Zhu, Hollerbach, Leber, & Andrews, 2006). My recent data showed that cell death, which followed multiple post-translational modifications of E-cadherin during TG treatment, was prevented by both Bcl2-ActA and Bcl2-cb5. Compared with the two types of cell death responses mentioned above, in Chapter 4 of this thesis we describe a novel type of cell death that was caused by the extended growth of breast cancer cells in charcoal stripped bovine serum and prevented only by Bcl2-cb5 and not Bcl2-ActA. Interestingly, the protection mediated by Bcl2-cb5 was abolished by the BH3 mimetic ABT-737. Intriguingly, this cell death was not caused by any of known cell death responses including UPR, autophagy or Bap31 cleavage.

To better examine the cell death described in Chapter 4, Chapter 5 of this thesis introduces a novel approach using multiparametric image analysis. Compared with the conventional approaches employed in Chapter 4, Chapter 5 describes a series of features extracted from the images of cells stained with NAO (Acridine Orange 10-nonyl bromide) to classify and distinguish cellular responses.

Overall, the investigations presented in this thesis reveal new insights into cell death mechanisms related to the endoplasmic reticulum, including the multiple post-translational modifications on E-cadherin and the endoplasmic reticulum-specific cell death pathway caused by estrogen deprivation. The details presented here provide valuable new information regarding the significance of cell-cell adhesion regulation during stress conditions. The characterization of novel cell death mechanisms sheds light on the ways which Bcl-2 functions at the endoplasmic reticulum.

Chapter 2 : Materials and methods

2.1 Materials

Human breast cancer cell line MCF-7 cells were grown in α-minimal essential medium (α-MEM, Invitrogen) supplemented with 10% fetal bovine serum (FBS, Thermo Scientific). Human breast cancer cell line BT474 andT47D cells were grown in Roswell Park Memorial Institute (RPMI, Invitrogen) 1640 medium supplemented with 10% FBS (Thermo Scientific). Madin-Darby Canine Kidney (MDCK) cells and Human breast cancer cell lines CAMA1, MDA-MB-361, MDA-MB-134, and MDA-MB-415 were grown in Dulbecco's Modified Eagle Medium (DMEM)/F12 medium (Invitrogen) supplemented with 10% FBS (Thermo Scientific). Thapsigargin (Invitrogen), Brefeldin A (Sigma), Tunicamycin (Sigma), Furin Inhibitor Decanoyl-Arg-Val-Lys-Arg-chloromethylketone (BACHEM), and C2-ceramide (Sigma) were dissolved in dimethylsulfoxide (DMSO) while DTT (Sigma) was dissolved in dH_2O and then they were diluted into culture medium according to indicated concentration. Leupeptin and E64d were purchased from Sigma.

The antibodies including mouse monoclonal antibody (mAb) against E-cadherin cytoplasmic domain (IC) (BD Biosciences) and p120-catenin (BD Biosciences), mouse mAb against E-cadherin extracellular domain (EC) SHE78-7 (Invitrogen), mouse mAb against Hemaglutinin (HA) tag (Covance Research Inc), mouse mAb against KDEL (Enzo Life Sciences), mouse mAb against PARP (Enzo Life Sciences) and β-actin (Santa Cruz Biotechnology) were used for immunoblots. Wheat germ agglutinin (WGA)-agarose was obtained from Sigma. For immunoprecipitation, mouse anti-E-cadherin cytoplasmic domain (BD Biosciences) and mouse mAb against HA tag (Covance Research Inc) were used. For immunofluorescence, mouse mAb against E-cadherin extracellular domain SHE78-7 (EC) was used. Antibodies against caspase-7 and light chain 3 (LC3) were purchased from Cell Signaling. Antibody against activated Bak (AM03) was purchased from EMD Chemical. Nitrocellulose and PVDF membranes were purchased from Pall

Corporation. Chemiluminescence reagent was purchased from Perkin Elmer, while an ultra-sensitive Enhanced Chemiluminescence reagent was purchased from Millipore. Bicinchoninic assay (BCA) reagent was purchased from Pierce. Gammabind G Sepharose beads were purchased from GE Healthcare.

Deoxyribonucleic acid (DNA) primers used for cloning were purchased from either Sigma Genosis or the Mobix Lab (McMaster University). The DNA modifying enzymes Pfu DNA polymerase and T4 DNA ligase were purchased from MBI Fermentas. All other DNA modifying enzymes (including restriction endonucleases) were purchased from New England Biolabs.

2.2 Methods

Constructs

cDNA for human wild type E-cadherin (E-cad WT) hEcad/pcDNA3 was provided by Dr. Cara J. Gottardi (Northwestern University, Chicago, IL). E-cadherin cytoplasmic domain truncated mutant (E-cadΔcyto) was amplified by PCR using 5′ (5′-ACTCGAGCGGCCGCATGGGCCCTTGGAGCCGCAGC-3′) and 3′ (5′-GCTGACTCTAGACTATCAAAGAGCGTAATCTGGAACATCGTATGGGTACATA AGAAACAGCAAGAGCAG -3′) oligonucleotide primers between nucleotides 125 and 2317 as defined as previously (Gottardi, Wong, & Gumbiner, 2001). cDNA encoding E-cadΔpSer was provided by Dr. Patrick J. Casey (Duke University, Durham, NC). All these three cDNAs were subcloned into pRc/CMV vectors with a coding sequence for the HA tag reengineered on the COOH-terminal. All cloning procedures described above were verified by sequencing (Mobix labs, McMaster University).

Stable expression of WT E-cadherin and E-cadherin variants in MCF-7 cells

Plasmids encoding E-cad WT as well as E-cadΔcyto and E-cadΔpSer were transfected into MCF-7 cells or MDCK cells with ExGen 500 (Fermentas) and colonies were selected in G418 (500 μg/mL). Stable clones were first isolated with cloning cylinders, expanded, and screened for protein expression by western analysis. Cell clones expressing E-cad WT and E-cadherin mutants were screened by immunoblotting using HA tag antibody and high expression clones were picked for further studies.

Preparation of charcoal stripped bovine serum (CSBS)

To prepare charcoal charcoal stripped FBS, 50 g activated charcoal (Sigma) was added to 500 mL of FBS (HyClone, Thermo Fisher) and mixed well. The mixture of charcoal and FBS was incubated at room temperature for 2 hours before it was filtered by 0.2 μm membrane (Pall). CSBS media was made by phenol red-free αMEM (Invitrogen) supplemented with 10% filtered charcoal stripped FBS.

The growth of cells in CSBS

The growth of cells in CSBS was performed as following. All the MCF-7 cells were split one day before the treatment and the cell density needs to be around 30%. Day 1: Prior to the treatment, MCF-7 cells were gently washed with 1X Phosphate buffered saline (PBS) buffer once and then cultured with phenol red-free αMEM supplemented with 10% charcoal stripped FBS. In addition, MCF-7 cells were also cultured with phenol red-free αMEM supplemented with 10% charcoal stripped FBS with the addition of 10 nM β-estradiol (Sigma) or 10 μg/mL insulin (Sigma). CSBS media were changed every two days during the treatment. Day 11: Harvest the cells cultured with phenol red-free αMEM supplemented with 10% charcoal stripped FBS in the absence or presence of β-estradiol or insulin and then perform cell death assay.

Surface biotinylation assay

To biotin-label cell surface proteins, EZ-Link™ biotin (Thermo Scientific) dissolved in PBS at 0.5 mg/mL was added to cells for 30 minutes as specified. Then cells were lysed and 30 µl of streptavidin-conjugated paramagnetic particles (Promega) was added to 100 µg biotinylated cell lysates, mixed for 6 hours at 4 ℃ and washed three times with cell lysis buffer. The beads were collected using a paramagnetic isolator and proteins released by incubation in sodium dodecyl sulfate (SDS) loading buffer at 100 ℃ for 10 minutes.

PNGase F and Endo H digestion

To perform Peptide: N-glycosidase F (PNGase F) and Endoglycosidase H (Endo H) digestion, protein bound beads derived from WGA binding or E-cadherin/HA tag immunoprecipitation were washed with 1% Triton buffer for 3 times and then were denatured in the denaturing buffer (5% SDS and 10% 2-mercatptoethnaol) for 5 minutes at 100 ℃. Denatured samples were then cooled and mixed with 1/10 volume each of concentrated PNGase F/Endo H reaction buffer (0.5 M sodium phosphate, pH 7.5, and 10% NP-40). Samples were then digested with 500 units of PNGase F (New England BioLabs) and Endo H (New England BioLabs) for 3 hours at 37 ℃. After this step, the reaction was stopped by the addition of the sample buffer (New England BioLabs) containing 2-mercaptoethanol.

TCA precipitation

100% (w/v) Trichloroacetic acid (TCA, Thermo Scientific) was added to the digestion products to a final concentration of 20%. Then samples were vortexed and kept on ice for 15 minutes before the centrifugation. The pellets were washed with 50% Ethyl

Ether Anhydrous and 50% ethanol. Then pellets were dried in SpeedVac System and dissolved in SDS loading buffer. The samples were heated at 100 ℃ for 10 minutes before they were analyzed by immunoblotting.

Immunoprecipitation and immunoblotting

For immunoprecipitation, 1 x 10^7 cells were lysed in 1 mL of cell lysis buffer (10 mM Tris-HCl pH 7.5, 1% Triton X-100, 150 mM NaCl) for 15 minutes on ice, and passed through a 26 gauge needle four times. Cellular debris and nuclei were removed by centrifugation at 13000 rpm for 10 minutes in a microcentrifuge. Protein concentration was determined for the supernatant using BCA assay (Thermo Scientific), and 100 µg of total protein from each sample was immunoprecipitated with 1 µg of anti-E-cadherin or HA tag antibody. GammaBind G Sepharose (GE Healthcare) was added, and samples were mixed by rotation for 4 hours at 4 ℃. For binding with WGA-agarose beads (Sigma), 100 µg of total protein was incubated with beads, samples mixed by rotation. Then the beads were pelleted and washed three times before the addition of 10 µl of SDS loading buffer to the beads and being boiled at 90 ℃ for 10 minutes for immunoblotting. Proteins were separated on 8% denaturing SDS-PAGE gels and transferred to PVDF membrane. The membrane was incubated with various primary antibodies diluted by 1:1000. The membrane was then incubated with the corresponding secondary antibody coupled to horseradish peroxidase (Jackson ImmunoResearch Laboratories Inc) at 1:10000 dilution. Labeled proteins were visualized with Enhanced Chemiluminescence (Perkin Elmer).

Immunofluorescence

MCF-7 cells were seeded on coverslips and grown as described (Zhu et al., 2001). Non-permeabilized cells were stained with cell-permeable dye Syto-63 (Invitrogen) as an

internal standard for cell number/volume at 37 ℃ for 30 minutes. Eukaryotic cells incubated with Syto-63 dye generally show cytoplasmic staining as well as nuclear staining (Wlodkowic, Skommer, & Darzynkiewicz, 2008). After being washed twice in PBS, cells were fixed with 4% paraformaldehyde and then incubated with E-cadherin antibody directed against the external domain SHE78-7 (EC) at 37 ℃ for 1 hour, washed and incubated for 1 hour with fluorescent secondary antibody donkey anti-mouse IgG-fluorescein isothiocyanate (FITC) (Jackson ImmunoResearch Laboratories Inc) and observed by confocal microscope (Leica TCS SP5). For ZO-1 staining, cells were pre-extracted with 0.2% Triton X-100 in 100 mM KCL, 3 mM $MgCl_2$, 1 mM $CaCl_2$, 200 mM sucrose, and 10 mM Hepes (pH 7.1) for 2 minutes on ice. Then the cells were fixed with 4% paraformaldehyde for 30 minutes, washed twice in PBS for 5 minutes and incubated with 1% Bovine serum albumin (BSA) in PBS/0.5% Triton X-100 for 30 minutes at room temperature. Cells were incubated at room temperature with 5 μg/mL anti- ZO-1 antibody (Invitrogen) for an hour. To visualize the nuclei, cells were stained with 5 μM DRAQ5 (Biostatus) for 30 minutes at room temperature.

Phalloidin staining

To stain F-actin, MCF-7 cells were fixed with 4% paraformaldehyde for 30 minutes, washed twice in PBS for 5 minutes and incubated with 1% BSA in PBS/0.5% Triton X-100 for 30 minutes at room temperature. Then cells were incubated with Alexa-488-conjugated phalloidin (Invitrogen) for 30 minutes at room temperature and imaged on an Opera High Content Screening System (Evotec).

Cell adhesion assay

To assess cell adhesion, we used an assay that measures loss of attachment to a cell culture dish with lateral shaking. MCF-7 cells expressing E-cad WT and E-cadΔpSer

were seeded at the density of 5×10^6/10-cm dish. Cells were treated with TG, DMSO (negative control) and 5 mM EDTA (positive control). Then cells were shaken at 500 rpm on Thermomixer 5436 (Eppendorf) inside a tissue culture incubator. Floating cells were counted over time on a hemocytometer at time points of 0, 8, 16, 24 hours after TG treatment on a Telaval 3 Inverted Microscope (Jena). As the exposure to 5mM EDTA for 30 minutes at 37℃ causes detachment of cells by abrogating all calcium-dependent E-cadherin function, the percentage of floating cells at each time point was calculated by the floating cell count in TG treated dish divided by the number of floating cells in EDTA treated dish.

Confocal microscopy (for E-cadherin staining in Chapter 3)

Fluorescence images were taken at room temperature using a laser-scanning confocal microscope (Leica TCS SP5) with 63x plan apochromat glycerin immersion objective (1.3 NA) and steady state photomultiplier tubes (PMTs, Leica Microsystems Inc) to detect and digitize the image. The coverslips were mounted with mounting medium (Sigma). The excitation wavelength for FITC was 488 nm with emission collected at 530 ± 15 nm and the excitation wavelength of Syto 63 was 633 nm with emission collected at 673 ± 15 nm. A complete set of images were recorded using the Leica TCS SP5 software by setting and fixing the imaging parameters on the brightest samples to ensure no saturation. Images were analyzed using Acapella software (Acapella 2.5, Perkin Elmer). The intensity of E-cadherin staining was normalized against the Syto 63 intensity to correct for changes in cell shape.

Image analysis and quantification (for E-cadherin staining in Chapter 3)

MCF-7 cells transfected with plasmids encoding Neo (control vector), E-cad WT and E-cadΔpSer were treated with TG for 0, 5, 10, 15, 20, 25 hours respectively and

then were fixed without permeabilization of cell membranes. E-cadherin on the plasma membrane was stained by FITC (green) and cytoplasmic dye Syto63 (red) was applied as an internal control. Four cell images were collected for each sample using a deconvolution microscope all with the same exposure time. Acapella software was used to capture cellular matter in the green/red channels (for a green-red image, the same matter was used). The total green intensity and red intensity were collected in the cell area for each image. For each image we did:

$$\text{Ratio}=\text{Total green intensity}/\text{Total red intensity}$$

with replicates and plotted averages for each time period.

Since Syto63 stain (red) should be constant for each cell, we plotted the average value of red per cellular matter pixel. This was averaged for each time period and plotted.

PARP cleavage assay

During apoptosis PARP is cleaved into 24 kDa and 89 kDa fragments by caspase-7 in MCF-7 cells and can be degraded by lysosomal proteases to 62 kDa and 55 kDa or 74 kDa and 42 kDa fragments (Gobeil, Boucher, Nadeau, & Poirier, 2001). Thus loss of full-length PARP is the most appropriate measure of cell death since both cleavage and degradation are accounted for (Fiebig, et al., 2006). Full length PARP was shown by immunoblotting using PARP C-2-10 mAb (Enzo Life Sciences) and quantified as described previously (Fiebig, et al., 2006). The C-2-10 monoclonal antibody recognizes full-length and 89 kDa caspase cleaved PARP, but does not recognize the cleavage products of other proteases. Therefore, to assess PARP cleavage by caspase-7 as well as degradation we measured the decrease in the amount of the full-length PARP. In each experiment the amount of actin in the samples was also recorded. If the actin blots indicated uneven loading, transfer or development of the blots then the corresponding PARP data was not used. To analyze the PARP data, both PARP cleavage and

degradation are combined into a single apoptosis index determined by measuring the band intensities for the full-length PARP in untreated cells ($F_{untreated}$), and in cells grown in CSBS ($F_{treated}$) indicated above the lanes by analysis with ImageJ software (Fiebig, et al., 2006). For each blot we did:

$$\text{Apoptosis Index} = 100 \times (1 - F_{treated}/F_{untreated})$$

with replicates and plotted averages for each treatment

XBP-1 splicing analysis

Cells were lysed and total RNA was isolated using RNA extraction kit (RNAeasy, Qiagen). Then mRNA was reverse-transcribed from total RNA using the SuperScript-RT system (Invitrogen). cDNA was used as template for PCR amplification across the fragment of the XBP-1 cDNA bearing the intron target of IRE1α ribonuclease activity. Primers used included: human XBP-1, 5'-TTACGAGAGAAAACTCATGGC-3' and 5'-GGGTCCAAGTTGTCCAGAATGC-3'. PCR conditions were: 95°C for 5 minute; 95 ℃ for 30 second; 58 ℃ for 30 second; 72 ℃ for 1 minute; 72 ℃ for 5 minute with 35 cycles of amplification. A 289 bp amplicon was generated from unspliced XBP-1; a 263 bp amplicon was generated from spliced XBP-1. PCR products were resolved on a 5% agarose/1x TAE gel.

Quantitative Real-Time PCR Analysis

Cells were lysed and total RNA was isolated using RNA extraction kit (RNAeasy, Qiagen, Germany). Then mRNA was reverse-transcribed from total RNA using the SuperScript RT system (Invitrogen) and aliquots of cDNA were used as template for quantitative PCR. Primers used included:

human Rpl19 mRNA, 5'-ATGTATCACAGCCTGTACCTG-3' and 5'-TTCTTGGTCTCTTCCTCCTTG-3'; human Chop mRNA, 5'-ACCAAGGGAGAACCAGGAAACG-3' and 5'-TCACCATTCGGTCAATCAGAGC-3'; human IRE1α mRNA, 5'-TGGGTAAAAAGCAGGACATCTGG-3' and 5'-GCATAGTCAAAGTAGGTGGCATTCC-3'; Real time PCR was performed by using Mastercycler realplex Thermal Cyclers (Eppendorf). Rpl19 mRNA levels, a ribosomal protein whose transcription is not regulated by endoplasmic reticulum stress, served as an internal normalization standard. PCR conditions were: 95 ℃ for 5 minute; 95 ℃ for 30 second; 55 ℃ for 30 second; 72 ℃ for 1minute; 78 ℃ for 10 second; 72 ℃ for 5 minute, with 40 cycles of amplification.

Annexin V/PI double staining (Chapter 3)

Cell survival was also quantified using Annexin V- Alexa Fluor 488 and propidium iodide (PI) staining. This assay identifies viable cells (Annexin V −/PI−), apoptotic cells (Annexin V +/PI−) and necrotic cells (Annexin V +/PI+) (Vermes et al., 1995). MCF-7 cells were washed with cold PBS twice and then resuspended in 1X Binding Buffer (0.01 M HEPES, pH 7.4; 0.14 M NaCl; 2.5 mM $CaCl_2$) at a concentration of ~1 x 10^6 cells/mL. Annexin V Alexa Fluor 488 (Invitrogen) and PI (Sigma) were added to the cells prior to incubation on ice for 15 minutes. Cells were then analyzed by flow cytometry (Beckman Coulter Epics Altra).

Annexin V/DRAQ5 staining and image analysis (Chapter 4)

Cells were seeded on coverslips 24 hours prior to the treatment. After growth in CSBS for 10 days, aspirated the CSBS and added 500 µL 1X Binding Buffer (0.01 M HEPES, pH 7.4; 0.14 M NaCl; 2.5 mM $CaCl_2$) containing 5 µL Annexin V coupled to Alexa Fluor488 (Invitrogen) and 5 µM DRAQ5 (Biostatus) for each well. Incubated for 30 minutes at 37 ℃ and then viewed by confocal microscopy. Acapella software

(Acapella 2.5, Perkin Elmer) was used to segment cell objects based upon DRAQ5 staining. The intensity in green channel in the cytoplasm was measured for each object.

For the quantitative determination of Annexin V positivity, two sample sets were prepared by manually picking 20 objects per sample. The first sample (Sample 1) is of the objects that showed Annexin V-positive. The second sample (Sample 2) is of those objects with Annexin V-negative. Sample 1 was employed to find the average value of the green intensity (Annexin V channel) +/- standard deviation as a comparison with Sample 2. This provided the lower value for the green intensity of cells that showed Annexin V-positivity. This value was used as the threshold and all cells with green channel intensity above this threshold would be labeled Annexin V-positive. The above mentioned thresholds were used to find the fraction of cells showing Annexin V positivity per transfected protein (Neo, Bcl2-ActA, Bcl2-cb5, Bcl2-WT) for the entire dataset:

$$\text{Annexin V positivity (\%)} = \frac{\text{Count of Annexin V-positive cells}}{\text{Total cell count}} \times 100\%$$

The percentages were then plotted for each transfected protein (Neo, Bcl2-ActA, Bcl2-cb5, Bcl2-WT) expressing cells after grown in CSBS for 10 days and total cell counts were shown below corresponding column.

6A7/Cytochrome c staining and image analysis (Chapter 4)

MCF-7 cells expressing Neo, Bcl2-ActA, Bcl2-cb5 and Bcl2-WT were seeded on coverslips. Then the cells were grown in CSBS for 10 days before they were fixed with 4% paraformaldehyde. To permeabilize cells, they were incubated with 1% Triton X-100 in PBS for 10 minutes at room temperature, and then incubated with affinity-purified sheep polyclonal antibody directed against cytochrome c and 6A7 antibody against activated Bax (at a dilution of 1: 1000) or AM03 antibody against activated Bak (at a dilution of 1: 1000) at 37 ℃ for 1 hour. Then the cells were washed and incubated at 37 ℃

for 1 hour with fluorescent secondary antibody donkey anti-sheep IgG-fluorescein isothiocyanate (FITC, Jackson ImmunoResearch Laboratories Inc) to stain cytochrome c and Alexa Fluor 594 Goat Anti-Mouse IgG (H+L) (Invitrogen) to stain activated Bax or activated Bak. Nuclei were stained with 5 μM DRAQ5 (Biostatus) for 30 minutes at room temperature.

Fifteen cell images were collected for each transfected protein using a confocal microscope all with the same exposure time. Acapella software (Acapella 2.5, Perkin Elmer) was used to segment cell objects based upon DRAQ5 staining. The intensity in green (cytochrome c) and red (6A7) channels was measured in the cytoplasm for each object.

Two sample sets were prepared by manually picking 20 objects per sample. The first sample (Sample 1) is of the objects that showed the release of cytochrome c. The second sample (Sample 2) is of those objects with intact cytochrome c. Sample 1 was employed to find the average value of the green intensity (cytochrome c release channel) +/- standard deviation as a comparison with Sample 2. This provided the upper value for the green intensity of cells that showed cytochrome c release. This value was used as the threshold and all cells with green channel intensity below this threshold would be labeled cytochrome c release positive. The mentioned thresholds were used to find the fraction of cells showing cytochrome c release per transfected protein (Neo, Bcl2-ActA, Bcl2-cb5 and Bcl2-WT) for the entire dataset:

$$\text{Cytochrome c Releasing (\%)} = \frac{\text{Count of cytochrome c released cells}}{\text{Total cell count}} \times 100\%$$

The percentages were then plotted for each transfected protein (Neo, Bcl2-ActA, Bcl2-cb5 and Bcl2-WT) expressing cells after grown in CSBS for 10 days and total cell numbers were shown below corresponding column.

For the quantification of 6A7 staining, similar to Annexin V staining, two sample set were prepared by manually picking 20 objects per sample. The first sample (Sample 1) is of the objects that showed 6A7-positive. The second sample (Sample 2) is of those objects with 6A7-negative. Sample 1 was employed to find the average value of the red intensity (6A7 channel) +/- standard deviation as a comparison with Sample 2. This provided the lower value for the red intensity of cells that showed 6A7 positivity. This value was used as the threshold and all cells with red channel intensity above this threshold were labeled as 6A7-positive. Thus the fraction of cells showing 6A7 positivity was calculated as below:

$$\text{6A7 positivity (\%)} = \frac{\text{Count of 6A7-positive cells}}{\text{Total cell count}} \times 100\%$$

To quantitatively determine the double staining of activated Bak (AM03)/cytochrome c or tetramethylrhodamine ethyl ester (TMRE) staining, the same approach was applied.

Cell staining and microscopy (Chapter 5)

Cells were stained with either 100 nM nonyl-acridine orange (NAO, Sigma) and 5 μM DRAQ5 (Biostatus) or 1 μM PI (Sigma) with 1:1000 Annexin V-AlexaFluor 488 (Invitrogen) and 5 μM DRAQ5 in αMEM. After 30 minutes the cells were washed with PBS followed by αMEM. The plate was imaged using a Perkin Elmer Opera QEHS high content screening system maintained at 37 ℃ and 5% CO2 in the imaging chamber. Images were acquired using a 40×0.7NA water immersion objective. Images of NAO and Annexin V-AlexaFluor 488 staining were acquired with 488nm excitation and 540/40 emission filter; PI with 561 nm excitation and 600/40 emission; DRAQ5 with 633 nm excitation and 680/40 nm emission. The expression vector for the caspase-probe was a kind donation from Dr. R. Truant (McMaster).

The expression of mCherry-BH3 and cytochrome c release image and data analysis (Chapter 5)

MCF-7 cells and Bcl-XL expressing MCF-7 cells were seeded on coverslips. The next day, the cells were transfected with plasmids encoding mCherry (vector), or mCherry fused to the BH3 protein indicated to the left of the panels. The cells were washed twice in PBS and fixed with 4% paraformaldehyde 24 hours after transfection. To permeabilize cells, they were incubated with 1% Triton X-100 in PBS for 10 minutes at room temperature, and then incubated with affinity-purified sheep polyclonal antibody directed against cytochrome c (1: 1000) at 37 ℃ for 1 hour. Then the cells were washed and incubated at 37 ℃ for 1 hour with fluorescent secondary antibody (donkey anti-sheep IgG-fluorescein isothiocyanate (Jackson ImmunoResearch Laboratories Inc), dilution of 1: 500. Nuclei were stained with 5 μM DRAQ5 (Biostatus) for 30 minutes at room temperature, which was not shown.

Fifteen images of cells were collected for each condition using spinning disk confocal microscope (Leica Microsystems Inc), all with the same laser settings and exposure time. Acapella software (Acapella 2.5, Perkin Elmer) was used to automatically identify cells as well as the nuclear and cytoplasmic areas in the images by segmentation based on DRAQ5 staining (not shown). Images were scored for mCherry-protein expression and for cytochrome c release using an automated image analysis program. Comparison of the red intensity (mCherry-BH3 protein) in transfected and non-transfected cells (20 of each) was used to set an arbitrary threshold intensity to identify mCherry-BH3 expressing cells in the population. The same images were used to set a threshold for the green channel (fluorescein labeled immunostaining for cytochrome c) based on a linear combination of cytoplasmic staining intensity and standard deviation to permit automatic assignment for cytochrome c release. Cytochrome c release was then expressed as the percentage of the cells with mCherry intensity above the red threshold (expressing a mCherry-BH3 protein) that had cytochrome c intensity and standard

deviation below the green threshold (cytochrome c released). The bars on the histogram indicate the percentage of mCherry positive cells that had released cytochrome c. The actual number of cells that scored positive for cytochrome c release and the total number of mCherry positive cells in 15 images is indicated below the bars. Fewer mCherry positive cells were observed when the BH3-protein induced apoptosis because the dead cells did not remain on the dish. For example, mCherry-tBid retained significant cytotoxicity as only 35 mCherry-positive cells were observed, 16 of which had released cytochrome c. In contrast, in cells expressing the inactive tBid control mutant tBidG94E, 422 mCherry positive cells were observed only 22 of which had released cytochrome c.

Chapter 3 : Multiple post-translational modifications regulate E-cadherin transport during apoptosis

3.1 Preface

All of the work presented in this chapter was published in:

Geng F, Zhu W, Anderson RA, Leber B, Andrews DW. (2012) J Cell Sci. 125:2615-25

Permission has been granted by the publishers to reproduce the material here.

3.2 Introduction

Epithelial cell-cell adhesion determines tissue organization, and loss of cell adhesion activates anoikis (Grossmann, 2002; Yap, Crampton, & Hardin, 2007). An important component of this process is E-cadherin, a single-membrane-spanning protein with a conserved cytoplasmic domain and divergent extracellular regions composed of five cadherin domains separated by interdomain Ca^{2+} binding sites (Gumbiner, 2000). Cadherins mediate cell-cell adhesion via interactions between N-terminal cadherin domains on opposing cell surfaces and by organization of the actin cytoskeleton through α-catenin (Nelson, 2008).

Assembly of E-cadherin based AJ is obligatory for establishment of polarized epithelia. Rab11 (Lock & Stow, 2005), p120-catenin (Peifer & Yap, 2003), tyrosine phosphorylation (Behrens, et al., 1993), and ubiquitination (D'Souza-Schorey, 2005) control the trafficking and assembly of E-cadherin in mammalian cells. Recent studies have shown that PIPKIγ acts as a signaling scaffold that links an adaptor protein complex to E-cadherin (Ling, et al., 2007; Ling, et al., 2002). The depletion of PIPKIγ or disruption of PIPKIγ binding to either E-cadherin or adaptor protein complexes results in defects in E-cadherin transport and blocks AJ formation (Ling, et al., 2007).

E-cadherin is synthesized as a 140 kDa precursor that undergoes cleavage by proprotein convertase family proteins associated with the trans-Golgi network (TGN) that remove an amino-terminal pro-region (Beavon, 2000; Posthaus, et al., 1998). Furin, a member of the proprotein convertase family, efficiently cleaves the E-cadherin precursor (Posthaus, et al., 1998). This processing is essential for correct folding of the extracellular portion of the mature molecule and required to mediate the homotypic calcium-dependent binding of E-cadherin extracellular domains (Beavon, 2000; Ozawa & Kemler, 1990).

We previously reported that the cytoplasmic domain of E-cadherin is modified by the addition of O-GlcNAc after treatment of cells with TG, an irreversible inhibitor of the sarcoplasmic/endoplasmic reticulum calcium ATPase (Denmeade & Isaacs, 2005; Lytton,

et al., 1991; Zhu, et al., 2001). In TG treated cells, the apparent molecular weight of E-cadherin increased by 20 kDa, a molecular weight change unlikely to be due solely to the addition of O-GlcNAc to serine and threonine residues (Vosseller, et al., 2001; Zhu, et al., 2001). The nature and functional significance of this other modification are unknown.

We present evidence here that cytoplasmic O-GlcNAcylation blocks exit of E-cadherin precursors from the endoplasmic reticulum and interferes with PIPKIγ binding. We identify the second modification as loss of pro-region processing that presumably results from inhibition of proprotein convertases and show that this is regulated separately from O-GlcNAcylation. Loss of the plasma membrane localization of E-cadherin accelerates the induction of apoptosis, as prevention of O-GlcNAcylation by deletion mutagenesis restored PIPKIγ binding, E-cadherin trafficking, and attenuated apoptosis. Our data suggest that in response to some agonists, both independent post-translational modifications contribute to the rapid induction of apoptosis by inhibiting the assembly of E-cadherin complexes on the plasma membrane.

3.3 Results

E-cadherin is independently modified by O-GlcNAcylation and pro-region retention

We previously reported that in the MCF-7 and MDCK epithelial cells exposure to TG, an agent that causes endoplasmic reticulum stress by depleting intraluminal calcium, resulted in the addition of O-GlcNAc to the cytoplasmic domain of E-cadherin. O-GlcNAcylation was assayed as increased binding of the modified E-cadherin to the GlcNAc-binding lectin WGA that was abolished by treatment with β-hexosaminidase (Zhu, et al., 2001). This O-GlcNAcylation pattern is not bound by two monoclonal antibodies (mAb, 110.6 and RL2) that recognize specific patterns of O-GlcNAcylation (data not shown). Furthermore, in TG treated cells there is a 20 kDa change in electrophoretic mobility of E-cadherin (Figure 3.1A, lane 3) suggesting additional modification(s) may occur when cells are treated with TG (Zhu, et al., 2001).

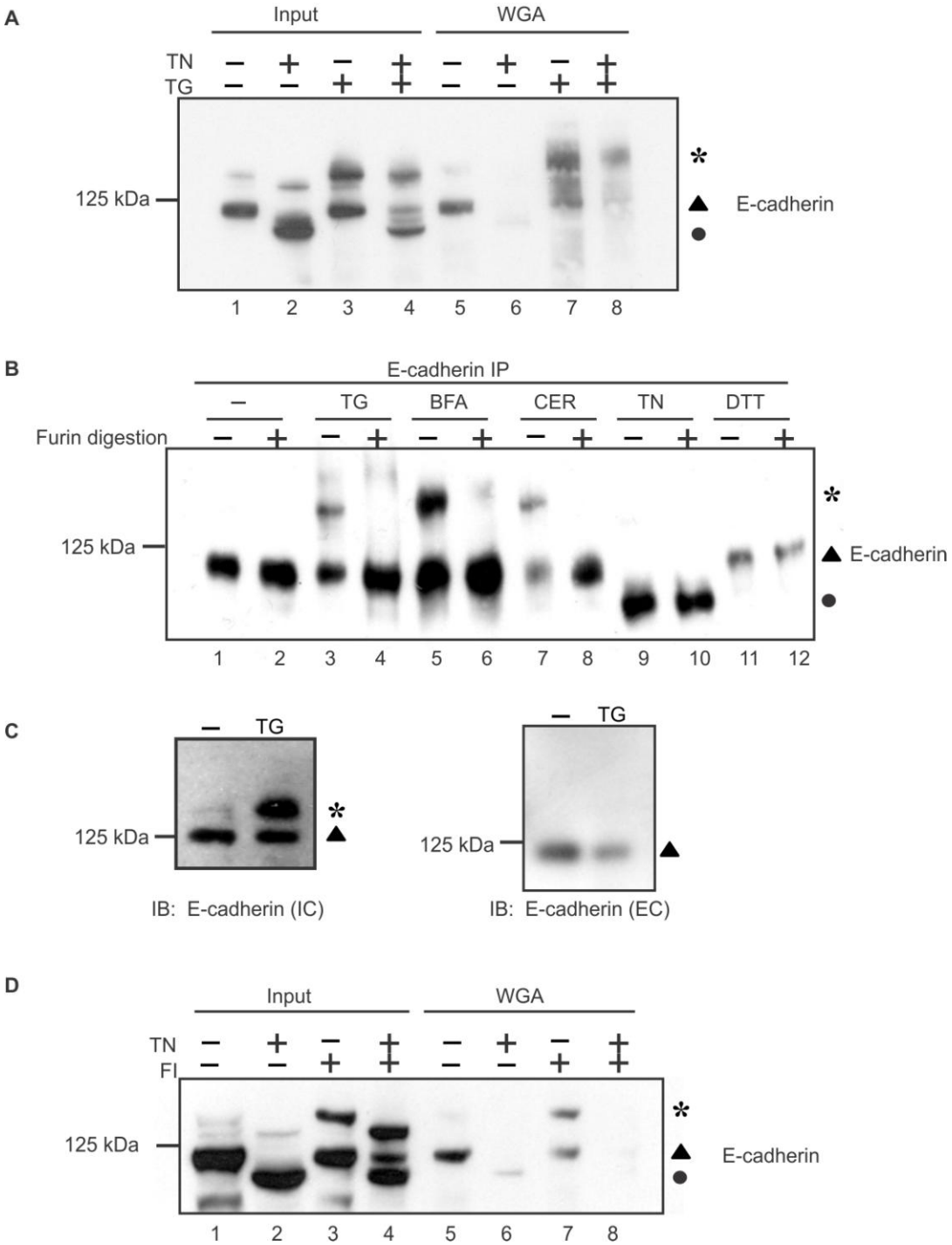

Figure 3.1 E-cadherin undergoes two independent post-translational modifications in stressed cells. Legend see next page.

(A) Lysates prepared from MCF-7 cells treated with DMSO control (−), 10 μg/mL TN, 400 nM TG, or both for 24 hours were analyzed by E-cadherin immunoblotting directly or after WGA binding. In all blots ▲ indicates mature E-cadherin, * indicates modified E-cadherin and ● indicates E-cadherin with N-glycosylation prevented by TN. (**B**) Lysates prepared from MCF-7 cells 400 nM TG for 24 hours, 10 μg/mL BFA for 24 hours, 100 μM CER for 8 hours, 10 μg/mL TN for 48 hours, 10 mM DTT for 6 hours respectively were immunoprecipitated (IP) with E-cadherin antibody, subjected to furin digestion, then TCA precipitated and analyzed by immunoblotting for E-cadherin. These drug treatment conditions apply to all figures unless otherwise specified. (**C**) MCF-7 cells without or with TG treatment were analyzed by immunoblotting with an E-cadherin antibody raised against an epitope in the cytoplasmic domain (IC; unless otherwise specified, all subsequent E-cadherin immunoblots were probed with this antibody) or E-cadherin antibody SHE78-7 (EC) recognizing an epitope in the extracellular domain of mature E-cadherin. (**D**) Lysates prepared from MCF-7 cells treated with DMSO control (−), TN, 200 μM furin inhibitor (FI) or both for 24 hours were immunoblotted for E-cadherin either directly (Input) or after WGA binding (WGA). FI treatment condition applies to all figures.

To determine if E-cadherin modifications are unique to TG treated cells we tested a variety of other agents that cause cell stress including TN, DTT, BFA and ceramide (CER). The addition of TG, BFA and CER but not TN resulted in the appearance of 140 kDa E-cadherin (Figure 3.1B, *), indicating that this modification is common but not an obligate result of endoplasmic reticulum stress or apoptosis (Figure 3.8A). O-GlcNAcylation of E-cadherin was examined by binding to WGA a lectin that binds with high affinity to O-GlcNAc, but with low affinity also binds to N-linked glycans (Natsuka et al., 2005). To permit unambiguous identification of O-GlcNAc modified proteins, N-linked glycan formation was inhibited by treating the cells with TN before the glycoproteins were isolated by binding to WGA agarose. As expected, treatment with TN prevented N-linked glycosylation of E-cadherin and therefore decreased the molecular weight of the mature protein (Figure 3.1A, lane 2, ●). Although TN treatment abolished the binding of 120 kDa E-cadherin (▲) to WGA, a substantial fraction of 140 kDa E-cadherin still bound to WGA (Figure 3.1A, lane 7 and 8, *), indicating that either 140 kDa E-cadherin is a preferential substrate for O-GlcNAcylation or that O-GlcNAcylation leads to the increase in apparent molecular weight. Treatment of cells with CER yielded

the 140 kDa E-cadherin without O-GlcNAcylation, confirming that most of the apparent increase in molecular weight is due to a second independent post-translational modification. Exposure to BFA gave rise to both modifications as did exposure to TG (Figure 3.8D, 3.8E).

The apparent molecular weight of the modified E-cadherin (140 kDa) is similar to the molecular weight of an E-cadherin precursor that contains the pro-region normally removed by proprotein convertases in the trans-Golgi. Therefore, we probed immunoblots with a monoclonal antibody (SHE78-7, EC) that recognizes an epitope created by processing E-cadherin to the mature form (Laur, Klingelhofer, Troyanovsky, & Troyanovsky, 2002). As EC bound the 120 kDa but did not bind to 140 kDa form of E-cadherin induced by both TG (Figure 3.1C) and BFA (Figure 3.8E) we conclude that the latter does not contain the epitope characteristic of the mature protein. Furthermore, after immunoprecipitation (IP) the 140 kDa E-cadherin induced by TG, BFA and CER, incubation with the proprotein convertase furin yielded a product with the same ~120 kDa electrophoretic mobility as mature E-cadherin (Figure 3.1B). Therefore, we conclude that the 140 kDa form of E-cadherin is the pro-form of the protein. Since CER does not lead to O-GlcNAcylation of E-cadherin, the common effect of these three agents is to inhibit the activity of a furin-like protease in cells.

To determine the relationship between inhibition of E-cadherin pro-region cleavage and O-GlcNAcylation, MCF-7 cells were treated with furin inhibitor (FI) and E-cadherin alterations and the cellular response were analyzed (Hallenberger, et al., 1992). In contrast to TG, FI did not cause endoplasmic reticulum stress or apoptosis (Figure 3.9A, top two panels), but it inhibited E-cadherin processing in cells, as the 140 kDa form of E-cadherin was evident (Figure 3.1D, lane 3). As expected for N-glycosylated proteins, both forms of E-cadherin bound to WGA (Figure 3.1D, lane 7). However in FI treated cells, binding of both species to WGA was abrogated by TN treatment (Figure 3.1D, lane 8), indicating that the 140 kDa E-cadherin that resulted from furin inhibition was not O-

GlcNAcylated. Thus retention of the E-cadherin pro-region is regulated independently from O-GlcNAcylation.

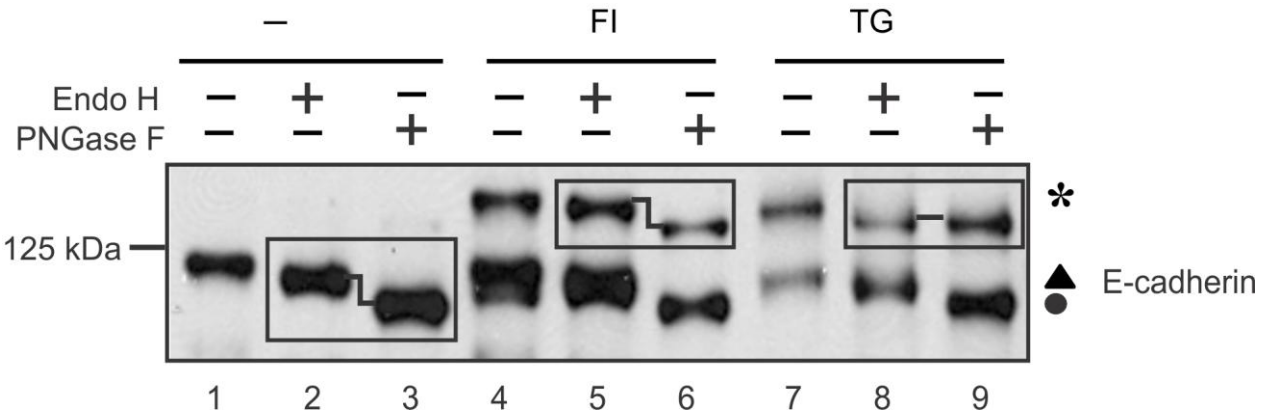

Figure 3.2 E-cadherin O-GlcNAcylation inhibits its trafficking to cell surface by preventing E-cadherin exit from the endoplasmic reticulum.
Lysates from MCF-7 cells treated with DMSO control (−), FI or TG were digested with Endo H or PNGase F and analyzed by immunoblotting for E-cadherin. The increased mobility after PNGase F digestion in untreated or FI treated cells is indicated with a stepped line (lane 2-3, 5-6).

O-GlcNAcylation prevents E-cadherin trafficking by inhibiting export from the endoplasmic reticulum

We examined the effect of the separate modifications on E-cadherin trafficking by exploiting the differential sensitivity of N-linked glycosylation to peptide:N-glycosidase F (PNGase F) and Endoglycosidase H (Endo H) digestion (Maley, Trimble, Tarentino, & Plummer, 1989). Endo H removes the high mannose sugars added in the endoplasmic reticulum but does not hydrolyze complex type N-glycosylation that occurs in the cis to medial Golgi cisternae. PNGase F hydrolyzes both types of N-glycosylation (Maley, et al., 1989). Thus Endo H resistance with PNGase F sensitivity reflects export from the endoplasmic reticulum and transit through the cis-Golgi, whereas sensitivity to both glycosidases indicates retention in the endoplasmic reticulum (Spellman, 1990).

As expected after treatment with either TG or FI, both the processed and pro-region containing forms of E-cadherin were sensitive to PNGase F (Figure 3.9B). This indicates that all of the E-cadherin species were N-glycosylated. In addition, the bulk of the E-cadherin from untreated cells (a control for authentic transport to the plasma membrane) was resistant to Endo H digestion but sensitive to PNGase F indicative of efficient export from the endoplasmic reticulum (Figure 3.2, lane 1-3). In FI treated cells, pro-E-cadherin was also resistant to Endo H digestion and sensitive to PNGase F digestion, indicating that this protein also exits the endoplasmic reticulum (Figure 3.2, lane 4-6) even though it does not transit to the cell surface ((Ozawa & Kemler, 1990); Figure 3.9A, bottom panel, lane 5).Thus retention of the pro-region is not sufficient to abolish export from the endoplasmic reticulum as expected, since the pro-region is normally removed later in the secretory pathway. By contrast in lysates from TG treated cells either Endo H or PNGase F digestion reduced the apparent molecular weight of the 140 kDa modified E-cadherin bands similarly (Figure 3.2, lane 7-9). Taken together with our previous report showing that TG treatment does not cause a general block in protein exit from the endoplasmic reticulum (Zhu, et al., 2001), these data indicate that TG induced O-GlcNAcylation selectively prevents pro-E-cadherin from exiting from the endoplasmic reticulum.

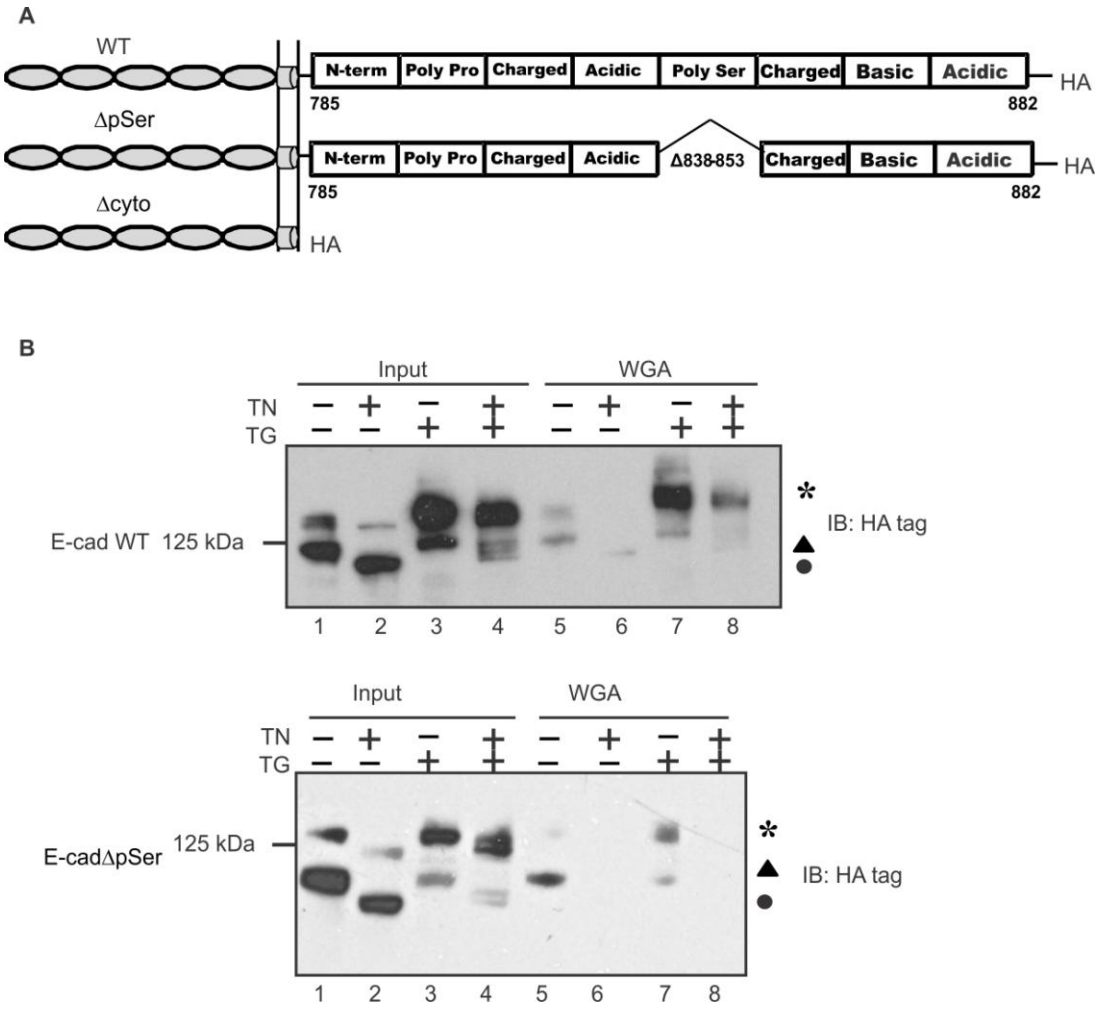

Figure 3.3 The polyserine region in the E-cadherin cytoplasmic domain is required for TG induced E-cadherin O-GlcNAcylation.
(**A**) Defined regions of wild type E-cadherin cytoplasmic domain were demonstrated previously. The corresponding diagram for HA tagged E-cad WT and E-cadΔpSer are indicated. (**B**) MCF-7 cells expressing HA tagged E-cad WT (top) and E-cadΔpSer (bottom) were treated with DMSO control (−), TN, TG or both for 24 hours. Cell lysates were analyzed by immunoblotting for HA tag (Input) or by WGA binding followed by immunoblot (IB).

The polyserine (pSer) region is required for O-GlcNAcylation of E-cadherin

On cytoplasmic and nuclear proteins, as well as the cytoplasmic domains of some transmembrane proteins O-GlcNAc can be attached via the hydroxyl group of serines or

threonines (Wells & Hart, 2003). Studies on non-glycosylatable mutants of these target proteins have increased our understanding of the biological function of O-GlcNAcylation (Comer & Hart, 2000). To map the region(s) of E-cadherin that are subject to O-GlcNAcylation, we generated a hemaglutinin (HA) tagged E-cadherin with a deletion of the pSer region located in cytoplasmic domain (deletion of amino acids 838-853, E-cadΔpSer) as this sequence is a potential candidate for the multiple O-GlcNAcylation site(s) required to result in binding to WGA (Figure 3.3A; (Vosseller, et al., 2001)). HA tagged constructs of wild type E-cadherin (E-cad WT) and a mutant with the entire cytoplasmic domain deleted (deletion of amino acids 728-882, E-cadΔcyto) served as controls that can and cannot be O-GlcNAcylated, respectively.

To assess O-GlcNAcylation and pro-region retention MCF-7 and MDCK cell clones stably expressing the proteins (Figure 3.10) were exposed to TG and/or TN and whole cell lysates or WGA precipitates were analyzed by immunoblotting as above (Figure 3.3B). In response to TG treatment the HA-tagged proteins migrated as higher molecular weight species consistent with pro-region retention as seen with the endogenous E-cadherin (Figure 3.3B, *). A fraction of the higher molecular weight E-cad WT protein was also O-GlcNAcylated in response to TG and TN and therefore bound to WGA (Figure 3.3B, top panel lane 8). In contrast, no detectable E-cadΔpSer bound to WGA after TG and TN treatment (Figure 3.3B, bottom panel, lane 8) despite the fact that most of this protein also retained the pro-region (Figure 3.3B, bottom panel, lane 4). The most likely explanation for loss of O-GlcNAcylation of E-cadΔpSer is that the deleted region contains the serines that are modified. Alternatively, deletion of the pSer region may affect the folding and accessibility to O-GlcNAcylation at another site.

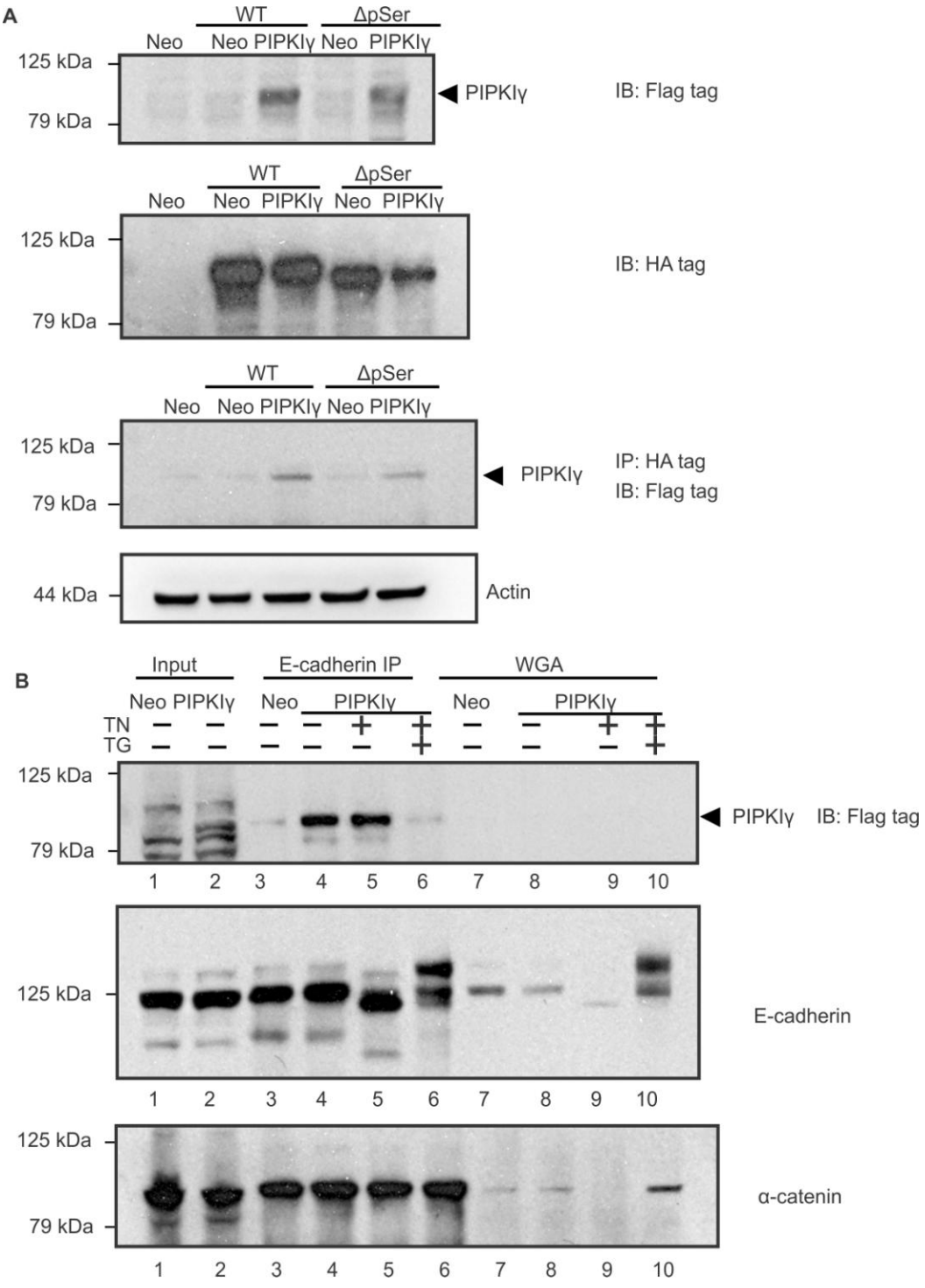

Figure 3.4 The E-cadherin-PIPKIγ interaction is intact after pSer region deletion but is disrupted by O-GlcNAcylation. Legend see next page.

(A) HEK 293 cells were cotransfected with either HA tag empty vector (Neo), HA tagged E-cad WT or E-cadΔpSer and either Flag tag control vector (Neo) or Flag tagged PIPKIγ. The expression of HA tagged E-cadherin and Flag tagged PIPKIγ was analyzed by immunoblotting for Flag tag (top panel) and HA tag (the second panel). The interaction between PIPKIγ and E-cad WT or E-cadΔpSer was analyzed by immunoprecipitation with HA tag antibody and immunoblotting for Flag tag (the third panel). Actin blot was provided as loading control (bottom panel). (**B**) MCF-7 cells transfected with PIPKIγ or control vector (Neo) were treated with DMSO control (-), TN, or TN plus TG for 24 hours. Total cell lysates (Input, lanes 1-2), immunoprecipitates with E-cadherin antibody (lanes 3-6) or WGA pull down (lanes 7-10) were immunoblotted for Flag tag (top panel), E-cadherin (middle panel) or α -catenin (bottom panel).

O-GlcNAc modified E-cadherin does not bind PIPKIγ

The PIPKIγ interacting region on E-cadherin overlaps with the pSer region required for O-GlcNAcylation (Ling, et al., 2007). To determine if deletion of the pSer region from E-cadherin interfered with PIPKIγ binding to E-cadherin, we examined complex formation in HEK 293 cells cotransfected with plasmids encoding Flag tagged PIPKIγ and HA tagged E-cadΔpSer or HA tagged E-cad WT (Figure 3.4A, top panel and the second panel). Immunoprecipitation with HA tag antibody followed by immunoblotting for Flag tag on PIPKIγ revealed that PIPKIγ bound to E-cadΔpSer and E-cad WT similarly (Figure 3.4A, the third panel).

To investigate the effect of O-GlcNAc modification of E-cadherin on the interaction between PIPKIγ and E-cadherin, MCF-7 cells stably expressing Flag tagged PIPKIγ were treated with TN and TG as above. In MCF-7 cells, the interaction between PIPKIγ and E-cadherin was not affected by TN (inhibited N-glycosylation) but was greatly decreased in response to TG (stimulated O-GlcNAcylation) (Figure 3.4B, top panel, lane 4-6). More importantly, precipitation with WGA revealed that PIPKIγ does not bind to O-GlcNAc modified E-cadherin (Figure 3.4B, top panel, lane 10). Overexpression of PIPKIγ did not inhibit O-GlcNAcylation of E-cadherin as it still bound to WGA (Figure 3.4B, middle panel, lane 10). Because O-GlcNAcylation disrupts the interaction between E-cadherin and PIPKIγ, we examined whether O-GlcNAcylation affects the interaction between E-cadherin and α-catenin as a “bridge” to the cytoskeleton

(Drees et al., 2005). We noted that α-catenin bound to total E-cadherin in the absence or presence of TG (Figure 3.4B, bottom panel, lane 4-6) and to O-GlcNAcylated E-cadherin as indicated by immunoblotting after WGA-Sepharose precipitation (Figure 3.4B, bottom panel, lane 9-10). We reported previously that treatment with TG did not affect binding of β-catenin or γ-catenin to E-cadherin (Zhu, et al., 2001). Furthermore, deletion of the pSer region did not affect the E-cadherin-β-catenin interaction or E-cadherin-γ-catenin interaction (Figure 3.11), even though phosphorylation on serines in this region of E-cadherin has been reported to enhance β-catenin binding affinity (Lickert, Bauer, Kemler, & Stappert, 2000; Stappert & Kemler, 1994). Taken together, these data suggest that O-GlcNAcylation selectively inhibits E-cadherin binding to PIPKIγ.

Preventing O-GlcNAcylation maintains transport of E-cadherin to the plasma membrane during cell stress

Because PIPKIγ is essential for trafficking of E-cadherin to the plasma membrane, we examined the effect of the deletion mutants on the cell surface expression of E-cadherin after TG exposure. We detected surface proteins by biotinylation, streptavidin precipitation and subsequent immunoblotting. After exposure of the cells to TG for 24 hours, HA-tagged full-length E-cadherin was not detected at the cell surface (Figure 3.5A, compare lane 1-2), suggesting a profound block in cell surface transport. In the same conditions both E-cadΔcyto and E-cadΔpSer transport was reduced by TG treatment but the mature forms of the proteins continued to be detected on the plasma membrane (Figure 3.5A). The decrease in intensity of the bands corresponding to E-cadΔcyto and E-cadΔpSer after treatment with TG is likely due to retention of the unprocessed (pro-region containing) forms of the proteins at a post-Golgi location in the secretory pathway as we noted for endogenous E-cadherin (Figure 3.2) and consistent with our previous observation that transport of unprocessed form is arrested in the late secretory pathway (Zhu, et al., 2001).

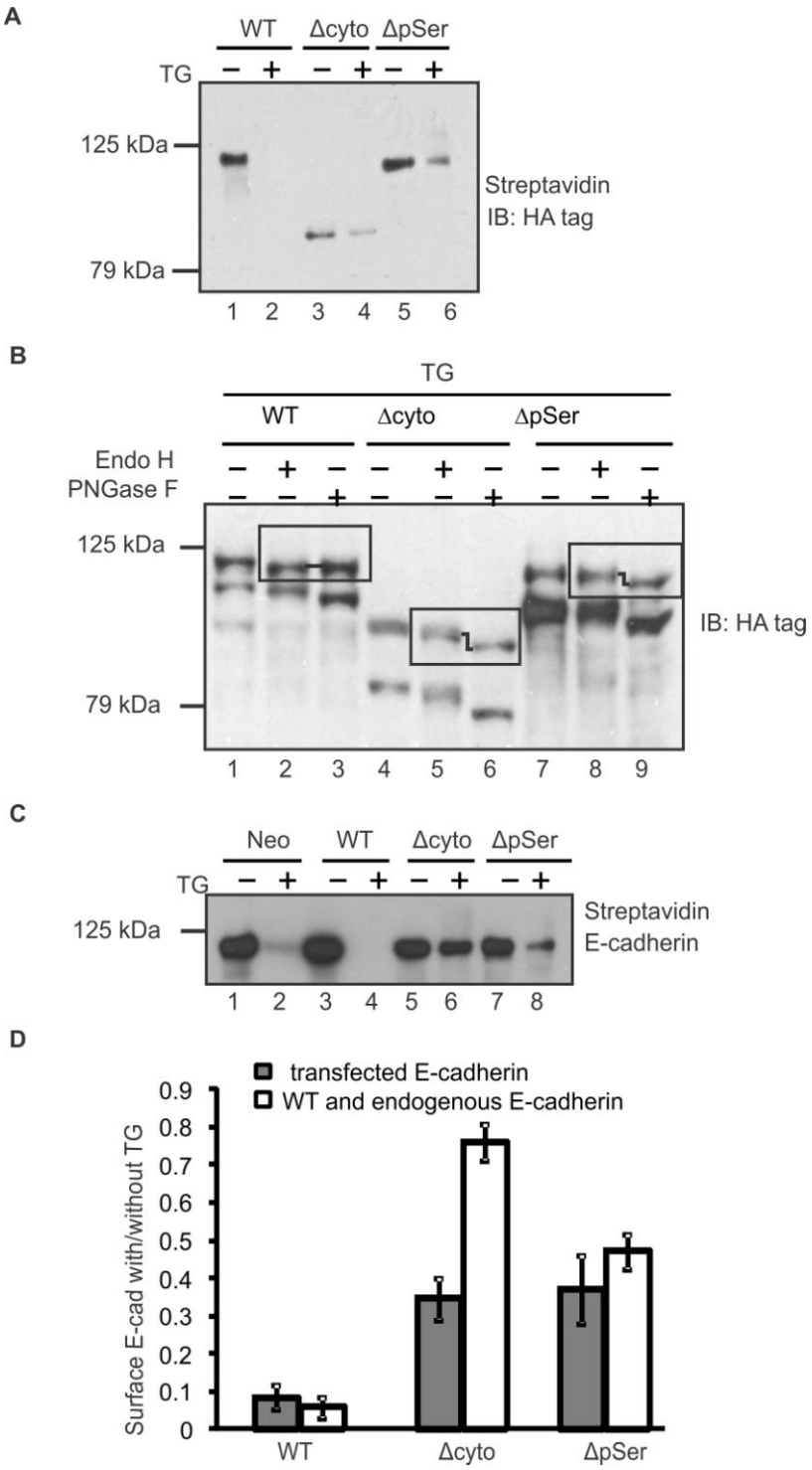

Figure 3.5 Prevention of E-cadherin O-GlcNAcylation maintains both endogenous and transfected E-cadherin targeting to the plasma membrane. Legend see next page.

(**A**) After surface biotinylation, cell surface E-cadherin expression in MCF-7 cells expressing HA tagged E-cad WT, E-cadΔcyto or E-cadΔpSer were examined by immunoblotting for HA tag. (**B**) Lysates from MCF-7 cells expressing HA tagged E-cad WT, E-cadΔcyto and E-cadΔpSer treated with TG were digested with Endo H or PNGase F and analyzed by immunoblotting for HA tag. (**C**) After surface biotinylation, cell surface E-cadherin expression in MCF-7 cells expressing HA tagged E-cad WT, E-cadΔcyto or E-cadΔpSer were examined by immunoblotting for E-cadherin with the antibody (IC) that recognizes cytoplasmic domain on endogenous E-cadherin and E-cad WT. (**D**) The relative proportion of transfected or endogenous E-cadherin remaining on cell membrane after TG treatment for 24 hours. The ratio was calculated based on the measurements of the intensity of the relevant bands (Figure 3.12C) shown in the immunoblots of Figure 3.5A, C.

We also noted a separate mechanism whereby the E-cadherin mutants increased surface expression of E-cadherin. By using a monoclonal antibody to the cytoplasmic domain that does not recognize either deletion mutant (Figure 3.12A), any cell surface E-cadherin detected in biotin-labeled cells using this antibody represents endogenous or transfected wild type protein. Remarkably in TG treated cells, expression of either E-cadΔcyto or E-cadΔpSer but not WT increased the amount of endogenous mature E-cadherin on the cell surface (Figure 3.5C, compare lane 4 with lane 6 and 8). Quantification of multiple blots revealed that this effect of increased cell surface expression of endogenous E-cadherin is particularly pronounced in cells expressing E-cadΔcyto (Figure 3.12C). Thus transfection of the non-glycosylatable mutants attenuated the decrease in total cell surface E-cadherin after TG treatment by two mechanisms: increased transport of the mutants themselves (Figure 3.5D, dark bars), and by facilitating the transport or stabilization of endogenous E-cadherin “in trans” (Figure 3.5D, open bars).

To confirm these results, we also measured the amount of cell surface protein by immunofluorescence staining of non-permeabilized MCF-7 cells stably expressing either E-cad WT or E-cadΔpSer. E-cadherin was labeled with an antibody directed against the extracellular domain (EC) (detecting both WT and mutant E-cadherin equally) and visualized using a fluorescein labeled secondary antibody (Figure 3.13A). Cell number

was estimated by staining with Syto 63 dye. The rate at which the green/red ratio decreases after TG treatment was used to estimate the rate at which E-cadherin disappears from the cell surface. Loss of cell surface E-cadherin was significantly greater in cells expressing exogenous HA tagged E-cad WT than that observed in cells expressing E-cadΔpSer (Figure 3.13B, p=0.047 by two way ANOVA), consistent with what was observed with the biotin labeling and immunoblotting results summarized above. In comparison, BFA and CER that cause O-glycosylation and/or pro-region retention also prevent E-cadherin transport to the cell surface (Figure 3.14). This is not an invariant feature of cells undergoing programmed cell death as it is not observed in MCF-7 cells treated with TNF .

To examine potential differences in exit from the endoplasmic reticulum during cell surface trafficking of E-cadherin and the deletion mutants, the sensitivity of N-linked glycosylation to PNGase F and Endo H digestion was determined. In untreated cells most exogenous E-cad WT, E-cadΔcyto and E-cadΔpSer was PNGase F sensitive and Endo H resistant (Figure 3.12B), demonstrating that they exited the endoplasmic reticulum and proceeded to the Golgi apparatus. By contrast, after treatment with TG, the 140 kDa form of E-cad WT was sensitive to Endo H digestion, consistent with O-GlcNAcylation serving as an endoplasmic reticulum retention signal and thereby preventing processing of E-cadherin in the Golgi (Figure 3.5B, lane 1-3). However, the pro-region containing forms of both E-cadΔcyto and E-cadΔpSer were Endo H resistant but PNGase F sensitive (Figure 3.5B, lane 4-6 and 7-9, respectively), indicating that the pro-region containing forms of the deletion mutants exited the endoplasmic reticulum.Thus O-GlcNAcylation, not pro-region retention, prevented trafficking from the endoplasmic reticulum to the Golgi.

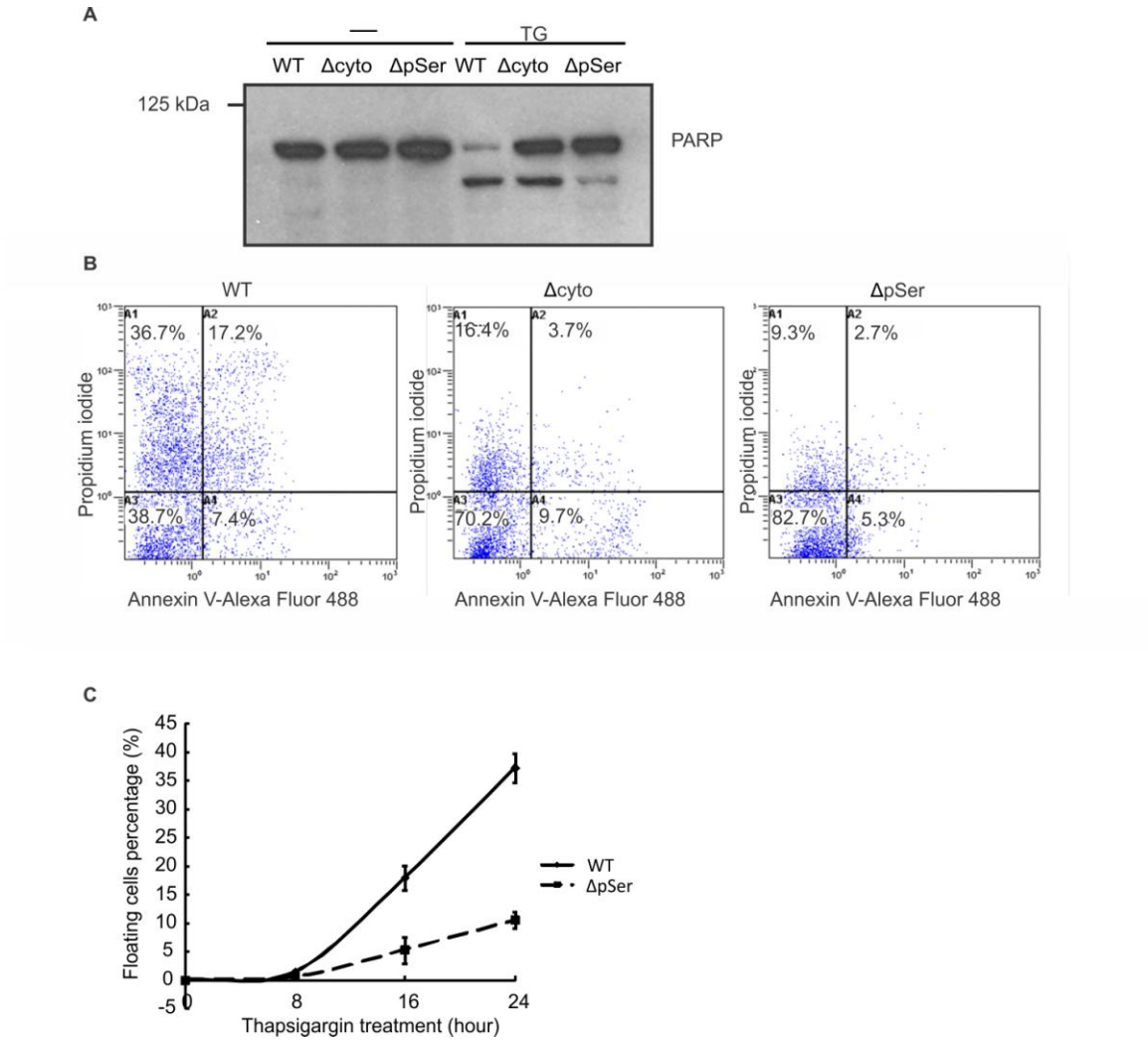

Figure 3.6 Prevention of E-cadherin O-GlcNAcylation maintains E-cadherin function and protects cells from stress induced apoptosis.

(**A**) Lysates from MCF-7 cells expressing HA tagged E-cad WT, E-cadΔcyto and E-cadΔpSer that were either treated with DMSO control (-) or TG for 24 hours were analyzed for PARP cleavage by immunoblotting. (**B**) MCF-7 cells expressing HA tagged E-cad WT, E-cadΔcyto or E-cadΔpSer were treated with TG for 24 hours, then stained with Annexin V coupled to Alexa Fluor488 and PI and analyzed by flow cytometry. Data were shown for a single experiment representative of three independent experiments. (**C**) MCF-7 cells expressing E-cad WT and E-cadΔpSer were treated with TG. After shaking at 500 rpm on the Eppendorf Thermomixer inside the tissue culture incubator, non-adherent cells were counted at the time point of 0, 8, 16, 24 hours.

Prevention of E-cadherin O-GlcNAcylation maintains E-cadherin function and delays apoptosis

To investigate the effect of O-GlcNAcylation of E-cadherin on cell death, MCF-7 cells expressing E-cad WT, E-cadΔpSer or E-cadΔcyto were treated with TG and apoptosis was assessed by PARP cleavage and Annexin V staining. PARP cleavage was delayed in cells expressing E-cadΔcyto or E-cadΔpSer at a time point at which PARP cleavage was almost complete and much of the cleaved product was been further degraded in control cells (Figure 3.6A). Delayed cell death in cells expressing the mutant forms of E-cadherin that were not O-GlcNAcylation substrates was confirmed by two color flow cytometric analysis measuring Annexin V-FITC and PI staining (Figure 3.6B). In these experiments TG treatment reduced the fraction of viable cells expressing E-cad WT to 38.7% (Annexin V-/PI-) whereas at the same time point 70.2% and 82.7% of the cells expressing E-cadΔcyto or E-cadΔpSer were viable respectively (Figure 3.6B). Thus expression of either E-cadΔcyto or E-cadΔpSer substantially reduced TG induced cell death. To confirm that these changes are not cell line or species specific, we examined the non-transformed, canine renal epithelial cell line MDCK expressing HA-tagged human E-cad WT and E-cadΔcyto (Figure 3.10C). Consistent with the results in MCF-7 cells after treatment with TG, less PARP cleavage was observed for MDCK cells expressing human E-cadΔcyto than for cells expressing E-cad WT.

To link the modification of E-cadherin with the effect on cell survival, we directly measured the adhesive activity of E-cad WT and E-cadΔpSer in the presence or absence of TG treatment (Figure 3.6C). After shaking in an incubator, the percentage of floating cells was 17% and 37% at 16 and 24 hours of TG treatment respectively, in WT E-cad expressing cells, but only 5% and 11% in E-cadΔpSer expressing cells. Thus prevention of O-glycosylation maintains the cell adhesion function of E-cadherin. Furthermore, F-actin formation and cell polarity were maintained by preventing O-glycosylation during TG treatment (Figure 3.15).

3.4 Discussion

As a critical component of epithelial junctional complex, E-cadherin is known to be post-translationally modified by phosphorylation and N-glycosylation (Gumbiner, 2005; Jeanes, Gottardi, & Yap, 2008; Liwosz, et al., 2006). As shown here, E-cadherin can also be modified by O-GlcNAcylation (Zhu, et al., 2001) and retention of the pro-region. The later effect is likely due to the inhibition of a luminal furin-like protease. Recent reports indicated that O-GlcNAc transferase (OGT) also has intrinsic proteolytic activity (Capotosti, et al., 2011). Both enzymatic functions are required sequentially to activate the mitotic regulator, HCF-1. In our case, selected cellular stressors activate the transferase activity of OGT while repressing the activity of a separate protease, and these effects occur in distinct cellular compartments (cytoplasm and endoplasmic reticulum lumen, respectively). Both of these independently regulated changes have a profound effect on E-cadherin trafficking and on the susceptibility of cells to apoptosis.

O-GlcNAcylation of E-cadherin inhibits both the binding of PIPKIγ to E-cadherin (Figure 3.4) and trafficking is blocked in the endoplasmic reticulum. As a result, the N-linked glycans on the extracellular domain of E-cadherin remain Endo H sensitive while pro-region which is normally removed by furin like proprotein convertases in the TGN is retained. Retention of E-cadherin in the endoplasmic reticulum reduced the total amount of the protein at the cell surface (Figure 3.2 and 3.5) and exacerbated apoptosis. Consistent with this interpretation, expression of mutant E-cadherin which lacks the pSer region that we identified as necessary for O-GlcNAcylation (Figure 3.3) prevented apoptosis induced by drugs that increased O-GlcNAcylation (Figure 3.6). A schematic overview of these effects is shown in Figure 3.7.

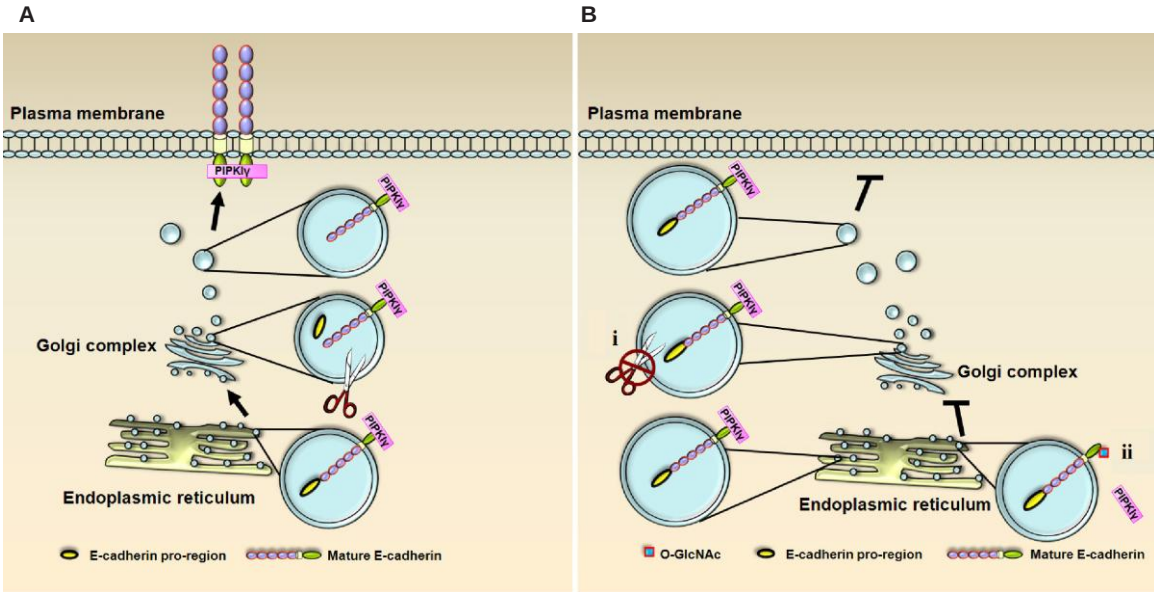

Figure 3.7 Cellular stress induces multiple modifications of E-cadherin that prevent trafficking to the plasma membrane.
(**A**) The E-cadherin trafficking pathway in healthy cells; (**B**) Cellular stress disrupts E-cadherin transport to the plasma membrane through two independent mechanisms: Inhibition of furin cleavage of the pro-region from E-cadherin in the TGN (i); Pro-E-cadherin is not transported to the plasma membrane. O-GlcNAcylation of the cytoplasmic domain of E-cadherin prevents the binding of PIPKIγ, and the O-GlcNAcylated E-cadherin is retained in the endoplasmic reticulum (ii). In this simplified diagram, signal peptide cleavage, other post-translational modifications and binding partners for E-cadherin are omitted.

The O-GlcNAc modification has been found to regulate a number of cellular functions (Gambetta, Oktaba, & Muller, 2009; Kreppel & Hart, 1999). However, the regulatory effects of O-GlcNAcylation on E-cadherin trafficking and PIPKIγ interaction have not been reported previously. Thus our data represent the first report that O-glycosylation prevents the binding of a kinase to the glycosylated substrate -this is the opposite of the effect that O-glycosylation of keratin has on the binding of Akt (Ku, Toivola, Strnad, & Omary, 2010). Moreover, little is understood about how O-GlcNAcylation is regulated in cells. Although we observed increased O-GlcNAcylation during certain forms of cell stress, it is likely that O-GlcNAcylation of E-cadherin also

occurs in response to less drastic stimuli and therefore, contributes to other forms of regulation of intracellular adhesion. The E-cadherin-PIPKIγ-AP1B interaction serves as a foundational signal for exocytic targeting and basolateral sorting of E-cadherin (Ling, et al., 2007). Furthermore, recent reports indicate that the association of increased PIPKIγ expression with invasiveness and poor prognosis in breast cancer. This effect may be mediated by PIPKIγ decreasing the binding of E-cadherin to β-catenin, which in turn can become transcriptionally competent and activate cell proliferation and metastatic pathways (Sun, et al., 2010). However, the simplest interpretation of our data demonstrating O-GlcNAc modification disrupts PIPKIγ binding to E-cadherin (Figure 3.4B) and prevents cell surface transport is that these events are interconnected. The fact that E-cadΔpSer was not O-GlcNAc modified (Figure 3.3B), continued to bind PIPKIγ (Figure 3.4A) and transited to the plasma membrane (Figure 3.5) strongly suggests that inhibition of E-cadherin transport in response to TG is due to O-GlcNAcylation of E-cadherin rather than some other effect of TG such as loss of endoplasmic reticulum calcium. This also explains why during TG treatment, E-cadΔpSer continued to target to the plasma membrane where it delayed apoptosis (Figure 3.5 and 3.6). Although the adhesion assay time course and the apoptosis data (Figure 3.5 and 3.6) are not directly comparable, they suggest that loss of adhesion precedes AnnexinV staining. However, it is difficult to assign a specific time for apoptosis since it is cell autonomous and clearly more work will be required to fully understand the kinetics of all of the events at the single cell level.

Adhesion-dependent survival is a fundamental aspect of cell behavior (Gilmore, Owens, Foster, & Lindsay, 2009). It is not clear why expression of mutants lacking pSer region or entire cytoplasmic domain of E-cadherin delayed apoptosis in response to stimuli that trigger O-GlcNAcylation of wild-type E-cadherin. However, both mutants continued to transit to the cell surface in drug treated cells. It is possible that increased adhesion for these mutants is sufficient to delay apoptosis in MCF-7 cells. However, we have also noted that expression of the mutants allows more of the processed endogenous

WT E-cadherin to assemble, or remain on the plasma membrane. In the latter case the survival signal may be mediated by signaling through the intact cytoplasmic tail of endogenous WT E-cadherin (possibly in mixed complexes), or by a combination of both increased adhesion and E-cadherin signaling mechanisms.

The endocytic recycling of cell surface E-cadherin is susceptible to oncogenic dysregulation that is mediated by multiple processes, including the Cbl and Nedd4 ubiquitin ligases that represent potential targets for novel cancer therapies (Mosesson, Mills, & Yarden, 2008). We have shown here that the initial trafficking and assembly of the plasma membrane E-cadherin complex is also tightly regulated, and recent work has indicated that OGT is a good target for pharmaceutical intervention (Gloster, et al., 2011). Therefore, further dissection and manipulation of the regulatory mechanisms of O-GlcNAcylation in E-cadherin adhesion in a context of stress have important implications for diverse disease processes such as apoptosis, development and metastasis.

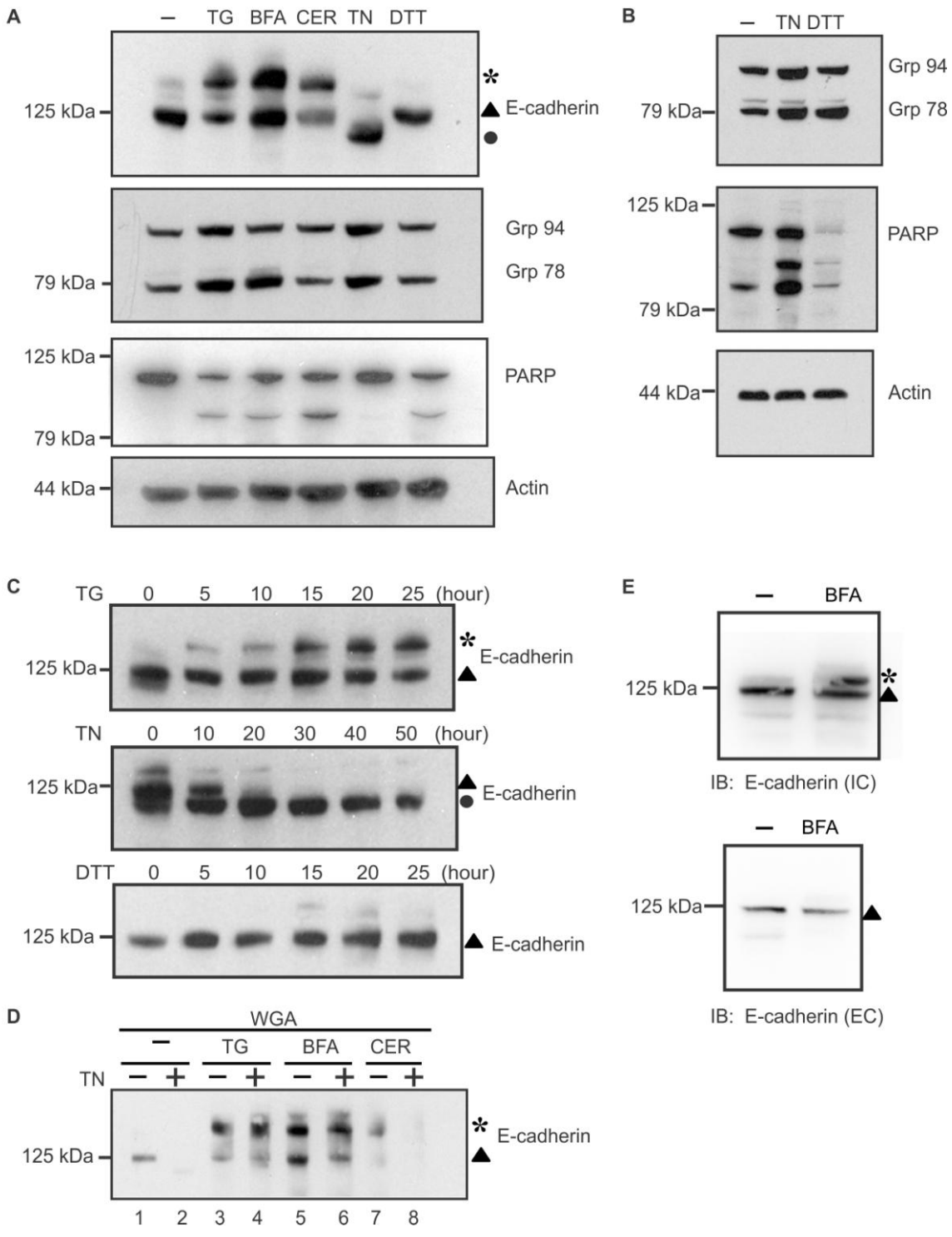

Figure 3.8 Multiple agonists cause E-cadherin modifications. Legend see next page.

(**A**) MCF-7 cells were treated with 400 nM TG for 24 hours, 10 μg/mL BFA for 24 hours, 100 μM CER for 8 hours, 10 μg/mL TN for 24 hours, 10 mM DTT for 6 hours respectively. Cell lysates were analyzed by immunoblotting and detected proteins are indicated on the right of the blots. Note that the modification of the E-cadherin is not directly associated with endoplasmic reticulum stress or apoptosis. TG and DTT both cause apoptosis, but modified E-cadherin only existed in TG treated cells. TN and BFA both cause endoplasmic reticulum stress with increased expression of Glucose-regulatory protein 78 (GRP78), but only the latter causes the E-cadherin modification. (**B**) The expression of Bip/GRP78 and PARP cleavage after extended treatment of MCF-7 cells with TN (10 μg/mL for 48 hours) or DTT (10 mM for 15 hours). (**C**) Detection of E-cadherin modification by immunoblotting after treatment of cells with TG or extended treatment with TN or DTT. (**D**) Lysates prepared from MCF-7 cells treated with DMSO control (-), TG, BFA or CER in the absence or presence of TN were analyzed by WGA binding and immunoblotting for E-cadherin. (**E**) Lysates prepared from MCF-7 cells treated with DMSO control (-) and BFA were analyzed by immunoblotting with an E-cadherin antibody raised against an epitope in the cytoplasmic domain (IC, top panel) or E-cadherin antibody raised against an epitope in the extracellular domain (EC, bottom panel).

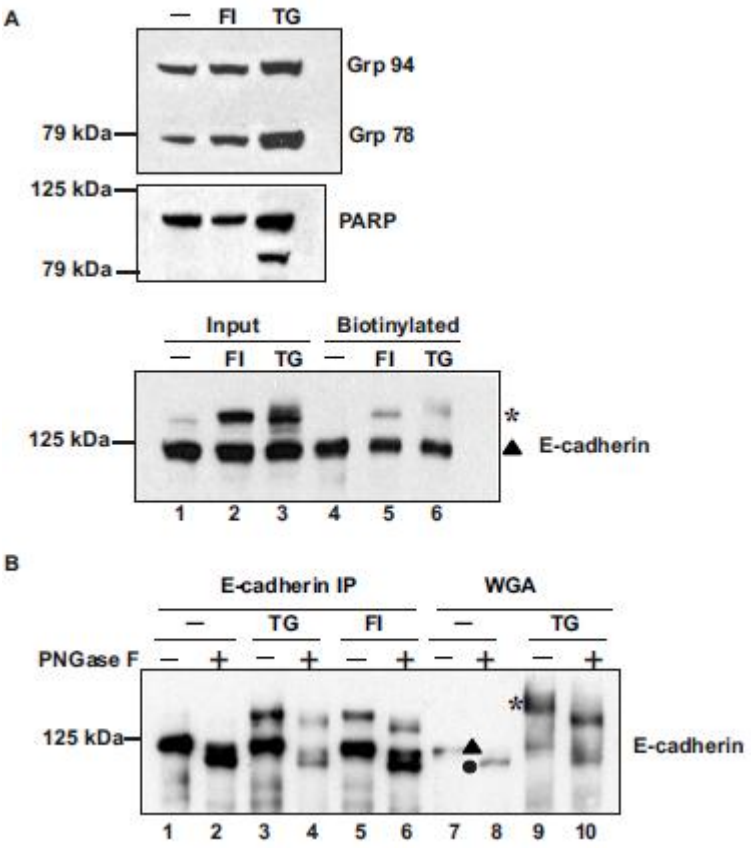

Figure 3.9 The effect of E-cadherin O-GlcNAcylation or pro-region retention on its plasma membrane trafficking.

(**A**) FI does not cause endoplasmic reticulum stress or apoptosis. Cell stress and apoptosis were monitored in cell lysates probed with antibodies to GRP78/GRP94 and PARP as indicated (top two panels). E-cadherin on the surface of MCF-7 cells treated with TG or FI was examined by surface biotinylation and immunoblotting (bottom panel, Biotinylated). The expression of E-cadherin in total cell lysates was shown as control (bottom panel, Input). (**B**) Lysates prepared from MCF-7 cells after treatment with DMSO control (−), TG or FI were immunoprecipitated with E-cadherin antibody or bound to WGA, digested by PNGase F and then analyzed by immunoblotting.

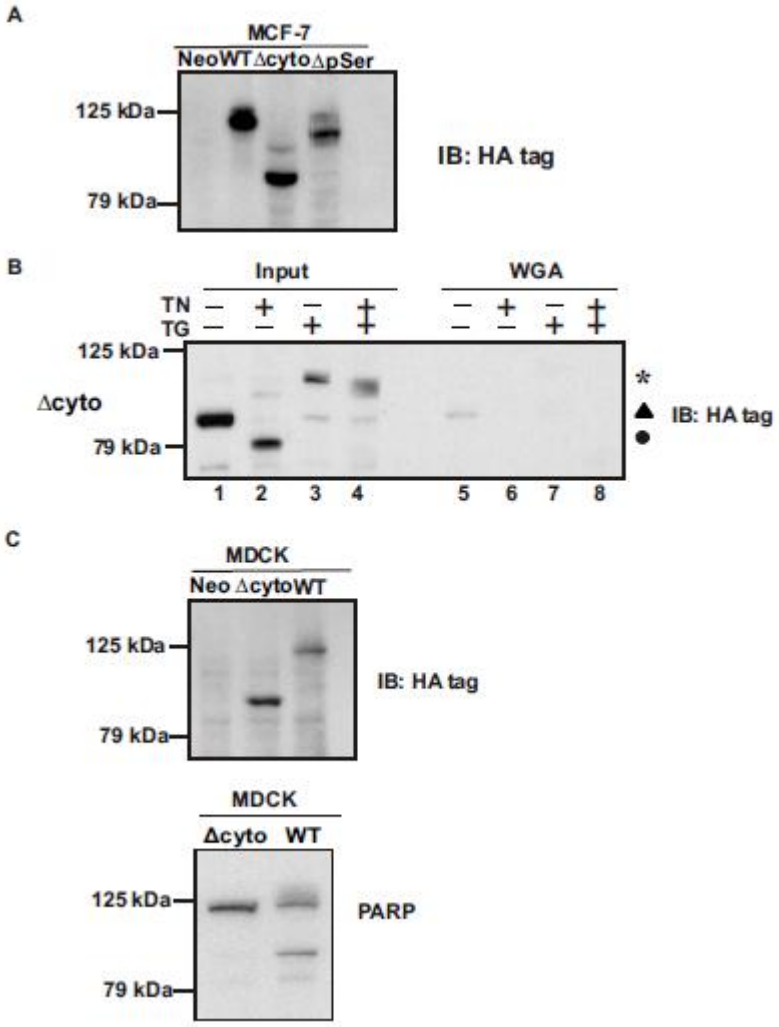

Figure 3.10 Functional evaluation of E-cadherin mutants.
(**A**) The expression profile of HA tagged E-cadherin WT and mutants in MCF-7 cells. Relative expression of HA tagged E-cad WT and E-cadherin mutants in MCF-7 cells was shown by immunoblotting for HA tag. (**B**) E-cadΔcyto is not O-GlcNAcylated in MCF-7 cells. MCF-7 cells expressing HA tagged E-cadΔcyto were treated with DMSO control (−), TN, TG or both for 24 hours. Cell lysates were analyzed by immunoblotting for HA tag (Input) or by WGA binding followed by immunoblotting. (**C**) E-cadΔcyto protects MDCK cells from TG induced apoptosis. The expression of HA tagged E-cadherin in MDCK cells transfected with E-cad WT or E-cadΔcyto was analyzed by immunoblotting for HA tag (top panel). The transfected MDCK cells were treated with TG for 24 hours, and assessed by immunoblotting for PARP (bottom panel).

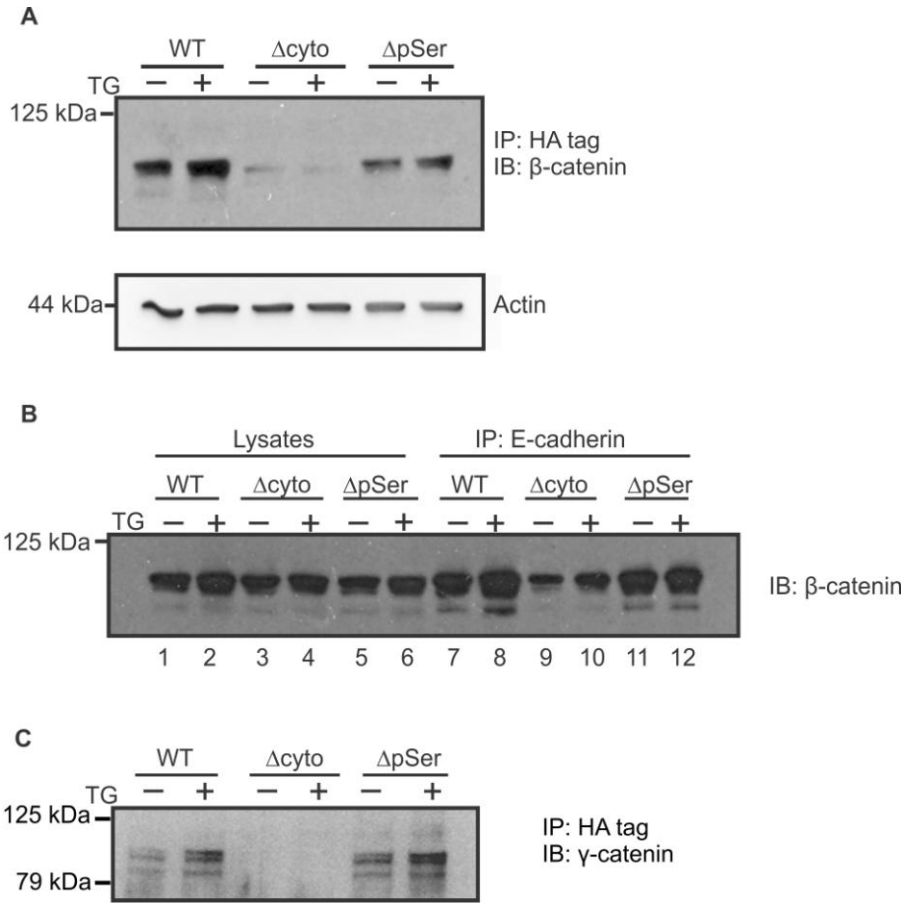

Figure 3.11 The interaction of E-cadherin with β-catenin or γ-catenin is not affected by the deletion of the pSer region.

(**A**) Deletion of the pSer region does not affect the E-cadherin-β-catenin interaction. Cell lysates prepared from the cells stably expressing E-cad WT, E-cadΔcyto and E-cadΔpSer were immunoprecipitated with HA tag antibody and then blotted with β-catenin antibody. Deletion of the cytoplasmic domain (E-cadΔcyto) eliminates this interaction, which is preserved in E-cadΔpSer (top panel). Actin blot was provided as loading control (bottom panel). (**B**) The amount of E-cadherin bound to β-catenin is less in cells transfected with E-cadΔcyto. Cells stably expressing E-cad WT, E-cadΔcyto and E-cadΔpSer were harvested and cell lysates were immunoprecipitated with antibody to extracellular (EC) domain of E-cadherin that detects both endogenous and all three transfected E-cadherin, immunoblotted for β-catenin. The amount of bound β-catenin is decreased in all transfected cells with E-cadΔcyto (lane 9-10) compared to E-cad WT (lane 7-8) or E-cadΔpSer (lane 11-12). (**C**) Deletion of the pSer region does not affect the E-cadherin-γ-catenin interaction. Cell lysates prepared from the cells stably expressing E-cad WT, E-cadΔcyto and E-cadΔpSer were immunoprecipitated with HA tag antibody and then immunoblotted for γ-catenin.

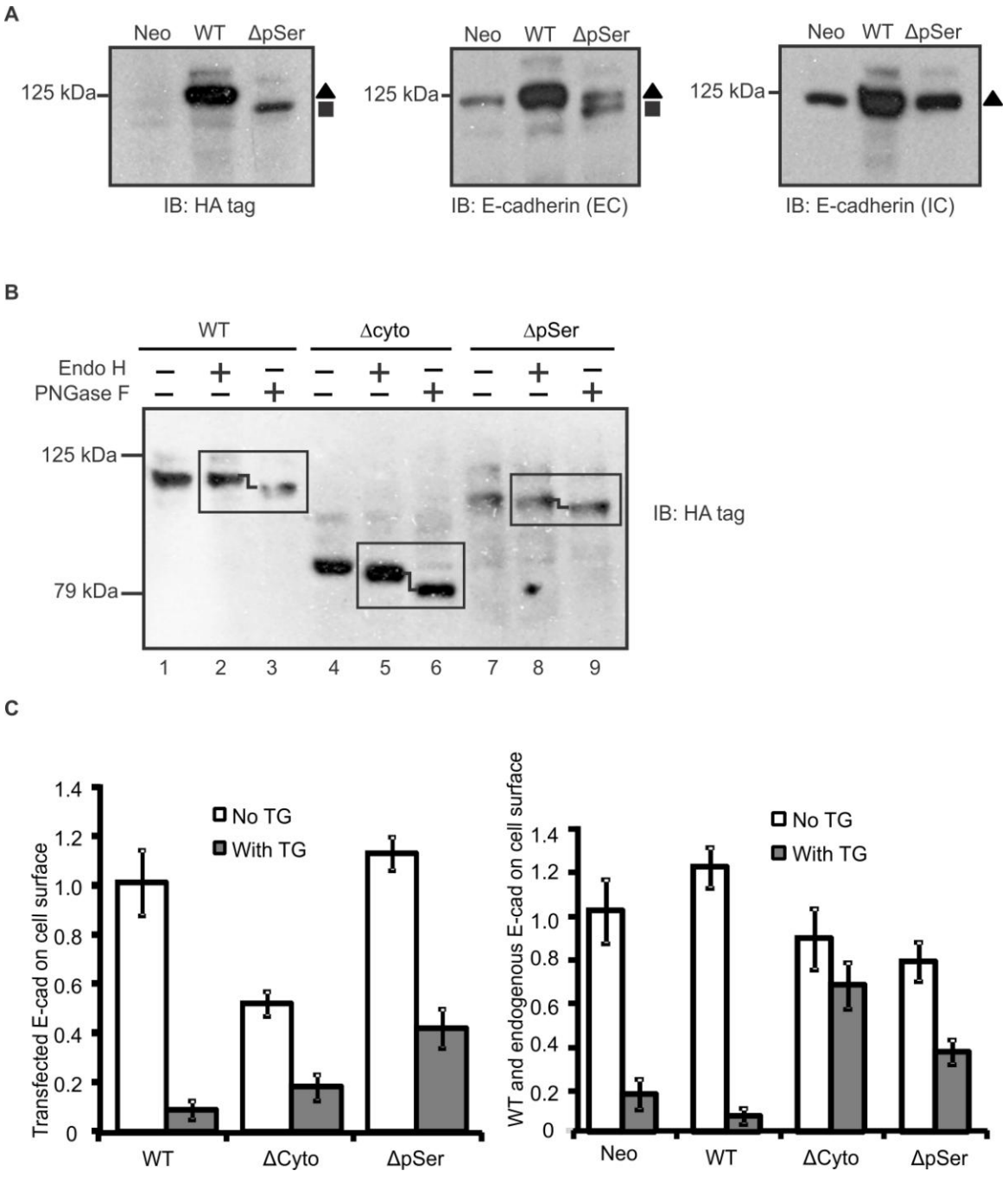

Figure 3.12 Characterization of intracellular transit and cell surface expression of WT E-cadherin and deletion mutants. Legend see next page.

(**A**) The antibody to E-cadherin cytoplasmic domain does not recognize E-cadΔpSer. Total cell lysates of MCF-7 cells expressing control vector (Neo), WT E-cad and E-cadΔpSer were analyzed by immunoblotting with HA tag antibody or antibodies with the epitope on cytoplasmic domain (IC, right panel) or extracellular domain of E-cadherin (EC, middle panel). As expected, the HA antibody detects E-cadΔpSer as a smaller species (■) compared to the transfected WT. The EC antibody recognizes both endogenous (▲) and transfected E-cadΔpSer (■) in E-cadΔpSer cells. Only the endogenous (▲) E-cadherin is recognized by the IC antibody (right panel) (**B**) Lysates from MCF-7 cells expressing HA tagged E-cad WT, E-cadΔcyto and E-cadΔpSer were digested with Endo H or PNGase F and analyzed by immunoblotting for HA tag. (**C**) Measurement of cell surface expression of transfected E-cadherin (representative data as shown in Figure 3.5A) and WT plus endogenous E-cadherin (representative data as shown in Figure 3.5C). Band intensities were measured by densitometry using the histogram feature in image J. Bars represent means ± standard deviation of three independent experiments, $P < 0.05$.

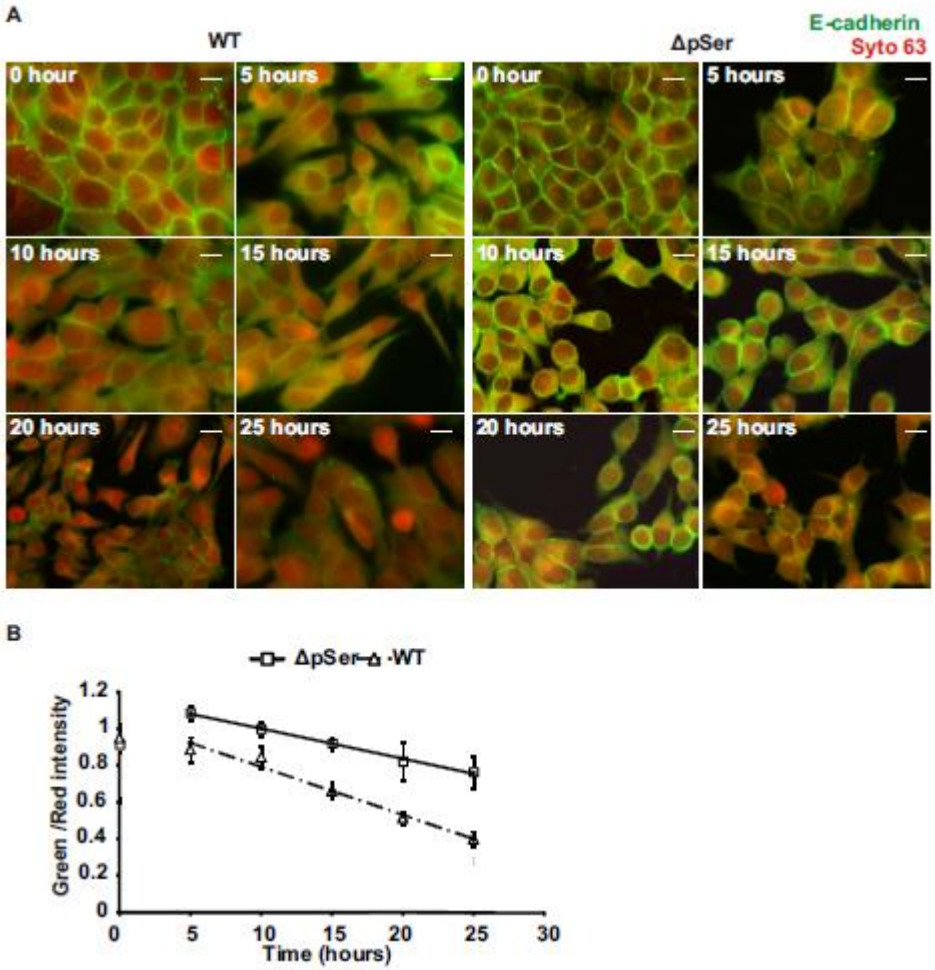

Figure 3.13 E-cadΔpSer maintains E-cadherin surface expression after TG treatment.

(**A**) MCF-7 cells expressing HA tagged E-cad WT and E-cadΔpSer were seeded on coverslips and grown for 24 hours before the following treatment of TG at indicated time points. Cell surface E-cadherin was stained with FITC (green) by immunofluorescence and cytoplasmic dye Syto63 (red) was applied as internal standard. Images were collected by confocal microscopy. Bars, 10 μm. (**B**) Measurement of the change in cell surface expression of E-cadherin after treatment with TG from images depicted in Figure 3.13A of cells transfected with HA tagged E-cad WT or E-cadΔpSer. Graphs represent means ± standard error of three independent experiments, $P < 0.05$.

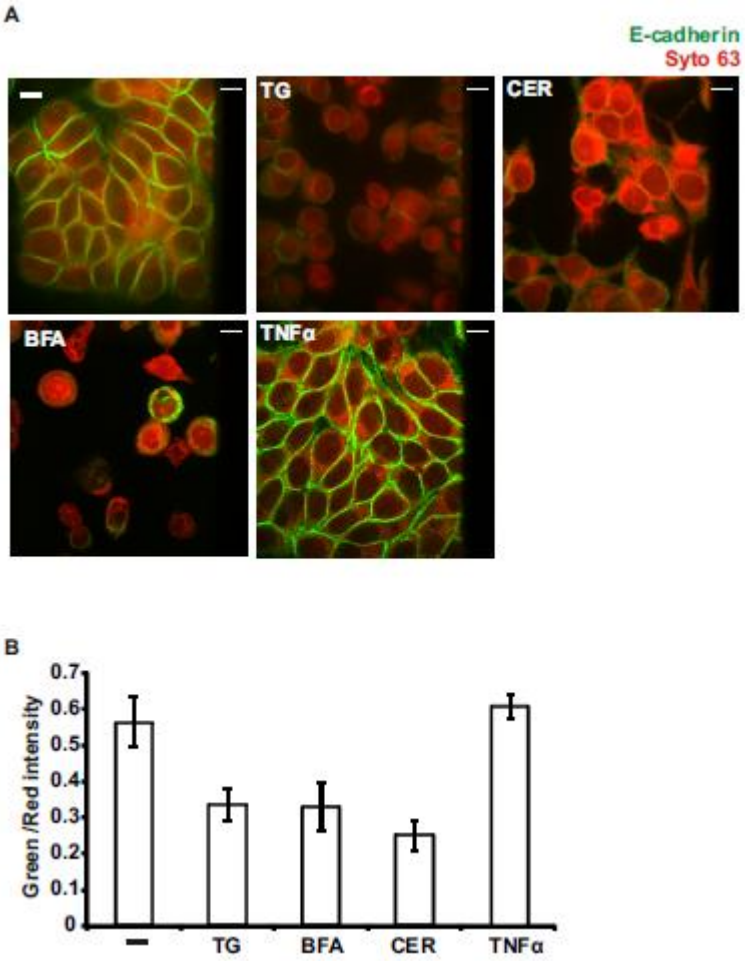

Figure 3.14 The effect of stressors on E-cadherin O-GlcNAcylation and plasma membrane targeting.

(**A**) MCF-7 cells were treated with DMSO control (-), TG, CER, BFA, or 30 ng/mL TNF-α for 24 hours. Cells were fixed and cell surface E-cadherin was stained with FITC (green) by immunofluorescence. The cytoplasmic dye Syto63 (red) was applied as internal standard. Images were collected by confocal microscopy. Bars,10 μm. (**B**) Measurement of cell surface expression of E-cadherin of cells treated as described in Figure 3.14A. Bars represent means ± SD of three independent experiments, $P < 0.05$. Thus the three agents that cause O-glycosylation and/or pre-region retention prevent E-cadherin transport to the cell surface. This is not an invariant feature of cells undergoing programmed cell death as it is not observed in MCF-7 cells treated with TNF-α.

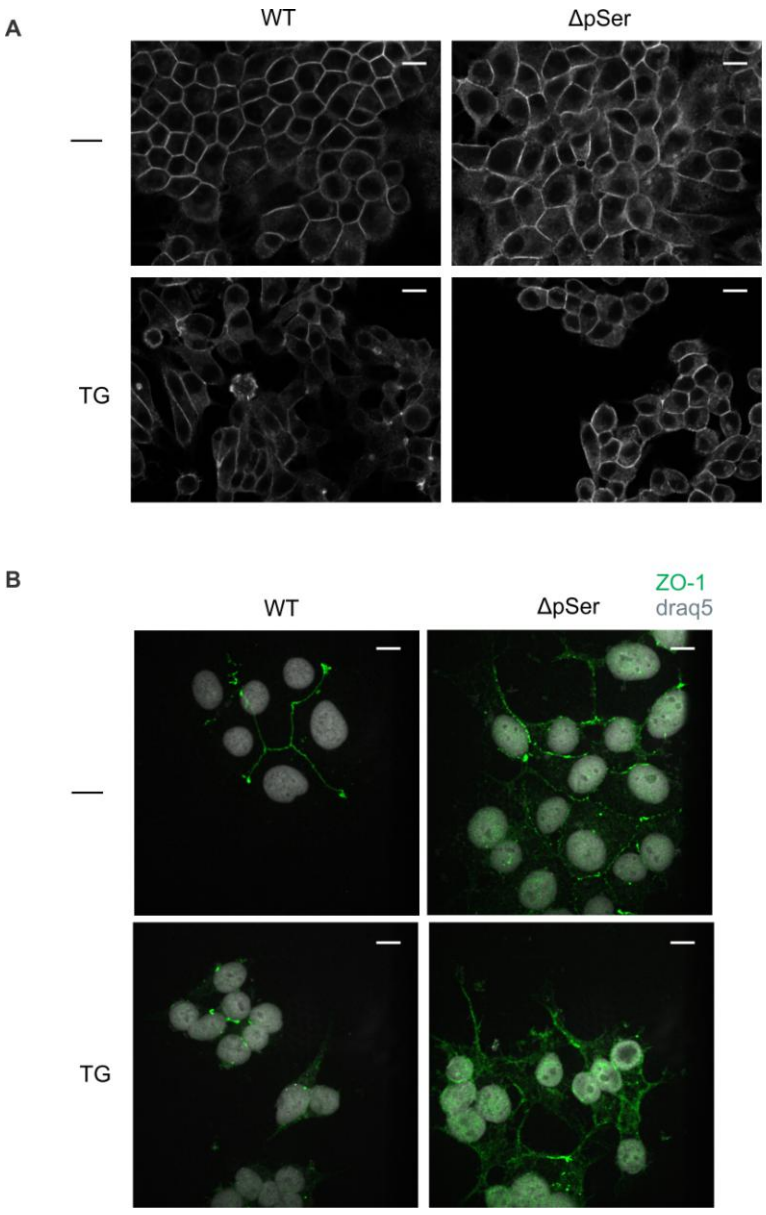

Figure 3.15 The prevention of E-cadherin O-GlcNAcylation maintains the formation of actin cytoskeleton and cell polarity.
(**A**) MCF-7 cells expressing E-cad WT and E-cadΔpSer were treated with TG or DMSO (negative control) for 24 hours. The treated cells were fixed, permeabilized and then stained with Alexa-488-conjugated phalloidin. Bars,15 μm. (**B**) MCF-7 cells expressing E-cad WT and E-cadΔpSer were grown to 50% confluence and then treated with TG or DMSO (negative control) for 24 hours. The cells were fixed, permeabilized and then stained with ZO-1 antibody by immunofluorescence (green) and nuclei were stained with DRAQ5 (grey). Bars,10 μm.

Chapter 4 : The characterization of endoplasmic reticulum-specific cell death in breast cancer cells

4.1 Preface

Although the modifications of E-cadherin that are induced during stress and the consequences of these modifications have been characterized by the experiments described in Chapter 3, the upstream steps that initiate this process are not defined. Our previous experiments indicate that cell death caused by stress conditions that induce E-cadherin modifications is prevented to the same extent by Bcl-2 mutant proteins targeted exclusively to either mitochondria or the endoplasmic reticulum to the same extent. This suggests that these forms of stress are neither initiated nor executed at specific organelles. However, we subsequently discovered a unique type of cell death which is prevented exclusively by Bcl-2 localized on the endoplasmic reticulum. In this chapter, we will examine this novel pathway and compare it with other stress conditions involving the endoplasmic reticulum, including those that elicit the E-cadherin modifications described in Chapter 3.

4.2 Introduction

The endoplasmic reticulum is primarily responsible for the synthesis and folding of secreted and membrane-bound proteins, as well as the biosynthesis of lipids and the storage of calcium. The endoplasmic reticulum has also emerged as a central player in other cellular responses including cell stress and programmed cell death pathways. Bcl-2 family members play an important role in regulating programmed cell death from this location (Hetz, 2007; Oakes, et al., 2006).

The anti-apoptotic protein Bcl-2, the prototype for the Bcl-2 family, is anchored to membranes by a carboxyl-terminal hydrophobic sequence called a tail-anchor. Unlike many other tail-anchor proteins that are targeted to a single subcellular location, Bcl-2 is localized to both the endoplasmic reticulum and the outer mitochondrial membrane in mammalian cells (Leber, et al., 2010; Zhu, et al., 1996). Over the past several years, extensive work has been done to elucidate the process whereby members of the Bcl-2 protein family at the mitochondrial outer membrane regulate the decision phase that commits cells to apoptosis (Shamas-Din, et al., 2011).

When located at the endoplasmic reticulum, Bcl-2 is a constituent of complexes with binding partners including Bap31, IP3R, BIK and SERCA (Leber, et al., 2010). Bcl-2 located at the endoplasmic reticulum has been reported to bind to the essential autophagy protein Beclin 1 and to inhibit Beclin 1- dependent starvation-induced autophagy (Pattingre, et al., 2005). Recently it has been reported that NAF-1 protein is required for Bcl-2 to antagonize the autophagy regulatory protein Beclin 1, suggesting that regulation of autophagy involves a multiprotein complex at the endoplasmic reticulum (Chang, et al., 2010).

Furthermore, Bcl-2 at the endoplasmic reticulum also regulates other modes of apoptosis including caspase activation through the interaction with Bap31, and Ca^{2+} signaling through the interaction with IP3R (Oakes, et al., 2006; Rong & Distelhorst, 2008). Furthermore other Bcl-2 family proteins also regulate apoptosis at this organelle as they are modified by signals emanating from the endoplasmic reticulum e.g. the pro-

apoptotic BH3 proteins Puma and Noxa are important mediators of apoptosis initiated by UPR (Hetz, 2007; Oakes, et al., 2006).

However, all of these pathways are also inhibited by Bcl-2 proteins located at mitochondria, suggesting these initiating stimuli eventually transmit pro-apoptotic signals to mitochondria and rely on interactions at that organelle to commit cells to apoptosis. To date, there is no known cell death pathway that is mediated primarily by events at the endoplasmic reticulum. Here we show that estrogen deprivation in estrogen receptor-positive breast cancer cell lines is a strong candidate for such a process. Aside from its importance in broadening our understanding of the mechanisms of cell death, the characterization of this pathway, which is involved in hormonally regulated apoptosis in breast cancer, may reveal novel drug targets for cancer therapeutics.

4.3 Results

Cell death induced by growth of cells in medium depleted of growth factors is prevented by Bcl-2 at the endoplasmic reticulum.

To discover a form of cell death which is prevented by Bcl-2 specifically at the endoplasmic reticulum, we chose MCF-7 cells for our initial studies, as this cell line has the important feature whereby the endogenous Bcl-2 levels can be dramatically reduced by growth in estrogen depleted medium (Fiebig, et al., 2006; Teixeira, Reed, & Pratt, 1995).This occurs because Bcl-2 expression is induced by 17β-Estradiol via two estrogen-responsive elements present in the coding sequence (Perillo, Sasso, Abbondanza, & Palumbo, 2000). Therefore as a convenient experimental tool, growth of MCF-7 cells in phenol red-free medium supplemented with Charcoal Stripped Bovine Serum (CSBS) for 5 days reduces the expression of endogenous Bcl-2 by depleting estrogen (and some other growth factors) from the serum (Fiebig, et al., 2006; Zhu, et al., 2001). By using these conditions, MCF-7 cells transfected with plasmids expressing Bcl-2 mutants either exclusively localized at the mitochondria (Bcl2-ActA) or the endoplasmic reticulum (Bcl2-cb5) can be used to examine the importance of organellar location.

For the cell lines we used in subsequent studies, we first confirmed that expression levels of wild type Bcl-2 (Bcl2-WT) and two Bcl-2 mutant proteins were similar (Figure 4.1A, top panel, lane 2-4). As expected, after estrogen deprivation, the endogenous Bcl-2 is expressed at lower levels than the transfected proteins as assessed by an overexposed immunoblot (Figure 4.1A, top right blot, compare lane 1 and lane 2-4). Annis et al. reported that Bcl2-cb5 inhibited cell death when a mitochondrial permeability transition preceded cytochrome c release, which provides the first hint that there might be a different pathway from the one in which commitment to cell death is mediated by proteins at the mitochondria (Annis, et al., 2001). Since Bcl2-ActA and Bcl2-cb5 are known to be as active as Bcl2-WT expressed at their corresponding organelle targets, with respect to protecting against apoptotic stimuli that are organelle non-specific (Annis et al, 2001), this model system should allow us to investigate this unknown pathway.

In pilot studies that led to this series of investigations, we had noticed that cells expressing Bcl2-cb5 appeared healthier than cells expressing Bcl2-Acta or Bcl2-WT when grown in CSBS. To examine this effect in more detail, we extended the growth time in CSBS from 5 days to 10 days (Figure 4.1B-G). Phase contrast micrographs demonstrated that MCF-7 cells expressing Neo, Bcl2-ActA and Bcl2-WT undergo loss of adhesion (become round) after growth in CSBS for 10 days while MCF-7 cells expressing Bcl2-cb5 remain unchanged (Figure 4.1B).

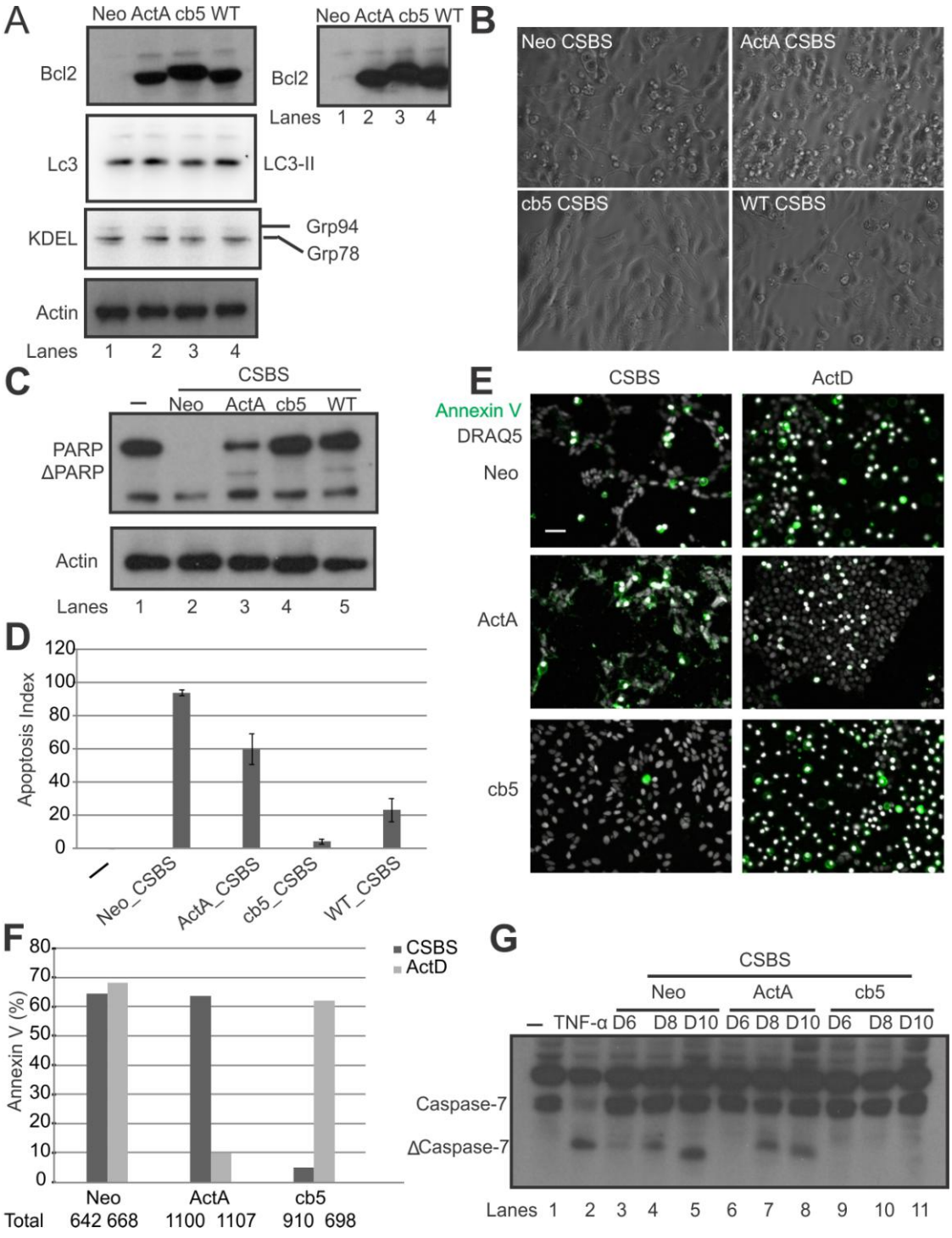

Figure 4.1 Growth in CSBS for 10 days led to endoplasmic reticulum-specific cell death in MCF-7 cells. Legend see next page.

(**A**) Cell lysates containing 20 μg of protein from MCF-7 cells transfected with vector control (Neo), wild type Bcl-2 protein (Bcl2-WT), mitochondria localized mutant (Bcl2-ActA) or endoplasmic reticulum localized mutant (Bcl2-cb5), as indicated above the lanes, were immunoblotted for: Bcl-2 with short exposure (top left blot) and long exposure (top right blot); the autophagy marker LC3 (the second blot); and the endoplasmic reticulum chaperone GRP78/94 (the third blot). An actin blot was used to control for equal protein loading in each lane (bottom blot). (**B**) Phase contrast microscopic images of MCF-7 cells expressing vector control (Neo), Bcl2-ActA, Bcl2-cb5 and Bcl2-WT grown in the phenol red-free medium supplemented with Charcoal Stripped Bovine Serum (CSBS) for 10 days. (**C**) Transfected MCF-7 cells expressing vector control (Neo), Bcl2-ActA, Bcl2-cb5 and Bcl2-WT were grown in CSBS for 10 days and then the cell lysates were immunoblotted for PARP. The migration position of the 89 kDa PARP fragment diagnostic of caspase cleavage is indicated to the left of the blots (ΔPARP, top panel). An actin immunoblot used as a control for equal protein loading in each lane is shown in the bottom panel. (**D**) Quantitative determination of PARP cleavage and degradation in MCF-7 cells expressing Neo, Bcl2-ActA, Bcl2-cb5 and Bcl2-WT following growth in CSBS for 10 days. The PARP antibody used for immunoblotting in Figure 4.1C does not recognize cleavage products generated by other proteases activated during apoptosis. Therefore, both PARP cleavage and degradation are combined into a single apoptosis index determined by measuring the band intensities for the116 kDa full-length PARP in untreated cells (−), and in cells grown in CSBS indicated above the lanes, by analysis with ImageJ software. Apoptosis Index= 100X ($1-F_{treated}/F_{untreated}$) (**E**) MCF-7 cells expressing Neo, Bcl2-ActA and Bcl2-cb5 were grown in CSBS for 10 days or treated with 20nM Actinomycin D (ActD) for 24 hours and then stained with Annexin V (green) and DRAQ5 (white). Representative images are shown. Bar, 30 μm. (**F**) The percentage of Annexin V-positive cells in Figure 4.1E determined by image quantification and supervised classification. (**G**) Cell lysates of MCF-7 cells expressing Neo, Bcl2-ActA and Bcl2-cb5 treated with CSBS at day 6 (D6), day 8 (D8) and day 10 (D10) were analyzed by immunoblotting for caspase-7. MCF-7 cells treated with DMSO control (-) or 33 ng/mL TNF-α/10 μg/mL cycloheximide (TNF-α) for 24 hours were applied as negative and positive controls for apoptosis.

Consistent with these morphological changes, inspection of PARP immunoblots revealed disappearance of full-length PARP in Neo control cells (Figure 4.1C, top panel, lane 2) and disappearance and cleavage of full-length PARP is shown in cells expressing Bcl2-ActA (Figure 4.1C, top panel, lane 3) compared to intact PARP in Bcl2-cb5 cells (Figure 4.1C, top panel, lane 4). Accordingly, the quantitative determination of combined PARP cleavage and degradation indicates a significant decrease of PARP in cells

expressing Neo or Bcl2-ActA (Figure 4.1D). The apoptosis index is approximately 90% and 60% in cells expressing Neo or Bcl2-ActA, respectively, after growth in CSBS for 10 days. By comparison, the apoptosis index is around 20% and less than 10% in cells expressing Bcl2-WT and Bcl2-cb5 respectively (Figure 4.1D).

In agreement with the PARP data, over 60% of cells expressing Neo or Bcl2-ActA became Annexin V-positive (green) after growth in CSBS (Figure 4.1E left panel and F). Comparatively, less than 10% Bcl2-cb5 cells were Annexin V-positive (Figure 4.1F). However, when cells were exposed to actinomycin D (ActD) which induces a form of mitochondria specific cell death (Hoye, Davoren, Wipf, Fink, & Kagan, 2008), only ~10% of Bcl2-ActA cells were Annexin V-positive compared to >60% in Bcl2-cb5 cells (Figure 4.1E right panel and F). Therefore Bcl2-ActA is functional but does not protect cells from CSBS-induced apoptosis.

MCF-7 cells lack caspase-3 due to a 47-base pair deletion in the caspase-3 gene (Janicke, Sprengart, Wati, & Porter, 1998), but undergo mitochondrial-dependent apoptosis via caspase-7 activation (Twiddy, et al., 2006). Caspase-7 is processed/cleaved by the Apaf-1-caspase-9 apoptosome from procaspase-7 into its active form (Twiddy, et al., 2006). Cleavage of a small amount of caspase-7 was detected in cells expressing Neo or Bcl2-ActA at day 8 and day 10 of growth in CSBS (Figure 4.1G, lane 4-5 and lane 7-8), but not in cells expressing Bcl2-cb5 (Figure 4.1G lane 9-11).

Since all the analyses above were performed after growth in CSBS for 10 days, we further extended the time period to 21 days and enumerated cells attached to the plate to assess the duration of the protective effect of Bcl2-cb5. The cell count revealed almost complete loss of attachment of cells expressing Neo, Bcl2-ActA and Bcl2-WT at this time point (Figure 4.2A). By contrast, not only did Bcl2-cb5 cells remain attached, they also increased in number compared to the input before being subjected to CSBS (Figure 4.2A) thus confirming the profound effect of Bcl2-cb5 against this form of cell death.

We then sought to determine if this specific pathway for cell death is shared by other known stimuli that elicit forms of endoplasmic reticulum stress (Figure 4.2B).

Based on our previous experiments we examined TG treatment (which causes O-glycosylation on E-cadherin in the endoplasmic reticulum as shown in Chapter 3) and TG combined with TN (another stressor than inhibits N-glycosylation) . Other stimuli previously reported to elicit endoplasmic reticulum stress were also tested, including glucose deprivation (Qu, et al., 2004), serum starvation (Annis, et al., 2001), UV light (Wu, et al., 2002) and CER (Annis, et al., 2001). Unlike CSBS, none of these conditions were protected exclusively by Bcl2-cb5 (Figure 4.2B and C).

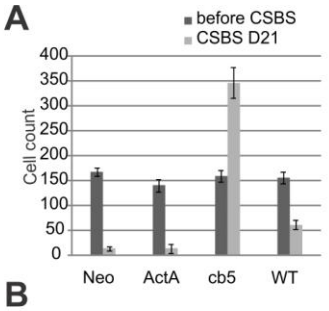

B

Conditions tested	Protected by ActA and cb5	Protected only by cb5
CSBS		v
Serum starvation	v	
No glucose	v	
TG	v	
TN+TG	v	
CER	v	
UV light	v	

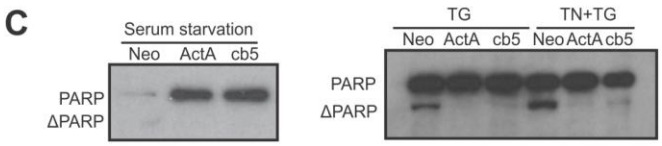

Figure 4.2 The protection of Bcl2-ActA and Bcl2-cb5 against cell death induced by CSBS compared with other tested conditions.
(**A**) Cell count of MCF-7 cells expressing Neo, Bcl2-ActA and Bcl2-cb5 before or after growth in CSBS for 21 days. (**B**) Summary of the response of MCF-7 cells expressing Neo, Bcl2-ActA and Bcl2-cb5 to different cell stressors. (**C**) MCF-7 cells expressing Neo, Bcl2-ActA and Bcl2-cb5 were treated with serum starvation for 48 hours, 400 nM TG for 24 hours or 10 μM TN plus 400 nM TG for 24 hours. Cell lysates were analyzed by immunoblotting for PARP.

Supplementation with 17β-Estradiol but not insulin prevents the CSBS-induced cell death

The data presented above suggest that charcoal stripping removed components from the serum required for viability of MCF-7 cells. The death of MCF-7 cells occurring as a consequence of the charcoal stripping of the serum in the growth medium is blocked by Bcl2-cb5 but not Bcl2-ActA. Therefore, we conclude that this pathway is an endoplasmic reticulum-specific cell death pathway. What critical component(s) is removed by this treatment? Previous reports (Dixit & Chang, 1984; Welshons, Grady, Engler, & Judy, 1992) indicate that activated charcoal treatment removes two separate factors that known to be relevant for breast cancer cell proliferation: 17β-estradiol (Pattarozzi, et al., 2008) and insulin (Chappell, et al., 2001). Therefore, we supplemented CSBS with 17β-estradiol or insulin and examined whether the cells were rescued from death.

Interestingly supplementation of 17β-estradiol decreased the Annexin V positivity from > 60% to <10% in Neo control cells, with a similar change noted in Bcl2-ActA expressing cells as well (Figure 4.3A middle panel and B). By contrast, insulin had no effect (Figure 4.3A right panel and B). This suggests that 17β-estradiol is the missing component in the CSBS media and that loss of estrogen signaling activates the endoplasmic reticulum-specific cell death pathway.

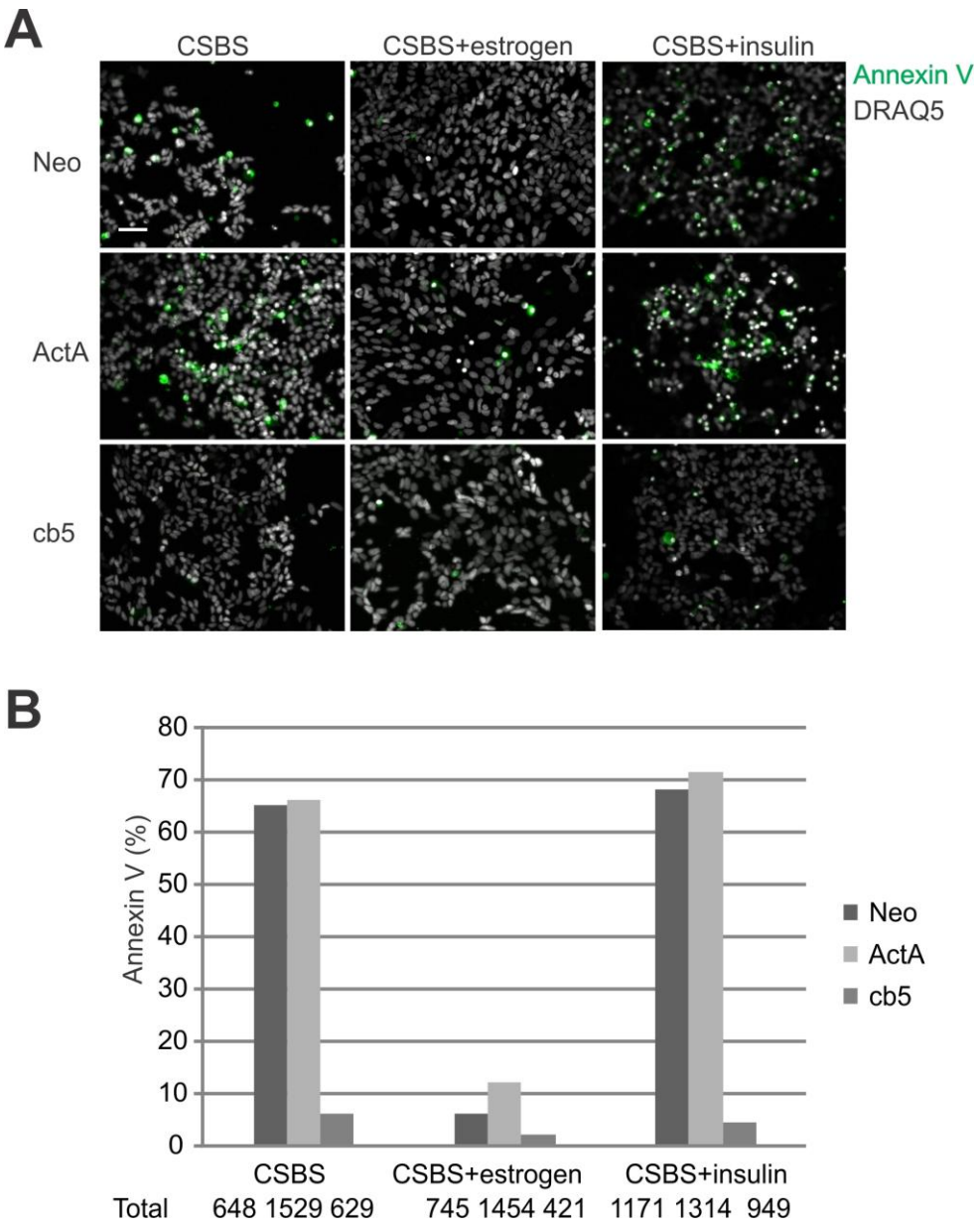

Figure 4.3 The supplementation of estrogen in CSBS prevents CSBS-induced cell death.

(**A**) MCF-7 cells expressing Neo, Bcl2-ActA and Bcl2-cb5 were treated with CSBS in the presence of no additives (−) or supplemented with 10 nM 17β-estradiol or 100 nM insulin for 10 days and then stained with Annexin V (green) and DRAQ5 (grey). Representative images are shown. Bar, 30 μm (**B**) The percentage of Annexin V-positive cells in Figure 4.3A quantified by image segmentation and classification as described in Chapter 2. The total cell counts are shown below the corresponding columns.

Characterization of CSBS-induced cell death parameters in MCF-7 cells

As this form of cell death differs from any previously reported mode of cell death we needed to determine how many components it shares with other well-recognized types of cell death. The expression of either Bax or Bak is required for almost all types of apoptotic cell death (Wei, et al., 2001; Zong, Lindsten, Ross, MacGregor, & Thompson, 2001). Conveniently there are monoclonal antibodies available that recognize specific epitopes in either Bax or Bak that are only detectable after the proteins have been activated (Griffiths, et al., 1999; Lalier, et al., 2007). Thus, these were logical candidates to investigate. Furthermore cytochrome c is released from the intermembrane space of mitochondria at the early stage of some forms of cell death which are inhibited only by Bcl-2 localized at the mitochondria (Q. Chen, Gong, & Almasan, 2000) and the cytochrome c release occurs at the end stage of some forms of cell death which are inhibited by both Bcl2-ActA and Bcl2-cb5 (Annis, et al., 2001; Jimbo, et al., 2003; Kroemer, Dallaporta, & Resche-Rigon, 1998; Tsujimoto & Shimizu, 2007). Therefore we analyzed the activation of either Bax or Bak and cytochrome c release in all the cell lines by immunofluorescence using the antibodies 6A7 for activated Bax (red channel of Figure 4.4A), the AM03 antibody for activated Bak (red channel of Figure 4.4B) and cytochrome c (green channel in Figure 4.4 A and B). The quantification of the experiment is shown in Figure 4.5B (Left panel: activated Bax/Cytochrome c release; Right panel: activated Bak/Cytochrome c release). This analysis indicated that while growth in CSBS kills both Neo control and Bcl2-ActA cells, different mediators are active. This is evident as the cytochrome c release as an end point of mitochondrial dysfunction is roughly comparable (~50% of Neo control cells and ~60% in Bcl2-ActA), activated Bax and/or Bak mediates this effect in the Neo control cells (50% 6A7 positive and 60% are AM03 positive) whereas these markers are essentially negative (<10% for either 6A7 or AM03) in Bcl2-ActA cells (Figure 4.5B). These data suggest that under normal circumstances activation of mitochondrial Bax and/or Bak contributes to cell death in MCF-7 cells grown in CSBS, but that this step is inhibited by Bcl2-ActA (Figure 4.5B). Nevertheless

Bcl2-ActA cells still die, and this cell death is accompanied by significant levels of cytochrome c release (Figure 4.5B). Whether this is due to the activation of a small amount of Bax and/or Bak that is too little to be detected in our assay or is due to the cell death that is Bax/Bak independent cannot be concluded from these studies. However, it is clear that the "default" form of cell death that is elicited by CSBS likely involves the canonical form of mitochondrial apoptosis when this is not inhibited. Here the death of Bcl2-ActA expressing cells in which this default process was inhibited by Bcl2-ActA uncovered an independent and equally potent parallel pathway (Figure 4.5B). This is highlighted by further differences: in response to growth in CSBS, Neo control cells become detached from the dish much more quickly and completely than Bcl2-ActA cells. Thus many Neo cells are removed during the washing steps of immunostaining. As a consequence, the quantitative determination of 6A7/Bak/cytochrome c release is an underestimate for Neo control cells. This might explain the difference in the number of dead cells in the Annexin V assay (Figure 4.1F) compared to cytochrome c staining as washing steps are required for cytochrome c staining but not for the Annexin V assay (Figure 4.5B).

It may appear paradoxical that cytochome c release is prevented by Bcl-2 targeted to the endoplasmic reticulum but not the mitochondria. However, our laboratory has previously reported that in Rat-1 fibroblasts some cell death signals are inhibited by Bcl2-cb5 that trigger loss of the mitochondrial membrane potential ($\Delta\psi_m$) thereby causing the mitochondrial permeability transition (Kroemer, 1999; Kroemer, et al., 1998). Thereafter the mitochondrial outer membrane will allow release of cytochome c, but not through the canonical Bax/Bak mediated pore (Annis et al, 2001). To determine whether cell death induced by CSBS also disrupts membrane potential across the mitochondrial inner membrane, cells were stained with potentiometric fluorescence probe tetramethylrhodamine ethyl ester (TMRE) after growth in CSBS for 10 days (Figure 4.4C). This dye provides a convenient measurement of stained with potentiometric fluorescence changes in $\Delta\psi_m$ in vitro after isolation or in living cells. Indeed, the results

indicate that mitochondrial membrane potential is lost in cells expressing Neo and Bcl2-ActA but not in Bcl2-cb5 cells (Figure 4.4C). Thus by three separate assays of cell death, the cytotoxic effects of CSBS were blocked by Bcl2-cb5 but not Bcl2-ActA.

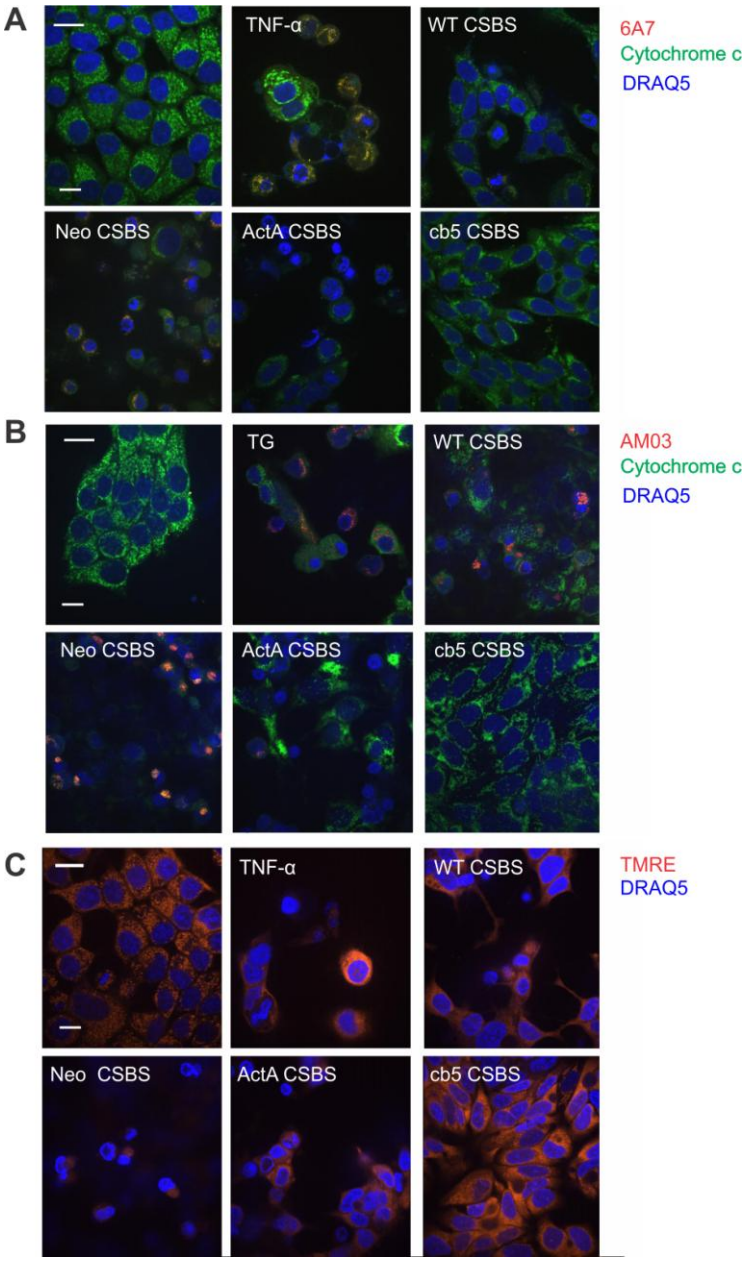

Figure 4.4 Bax/Bak activation and mitochondrial membrane potential changes during CSBS-induced cell death in MCF-7 cells. Legend see next page.

(**A**) MCF-7 cells expressing Neo, Bcl2-ActA, Bcl2-cb5 and Bcl2-WT were grown in CSBS for 10 days and then the immunofluorescent signal for activated Bax (6A7) (red) and cytochrome c (green) were recorded. Nuclei were stained with DRAQ5 (blue). MCF-7 cells treated with DMSO control (-) or 33 ng/mL TNF-α/10 μg/mL cycloheximide (TNF-α) for 24 hours were applied as negative and positive controls. Bar, 10 μm. (**B**) MCF-7 cells expressing Neo, Bcl2-ActA, Bcl2-cb5 and Bcl2-WT were grown in CSBS for 10 days and then the immunofluorescent signal for activated Bak (AM03) (red) and cytochrome c (green) was recorded. Nuclei were stained with DRAQ5 (blue). MCF-7 cells treated with DMSO control (-) or 400 nM TG for 24 hours were applied as negative and positive controls. Bar, 10 μm. (**C**) MCF-7 cells expressing Neo, Bcl2-ActA, Bcl2-cb5 and Bcl2-WT were grown in CSBS for 10 days and mitochondrial potential was assessed by TMRE staining (red). Nuclei were stained with DRAQ5 (blue). MCF-7 cells treated with DMSO control (-) or 33 ng/mL TNF-α/10 μg/mL cycloheximide (TNF-α) for 24 hours were applied as negative and positive controls. Bar, 10 μm.

The protective function Bcl2-cb5 against CSBS-induced cell death is abolished by the addition of ABT-737

Since Bcl2-cb5 blocks the cell death signal and maintains cell survival, this suggests that Bcl2-cb5 inhibits this pathway by directly or indirectly binding to at least one activator of the pathway. One activator likely activates Bax and or Bak and is inhibited by Bcl2-ActA also. The other activator is not inhibited by Bcl2-ActA and leads to loss of mitochondrial transmembrane potential and other manifestations of the cell death pathway not inhibited by Bcl2-ActA. As the function of anti-apoptotic Bcl-2 family members is mediated by binding the BH3 region of pro-apoptotic family members (Shamas-Din, et al., 2011; Youle & Strasser, 2008), we investigated this possibility by using a small-molecule inhibitor approach. ABT-737 developed by the pharmaceutical company Abbott, is a peptidomimetic that is based on the BH3 region of the sensitizer BH3 protein Bad (Bruncko, et al., 2007; Oltersdorf, et al., 2005; Shamas-Din, et al., 2011). Of further relevance to our investigations, ABT-737 has also been reported to displace Beclin 1 from Bcl-2 at the endoplasmic reticulum to induce autophagy (Maiuri, Criollo, et al., 2007). We reasoned that if a protein containing a BH3-like region mediates the cell death elicited by CSBS, then the protective effect of Bcl2-cb5 should be abolished by the addition of ABT-737. Interestingly, simultaneous addition of ABT-737

at the beginning of cell culture medium change to CSBS markedly enhanced the cell percentage of 6A7/Cytochrome c release in Bcl2-cb5 cells from less than 10% to over 60% (Figure 4.5B). Furthermore, the percentages of 6A7/Cytochrome c release in all the four cell lines become synchronized after the addition of ABT-737 (Figure 4.5B). This is not due to a general toxic effect of ABT-737 on MCF-7 cells under our experimental conditions as there is no evidence of Bax activation or cytochrome c release in cells treated with ABT-737 alone (Figure 4.5B). ABT-737 is likely killing the cells via the activator that is normally inhibited by Bcl2-ActA since cells expressing Bcl2-cb5 and Bcl2-ActA die equivalently under these conditions.

Therefore, as the long-term protective effect of Bcl2-cb5 is completely eliminated by the BH3 mimetic, it is likely that this protection is mediated by binding to a protein located at the endoplasmic reticulum that contains a BH3 region.

CSBS-induced cell death in several estrogen receptor-positive breast cancer cell lines

To rule out the possibility that these observations are specific to MCF-7 cells, we examined whether CSBS killed other estrogen receptor-positive breast cancer cell lines including T47D, CAMA1, MDA-MB-361, MDA-MB-134, BT474 and MDA-MB-415, and whether the effect was similarly abrogated by the addition of 17β-estradiol. In the absence of 17β-estradiol, loss of adhesion (cell rounding observed with phase contrast microscopy) was noted in T47D, CAMA1, MDA-MB-361and MDA-MB-134 cells (Figure 4.6A estrogen(-)). In the presence of 17β-estradiol, these morphological changes were reversed in T47D, CAMA1 and MDA-MB-361 (Figure 4.6A estrogen(+)). This suggests T47D, CAMA1 and MDA-MB-361 cells may also be sensitive to the cell death pathway activated by the depletion of estrogen. As expected, growth in CSBS has no effect on the estrogen receptor-negative breast cancer cell line MDA-MB-231 cells (Figure 4.6A).

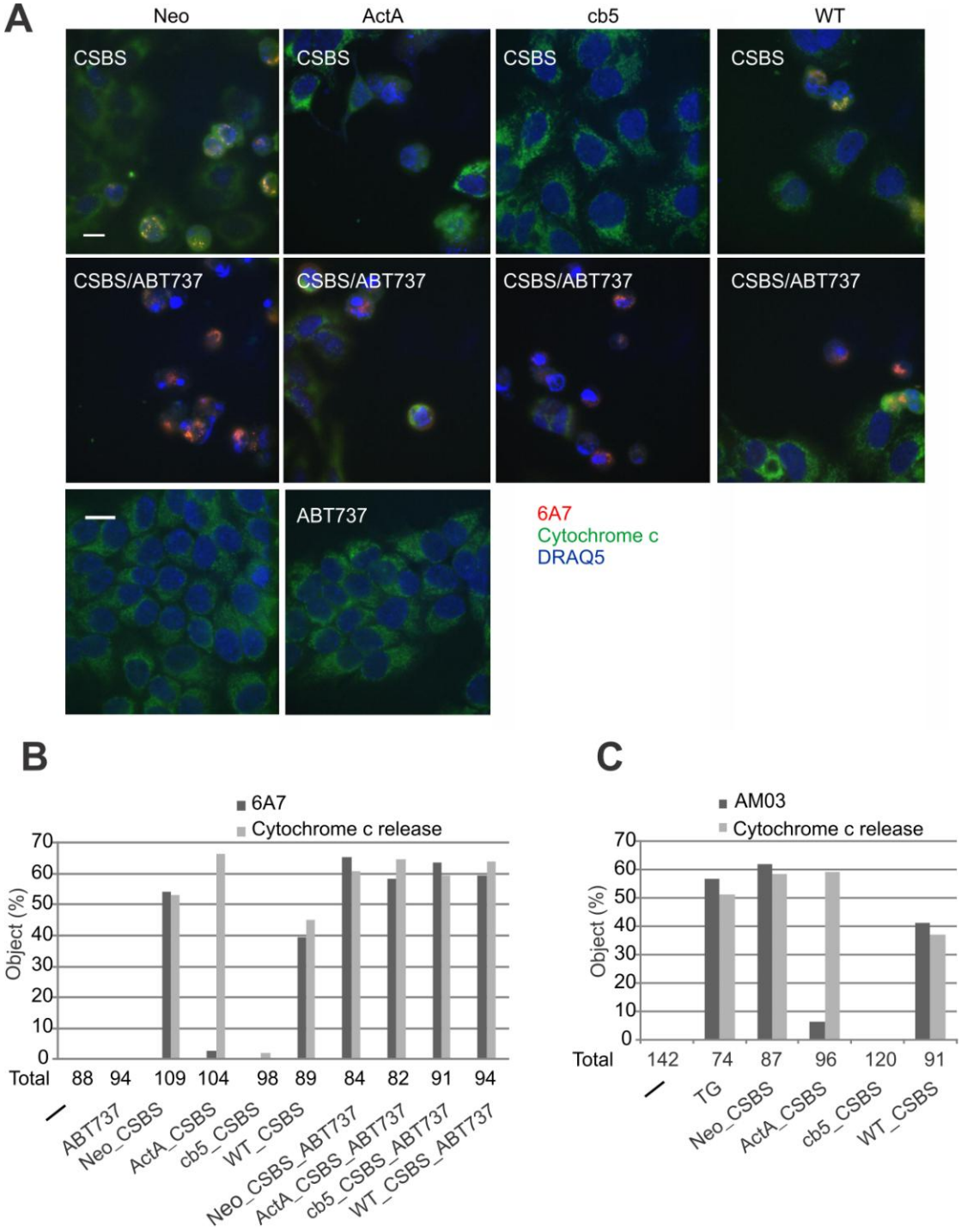

Figure 4.5 Bcl2-cb5 protects against CSBS-induced cell death and the addition of ABT-737 abolishes the protective effect of Bcl2-cb5 and Bcl2-ActA. Legend see next page.

(**A**) MCF-7 cells expressing Neo, Bcl2-ActA, Bcl2-cb5 and Bcl2-WT were grown in CSBS for 10 days in the presence or absence of 5 μM ABT-737 then the immunofluorescent signal for activated Bax (6A7) (red) and cytochrome c (green) was recorded. Nuclei were stained with DRAQ5 (blue). Representative images are shown. Bar, 10 μm. (**B**) Quantitative determination of the percentage of activated Bax (6A7)/cytochrome c release positive cells in Figure 4.5A by image segmentation and classification are described in Chapter 2. Cytochrome c intensity was quantified for each object and classified by automated analysis as having decreased intensity of cytochrome c staining. The total cell counts are shown below the corresponding columns. (**C**) Quantification of activated Bak (AM03)/cytochrome c release positive cells in Figure 4.4B by image segmentation and classification. The total cell counts are shown below the corresponding columns.

To determine if this novel endoplasmic-reticulum dependent cell death pathway is a general feature of estrogen receptor-positive breast cancer cell lines T47D cells were stably transfected with plasmid encoding either Bcl2-cb5, Bcl2-ActA or Neo control and the mitochondrial membrane potential was measured with TMRE after growth in CSBS (Figure 4.6B). Similar to what we observed with MCF-7 cells (Figure 4.4C), in T47D cells loss of mitochondrial membrane potential was noted in 40% of Neo control cells, 50% of Bcl2-ActA cells but < 10% of Bcl2-cb5 cells (Figure 4.6B) confirming the presence of this pathway.

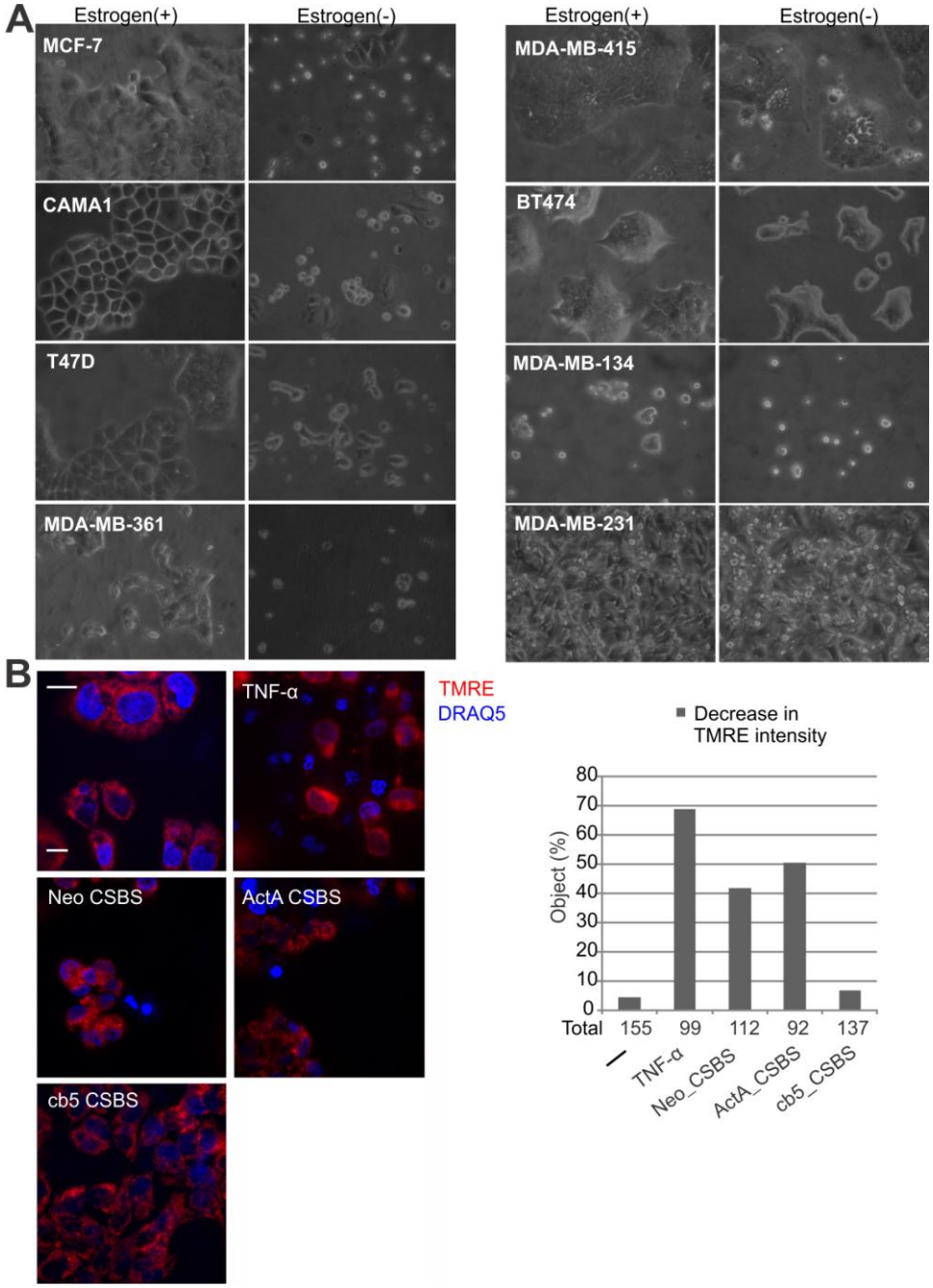

Figure 4.6 CSBS-induced cell death in estrogen-receptor positive breast cancer cell lines. Legend see next page

(**A**) Phase contrast images of breast cancer cell lines (MCF-7, MDA-MB-415, CAMA1, BT474, T47D, MDA-MB-134, MDA-MB-361 and MDA-MB-231) grown in CSBS in the presence or absence of 17β-estradiol. (**B**) TMRE staining of T47D cells expressing Neo, Bcl2-ActA and Bcl2-cb5 after the grown in CSBS and image analysis. T47D cells expressing Neo, Bcl2-ActA, Bcl2-cb5 and Bcl2-WT were grown in CSBS for 10 days and mitochondrial potential was assessed by TMRE staining (red). Nuclei were stained with DRAQ5 (blue) (left panel). T47D cells treated with DMSO control (−) or 33 ng/mL TNF-α/10 μg/mL cycloheximide (TNF-α) for 24 hours were applied as negative and positive controls. Bar, 10 μm. The intensity of TMRE staining was quantified for each object and classified by automated analysis as having decreased intensity of TMRE staining. The procedures of image analysis were performed in accordance with the procedures in Chapter 2 for cytochrome c release. Total cell counts are shown below the corresponding columns (right panel).

The unfolded protein response, autophagy or Bap31 cleavage does not mediate CSBS-induced cell death

Because of the endoplasmic reticulum location of this pathway, we sought to determine if other known cellular stress pathways that act through this organelle are involved as potential effectors or modulators. Therefore, to determine whether CSBS triggered the UPR (Breckenridge, Germain, Mathai, Nguyen, & Shore, 2003), autophagy (Kroemer, et al., 2010) or Bap31 cleavage (Breckenridge, Stojanovic, Marcellus, & Shore, 2003) we examined GRP78/94 expression, XBP-1splicing and CHOP expression, light chain 3 (LC3) expression and turnover, and Bap31 expression respectively.

In response to growth in CSBS, the expression of endoplasmic reticulum chaperone GRP78 and GRP94 are significantly elevated in MCF-7 cells expressing Bcl2-ActA, Bcl2-cb5 and Bcl2-WT as shown by KDEL blot (Figure 4.7A, top panel, lane 3-5). In comparison, the expression of GRP78/GRP94 is markedly less in Neo control MCF-7 cells after growth in CSBS (Figure 4.7A, top panel, lane 2).

BFA blocks protein transport from the endoplasmic reticulum and elicits UPR (Brostrom, et al., 1995), thus it was used as a positive control for XBP-1 splicing and CHOP expression, the two of effector arms of the UPR. Compared to BFA treated cells, growth in CSBS for all the cell lines (expressing Neo, Bcl2-ActA, Bcl2-cb5 or Bcl2-WT)

did not activate XBP-1 splicing (Figure 4.7B). This indicates that the IRE-1-XBP-1 pathway is not active in CSBS-induced cell death. However, CHOP mRNA levels are dramatically elevated in cells expressing Bcl2-ActA, Bcl2-cb5 and Bcl2-WT, but not in the Neo control cells (Figure 4.7C, left panel), consistent with changes in the endoplasmic reticulum chaperones that are transcriptional targets of CHOP (Figure 4.7A, top panel).Taken together these data indicate that activation of the UPR does not mediate the novel death pathway (it is absent in susceptible Neo cells), nor is it protective (absent in susceptible Bc2-ActA cells).

As another type of cell death involving the endoplasmic reticulum distinct from the UPR, autophagy is elicited by deprivation of growth factors in Bax- and Bak-deficient cells (Lum, et al., 2005). As an antagonist of estrogen receptor, TAM is known as autophagy inducer in MCF-7 cells (de Medina, Silvente-Poirot, & Poirot, 2009). Interestingly we observed vacuolation, a sign of autophagy in the cells grown in CSBS (data not shown). Thus, it is plausible that estrogen depletion is part of CSBS-activated autophagy. During autophagy cleavage of LC3 at the carboxyl-terminus immediately following synthesis yields the cytosolic LC3-I form which is converted to LC3-II through lipidation thus facilitating LC3 binding to autophagic vesicles (Klionsky & Emr, 2000). Hence the conversion of the LC3-1 to LC3-II that occurs during autophagy can be used as a biochemical assay to measure the induction of autophagy (Kabeya, et al., 2004) and autophagic flux can be measured by inhibiting LC3-II turnover using the protease inhibitors (leupeptin and E64D) (Klionsky, et al., 2008).

In the absence of leupeptin and E64D (thereby allowing lysosomal degradation), CSBS only causes subtle changes of LC3-II in Neo, Bcl2-ActA and Bcl2-cb5 expressing cells compared to the marked effect noted with TAM (Figure 4.7D, top panel, compare lanes 4-6 with lane 2). This was confirmed in the presence of leupeptin and E64D by monitoring LC3 turnover by western blotting (Figure 4.7D). The results demonstrate that LC3-II increases in the presence of protease inhibitor in Bcl2-ActA, Bcl2-cb5 and Bcl2-WT expressing cells, but not in Neo control cells (Figure 4.7D, top panel, compare lane

8-10 with lane 7). While some variation is found, this suggests a modest activation of autophagy in cells grown in CSBS.

The data suggest that both autophagy and UPR occur in cells expressing Bcl2-ActA, Bcl2-cb5 and Bcl2-WT but not in Neo control cells. Whether the decreased activation of these survival pathways contributed to the cell death elicited by CSBS in Neo cells (Figure 4.1) is not clear. But the fact that modest activation of both UPR and autophagy exist in both the surviving Bcl2-cb5 expressing cells, as well as the moribund Bcl2-ActA cells, indicates that neither of these processes is critically involved in mediating or inhibiting this novel cell death pathway but are likely reflections of a general stress response.

Another reported mediator of cell death that is located at the endoplasmic reticulum is Bap31 (Breckenridge, Stojanovic, et al., 2003; Wakana, et al., 2008). Bap31 is an endoplasmic reticulum transmembrane molecule (Annaert, Becker, Kistner, Reth, & Jahn, 1997; Wakana, et al., 2008), which contains a pseudo-death effector domain serving as a docking and activation platform for procaspase-8 (Ng, et al., 1997). After binding and activation of caspase-8, caspase-8 cleaves off a 20-kDa fragment of Bap31 (Breckenridge, Nguyen, Kuppig, Reth, & Shore, 2002; Ng, et al., 1997). Interestingly, Bcl-2 binds to Bap31 and prevents the activation of procaspase-8, the generation of the p20 fragment, and ultimately the transmission of the death signal to the mitochondria. To investigate the cell signaling involved in the CSBS-induced cell death pathway, we examined Bap31 cleavage (Figure 4.7E). Unfortunately, even though a distinct band was obtained by immunoblotting with the antibody used in previous publications, no cleavage was noted with any treatment (including CSBS) in any of the cell lines (Neo, Bcl2-ActA, Bcl2-cb5 and Bcl2-WT (Figure 4.7E, lane 3-6). Specifically, treatment with the extrinsic apoptosis inducers TNF-α and TRAIL, the intrinsic apoptosis inducer staurosporine (STS) and the UPR inducer BFA at doses and time point that cause significant cell death still did not elicit Bap31 cleavage (even with the long exposure of the blot Figure 4.7F, top panel and middle panel). Notably, TNF-α treatment has previously been used as a positive

control, as is recommended by the manufacturer. This discrepancy between our clear results and the published literature on Bap31 cleavage (B. Wang, et al., 2003) remains unexplained, and does not permit us to unambiguously conclude if it is a relevant player in our novel pathway.

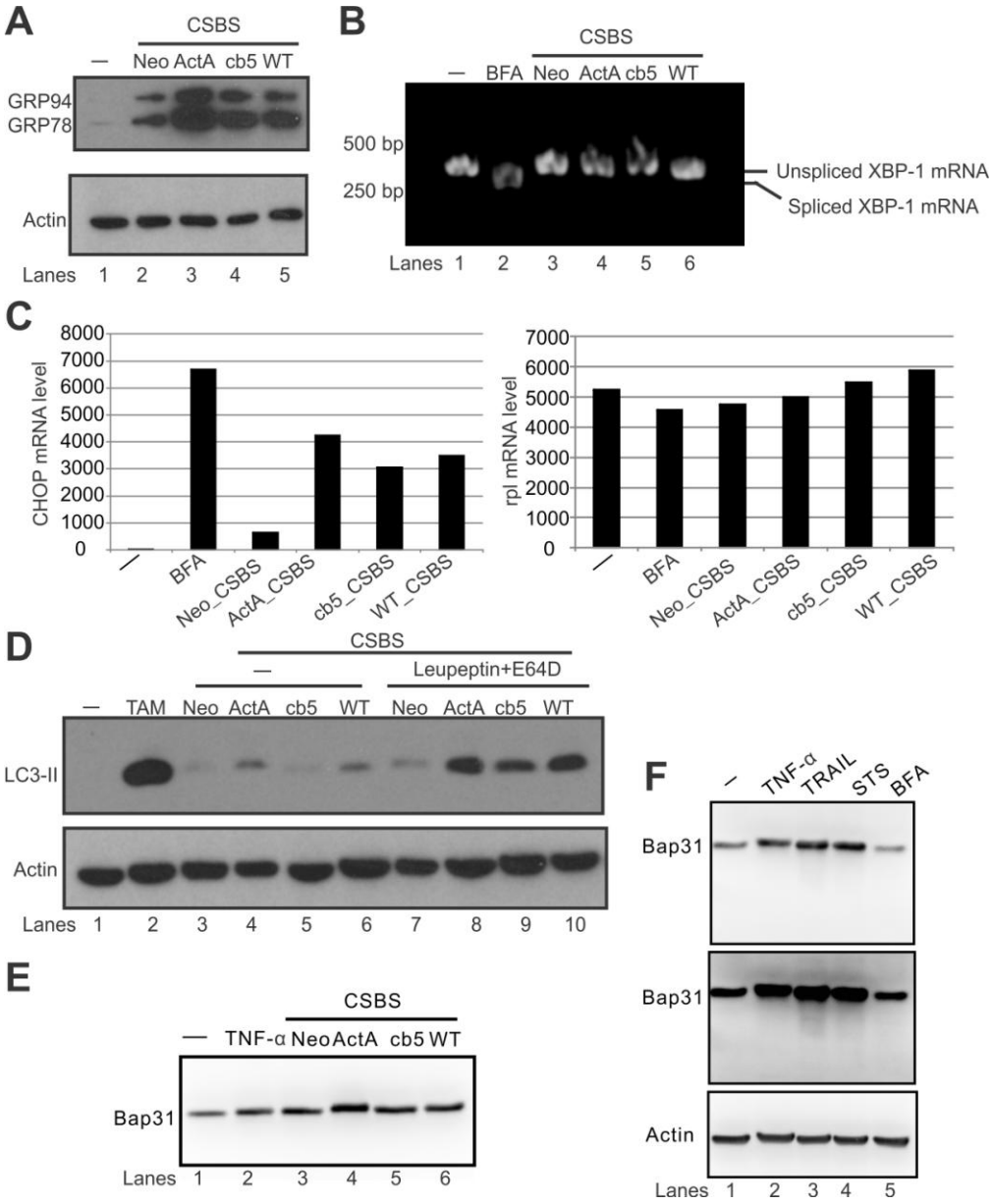

Figure 4.7 The unfolded protein response, autophagy or Bap31 cleavage does not mediate CSBS-induced cell death. Legend see next page.

(**A**) MCF-7 cells expressing Neo, Bcl2-ActA, Bcl2-cb5 and Bcl2-WT were grown in CSBS for 10 days and cell lysates analyzed by immunobloting for KDEL. Lysates from untreated parental MCF-7 cell are indicated by (−). (**B**) MCF-7 cells expressing Neo, Bcl2-ActA, Bcl2-cb5 and Bcl2-WT were grown in CSBS for 10 days and XBP-1 splicing assay performed by RT-PCR. BFA was used as a positive control for UPR. (**C**) MCF-7 cells expressing Neo, Bcl2-ActA, Bcl2-cb5 and Bcl2-WT were grown in CSBS for 10 days and the mRNA levels of CHOP monitored by real-time PCR. Rpl, a ribosomal protein not regulated by endoplasmic reticulum stress, was used as a negative control. And BFA was used as a positive control for UPR. (**D**) MCF-7 cells expressing Neo, Bcl2-ActA, Bcl2-cb5 and Bcl2-WT were grown in CSBS in the presence or absence of leupeptin and E64D for 10 days and the turnover of LC3 assessed by immunoblot. TAM is used as positive control for autophagy. An actin immunoblotblot as control for equal protein loading in each lane is shown. (**E**) MCF-7 cells expressing Neo were treated with DMSO control (−) or 33 ng/mL TNF-α/10 μg/mL cycloheximide for 24 hours. MCF-7 cells expressing Neo, Bcl2-ActA, Bcl2-cb5 and Bcl2-WT were grown in CSBS for 10 days and cell lysates were e analyzed by immunoblotting for Bap31. (**F**) MCF-7 cells expressing Neo were treated with DMSO control (−), 10 ng/mL TNF-α, TRAIL, 1 μM STS and 10 μg/mL BFA for 24 hours. Then the cell lysates were analyzed by immunoblotting for Bap31 and actin.

4.4 Discussion

Estrogen signaling is a complex and important pathway that controls a variety of functions including cell proliferation, apoptosis and invasion in breast cancer cells through estrogen receptor (Pearce & Jordan, 2004; Smith & O'Malley, 2004). The classic function of estrogen receptor is its role as a transactivator of genes involved in normal cellular function and tumor growth. As a result, the binding of estrogen to its receptor dynamically modulates the expression of hundreds of genes, some by upregulation and others by downregulation (Schiff, et al., 2004).

In the absence of estrogen, estrogen receptor is found predominantly in the nucleus, as part of a multiprotein complex consisting of a dimer of Hsp90 and a p23 monomer. Hsp90 is an ADP/ATP binding protein, which contains a nucleotide-binding pocket located at the amino terminal side. Once it is in its ATP bound state, Hsp90 recruits co-chaperone p23 which acts as a stabilizer of the complex (Knoblauch & Garabedian, 1999). Hsp90-based chaperone complex inactivates estrogen receptor's

transcriptional regulatory capabilities and maintains the estrogen receptor in a conformation competent for steroid binding. Upon binding estrogen, estrogen receptor dissociates from this complex, dimerizes, and recognizes specific DNA sequences, termed estrogen-response elements, within the promoters of estrogen-responsive genes (Klinge, 2001). Once bound to an estrogen-response element, estrogen receptor is believed to modulate transcription of the linked gene through direct or indirect interactions with general transcriptional factors (Knoblauch & Garabedian, 1999).

Estrogen receptor is not statically bound to DNA at promoter sites of genes regulating cell proliferation and differentiation, but rather behaves as a very mobile protein continuously shuttling between cytoplasm and nucleus (Knoblauch & Garabedian, 1999). This allows the receptor to generate both non-genomic and genomic responses. Estrogen can increase the expression of several ligands (Umayahara, et al., 1994) which activate the growth factor receptor pathways (A. V. Lee, Cui, & Oesterreich, 2001; Schiff, et al., 2004). On the other hand, estrogen signaling downregulates the expression of epidermal growth factor receptor and human epidermal growth factor receptor 2 (HER2) while increasing the expression of insulin-like growth factor receptor (Massarweh, et al., 2008). Therefore, charcoal stripped medium which sequesters growth factors and estrogen withdrawal can affect a number of pathways due to the downregulation of estrogen signaling.

Our data show that in the estrogen receptor-positive breast cancer cell line MCF-7, CSBS-induced cell death is protected by Bcl-2 localized on the endoplasmic reticulum (Bcl2-cb5) rather than Bcl-2 on the mitochondrial membrane (Bcl2-ActA) (Figure 4.1). Supplementation with 17β-estradiol prevents CSBS-induced cell death in Neo and Bcl2-ActA expressing cells (Figure 4.3A), which suggests that loss of estrogen signaling in the CSBS activates this novel cell death.

The endoplasmic reticulum has been established as an essential site in the regulation of apoptotic pathways (Szegezdi, et al., 2006). Cell stress stimuli as diverse as UPR or autophagy activate many of the endoplasmic reticulum-associated signaling

pathways including the activation of endoplasmic reticulum-localized BH3-only proteins and initiator caspases as well as Ca^{2+} signaling (Heath-Engel, et al., 2008). However, to date no cell death pathway mediated by the proteins exclusively localized on the endoplasmic reticulum has been described. Therefore, CSBS-induced cell death is unique in this respect.

To characterize this novel cell death pathway, we monitored key cellular events associated with known forms of cell death (Bax/Bak activation, cytochrome c release and loss of mitochondrial membrane potential). Although cytochrome c release and the loss of mitochondrial membrane potential occur in both Neo control cells and Bcl2-ActA cells, significant Bax/Bak activation is detected in Neo cells but not Bcl2-ActA cells (Figure 4.4 and 4.5). Due to the inhibition of Bax/Bak activation by Bcl-2 on the mitochondria, Bcl2-ActA cells either die from 6A7/Bak independent cell death or activation of residual amounts of Bax/Bak (Figure 4.4 and 4.5).

By contrast , Bcl-2 on the endoplasmic reticulum blocks this type of cell death as Bax/Bak activation, cytochrome c release or the loss of the mitochondrial membrane potential were not detected (Figure 4.4 and 4.5). However, these cells are not completely unaffected by growth in CSBS, as there is evidence of upregulated endoplasmic reticulum chaperones (UPR) and elevated LC3 levels (autophagy) (Figure 4.7). Finally, even after 21 days of growth in CSBS, cells expressing Bcl2-cb5 still maintain cell adhesion when the major population of three other cell lines shows almost complete loss of attachment (Figure 4.2A). Thus, CSBS induces a form of cell death that is effectively inhibited by Bcl-2 located at the endoplasmic reticulum and that is augmented by, but does not require activation of Bax or Bak and is at best poorly inhibited by Bcl-2 at mitochondria.

Although the cell death signal that Bcl2-cb5 blocks remains unclear, it leads to formation of mitochondrial permeability transition pores. The obvious candidate is Ca^{2+} but the TG data make this possibility unlikely as this type of cell death is blocked by Bcl2-ActA, whereas CSBS-induced cell death is not (Figure 4.1, Figure 4.2C). Therefore, to further dissect this novel cell death pathway we investigated the possible BH3

activators by targeting Bcl2-cb5 with peptidomimetic ABT-737. The intriguing observation that ABT-737 cotreatment with CSBS abolishes the protective effect of Bcl2-cb5 (Figure 4.5) suggests that Bcl2-cb5 might interact and suppress the activation of a BH3-only protein(s) on the endoplasmic reticulum membrane and thus maintain the cell death pathway switched off. Thus in the absence of f Bcl-2 on the endoplasmic reticulum in cells expressing Neo and Bcl2-ActA, growth in CSBS activates this unknown BH3-only protein(s) and the latter turns on the cell death pathway in these cells.

As mentioned in the introduction (Chapter 1), the known Bcl-2 binding partners at the endoplasmic reticulum include the BH3-only proteins BIK and Beclin 1. Since NAF-1 is displaced from the interaction with Bcl-2 at the endoplasmic reticulum by BH3-only protein BIK, the activator that ABT-737 transactivates could be BIK, Beclin 1 or NAF-1. Further studies including Small interfering RNA (siRNA) knockdown and protein pull-down assays will be performed to identify this activator(s). Although IP3R and SERCA mediate cell death via the modulation of endoplasmic reticulum Ca^{2+} homeostasis and both of them interact with Bcl-2 at the endoplasmic reticulum, this mechanism is less likely to be BH3 region dependent.

We examined the activity of other known stress-related pathways at the endoplasmic reticulum such as UPR, autophagy or Bap31 cleavage. UPR (shown by endoplasmic reticulum chaperone protein upregulation and increased transcription of CHOP) is detected in cells expressing Bcl2-ActA, Bcl2-cb5 and Bcl2-WT, but not Neo cells (Figure 4.7). Interestingly, autophagy (increased LC3-II levels) is also found in cells expressing Bcl2-ActA, Bcl2-cb5 and Bcl2-WT, but not in Neo cells (Figure 4.7). Whether this is due to extensive cell death in Neo control cells or this cell line is subject to a distinct cell death pathway differing from the other Bcl-2 expressing cell lines is a question which needs to be answered in the future. Since the presence of UPR or autophagy does not match the cell death observed in Figure 4.1 (Neo and Bcl2-ActA expressing cells die while Bcl2-cb5 expressing cells stay alive) this suggests that they are not directly involved. Unfortunately, technical limitations prevent us from definitively

concluding that Bap31 cleavage is not involved, although none was detected after growth in CSBS. The results related to our novel cell death are summarized in Table 4.1.

Analysis	Neo	Bcl2-ActA	Bcl2-cb5
6A7	+	–	–
Active Bak	+	–	–
Cytochrome c release	+	+	–
Membrane potential loss	+	+	–
PARP cleavage	+	+	–
GRP78	–	+	+
LC3	±	±	±

Table 4.1 Summary of cellular responses after growth in CSBS.

Although most of our studies were performed in MCF-7 cells, another six estrogen receptor-positive breast cancer cell lines and one estrogen receptor-negative breast cancer cell line were also examined (Figure 4.6). The corresponding expression profile of several known prognostic markers in human breast cancer for these cell lines is shown in Table 4.2. The six cell lines were chosen based upon the expression of different biologic prognostic factors (e.g. HER2 and P53 expression/mutant status) to obtain clues about factor(s) that may regulate this cell death pathway.

Of the six estrogen receptor-positive cell lines, only CAMA1, T47D and MDA-MB-361 were sensitive to CSBS-induced cell death (Figure 4.6). Based on the information in Table 4.2, the only common feature among these four lines is positivity for estrogen receptor expression. This indicates that there may be secondary regulatory mechanism(s) controlling the switch of cell death induction beyond expression of the estrogen receptor. Further research is underway to examine such features.

cell line	ER status	PR status	HER2 status	p53 expression status	TP53 mutational status
MDAMB231	-	-	-	++	MUT
T47D	+	+	-	++	MUT
MDAMB134VI	+	-	-	+/-	WT
MCF-7	+	+	-	+/-	WT
MDAMB361	+	-	+	-	WT
BT474	+	+	+	+	MUT
MDAMB415	+	-	-	+	MUT
CAMA1	+	-	-	+	MUT

Table 4.2 The profile of prognostic markers in breast cancer cell lines examined in Figure 4.6. ER: estrogen receptor; PR: progesterone receptor; HER2: human epidermal growth factor receptor 2; MUT: mutant; WT: wild type

Chapter 5 : Measuring cell death responses by automated image analysis

5.1 Preface

This chapter is a discussion chapter regarding the use of multiparametric image analysis to examine apoptosis.

Figure 5.1 presented in this chapter was published in:

Aranovich A, Liu Q, Collins T, Geng F, Dixit S, Leber B, Andrews DW. (2012) Mol. Cell 45: 754-63

Permission has been granted by the publishers to reproduce the material here.

Figure 5.2, Figure 5.3C and Figure 5.4C are contributed by Tony Collins.

5.2 Introduction

Inappropriate cell death has not only been recognized as one of the hallmarks of cancer (Hanahan & Weinberg, 2000), but also can be responsible for diseases such as atherosclerosis (Littlewood & Bennett, 2003), Alzheimer's disease (Cotman & Anderson, 1995; Shimohama, 2000), spinal cord injury (Y. Wang & Qin, 2010) and ischemia (Choi, 1996). Cell death can occur via a range of stresses or signals and result from the activation of multiple signaling cascades including those characteristic of apoptosis, endoplasmic reticulum stress and autophagy.

Cells undergoing apoptosis were originally identified based on typical, well-defined morphological changes, including plasma membrane blebbing, chromatin condensation, nuclear fragmentation and formation of apoptotic bodies. A common approach to quantifying apoptosis has been to image cells with a microscope and manually score cells to determine the fraction of the population undergoing apoptosis. The subjectivity of this approach combined with the requirement to analyze large numbers of images can lead to significant drift in these analyses. Apoptosis has also been characterized by several biochemical parameters including (1) cell surface exposure of PS on the outer leaflet of the plasma membrane detected by Annexin V staining with the loss of membrane integrity detected by PI staining; (2) loss of mitochondrial membrane potential detected by TMRE; (3) release of mitochondrial intermembrane space proteins such as cytochrome c detected by immunofluorescence, caspase activation detected by a variety of enzymatic assays including fluorescence lifetime imaging and the cleavage of a caspase-3/caspase-7 substrate PARP detected by western blot (Galluzzi, et al., 2009). Ideally apoptosis is quantified and differentiated from other forms of cell death in a population of cells using both morphological and biochemical markers.

In comparison, endoplasmic reticulum stress, which is caused by disruption of endoplasmic reticulum homeostasis, leads to the accumulation of unfolded proteins within the organelle lumen. The endoplasmic reticulum has developed an adaptive mechanism called the unfolded protein response to counteract compromised protein

folding. The UPR attempts to reduce the protein load by decreasing protein synthesis and increase the folding capacity of the endoplasmic reticulum by up-regulating the expression of luminal chaperones such as GRP78/GRP94. However, unresolved endoplasmic reticulum stress results in the activation of apoptosis. Although the unfolded protein response coordinates the production of endoplasmic reticulum proteins and membranes (Cox, Chapman, & Walter, 1997; Schuck, Prinz, Thorn, Voss, & Walter, 2009), no well-defined morphological changes are known to mark this response.

Compared with the two types of cellular response above, cells undergoing death associated with autophagy are characterized by the presence of double membrane autophagic vacuoles (Klionsky & Emr, 2000). Autophagy is foremost a survival mechanism that is activated in cells subjected to nutrient or obligate growth factor deprivation. When cellular stress continues, cell death may continue by autophagy alone, or else it often becomes associated with features of apoptotic or necrotic cell death. Morphological and biochemical markers have been determined for autophagy, including relocalization of LC3 to the autophagosomes and the lipidation of LC3, as detected by band shift in western blots (Klionsky, et al., 2008).

Although many assays have been developed to quantify specific aspects of these three cellular responses in the last decades (Galluzzi, et al., 2009), these indicators need to be integrated to meet the increasing demand for the investigation of the unknowns. The conventional measurement of various cell death and stress responses is based on measuring several morphological and biochemical parameters required to identify each pathway. The difficulty is that even the interpretation of dying cell morphology may be complex, because in the absence of rescue autophagic cells proceed to a stage called autophagic cell death, which shares many features of apoptosis (Maiuri, Zalckvar, et al., 2007). Features considered characteristic of apoptosis can also take place during endoplasmic reticulum stress induced cell death (Szegezdi, et al., 2006). Often multiple features are present because the pathways are not mutually exclusive. Finally the reliance

on observer judgement for many of these assays makes it difficult to identify unambiguously the type(s) of cellular responses to any particular agonist.

In Chapter 4 we used a variety of assays including PARP cleavage, KDEL blot and LC3 blot to probe apoptosis, endoplasmic reticulum stress and autophagy respectively. To improve this process, Sudeepa Dixit, Tony Collins and I have used automated image analysis and multiparametric approaches to analyze the feature data to distinguish cellular responses by statistical analysis. Multiparametric image analysis algorithms attempt to integrate as much of the information of each cell that can be extracted. This approach takes a broad variety of measurements (referred to as 'features') from each cell. These are then compared to reference images and each cell classified to the closest matching reference dataset.

In this chapter I first describe a relatively simple application of this approach that Sudeepa Dixit and I used to quantitatively determine the proapoptotic activity of mCherry-BH3 fusion proteins by measuring the expression level of those fusion proteins and the cytochrome c release in the corresponding cells (Aranovich, et al., 2012). Then we extended this approach to a more complex problem of deciphering the response of cells to different small molecules based on multiparametric analysis of images of cells stained with the lipophillic cationic dye nonyl-acridine-orange (NAO). With the preference for binding to cardiolipin (CL), NAO has been applied as a probe to visualize CL enriched membranes such as mitochondria (Mileykovskaya & Dowhan, 2009) an organelle intimately connected with many forms of cell death. We compared NAO staining based multiparametric classification with several traditional apoptosis assays and found that multiparametric classification is both quantitative and of high sensitivity. More importantly, this approach can measure both apoptosis and endoplasmic reticulum stress, which suggests its potential application in the quantification of the unknown cell death pathway induced by estrogen deprivation.

5.3 Results

The discovery of conventional cell markers relies on basic research including various "omic" studies. Even those markers identified in "omic" studies require extensive manual validation. As a result, there are few existing markers for the detection of cell responses and their limitations are apparent. Most of them are specifically dedicated to single response detection and therefore for a cellular event that involves multiple pathways conventional markers may give ambiguous results. As a results if the cellular response to an agonist is not known, identifying the mechanism by screening various markers is laborious, time consuming and often expensive (for the antibodies, unique dyes etc.). Furthermore, the information from conventional markers often can be interpreted in many ways. For example, the disappearance of full-length PARP often seen in PARP cleavage immunoblots can be due to multiple causes: PARP degradation by the proteasome, or loss of the epitope due to cleavage by caspases other than caspase-3/caspase-7, or by other enzymes such as calpain that are often activated by alternate pathways.

In comparison, in automated image analysis and machine learning a variety of cellular features are measured and then linked to different physiological responses in cells statistically. In supervised machine learning a computer program identifies those features that can be used to classify cellular responses based on images of cells exposed to stimuli that elicit different specific responses (e.g. apoptosis, endoplasmic reticulum stress, autophagy, or no treatment). The cells being tested can be assigned to the category that they match most closely. Furthermore, by using a large number of features extracted from the images, cells clustered into phenotypes which may be too complex to easily recognize visually. Thus this process of supervised clustering is an automatic, quantitative, explicit and objective way to compare unknown data with known data and to determine which it most resembles.

An example of multiparametric analysis and classification of images that we used is the measurement of cell death induced by expression of pro-apoptotic mCherry-BH3 fusion proteins in cells and its prevention by Bcl-XL. I performed the immunostaining and imaging for cytochrome c and mCherry-BH3 proteins (Figure 5.1A) while Sudeepa Dixit generated the classification algorithm that I then used to analyze the images (Figure 5.1B). The results published as part of paper that appeared in Aranovich et al. Mol. Cell 2012 are shown in Figure 5.1 (Aranovich, et al., 2012). In this example cells were classified as either apoptotic or normal based on the parameter of cytochrome c release from mitochondria. This was scored based on the measured cytoplasm intensity of immunofluorescence staining for cytochrome c and the standard deviation. In this case, a low intensity indicated release of cytochrome c. The cytochrome c release percentage was calculated by the number of objects with released cytochrome c versus the total number of cells expressing mCherry-BH3 proteins.

An additional criterion that was also useful was the fraction of the cells expressing detectable BH3 protein. Based on the expression level of mCherry-BH3 fusion protein identified by measuring the intensity of mCherry, the cells were classified as either BH3 positive or negative. It is noteworthy that the fraction of cells expressing high levels of the most potent BH3 proteins was low, possibly because this was toxic to the cells. However, variable transfection efficiency, protein synthesis and folding may also account for these differences.

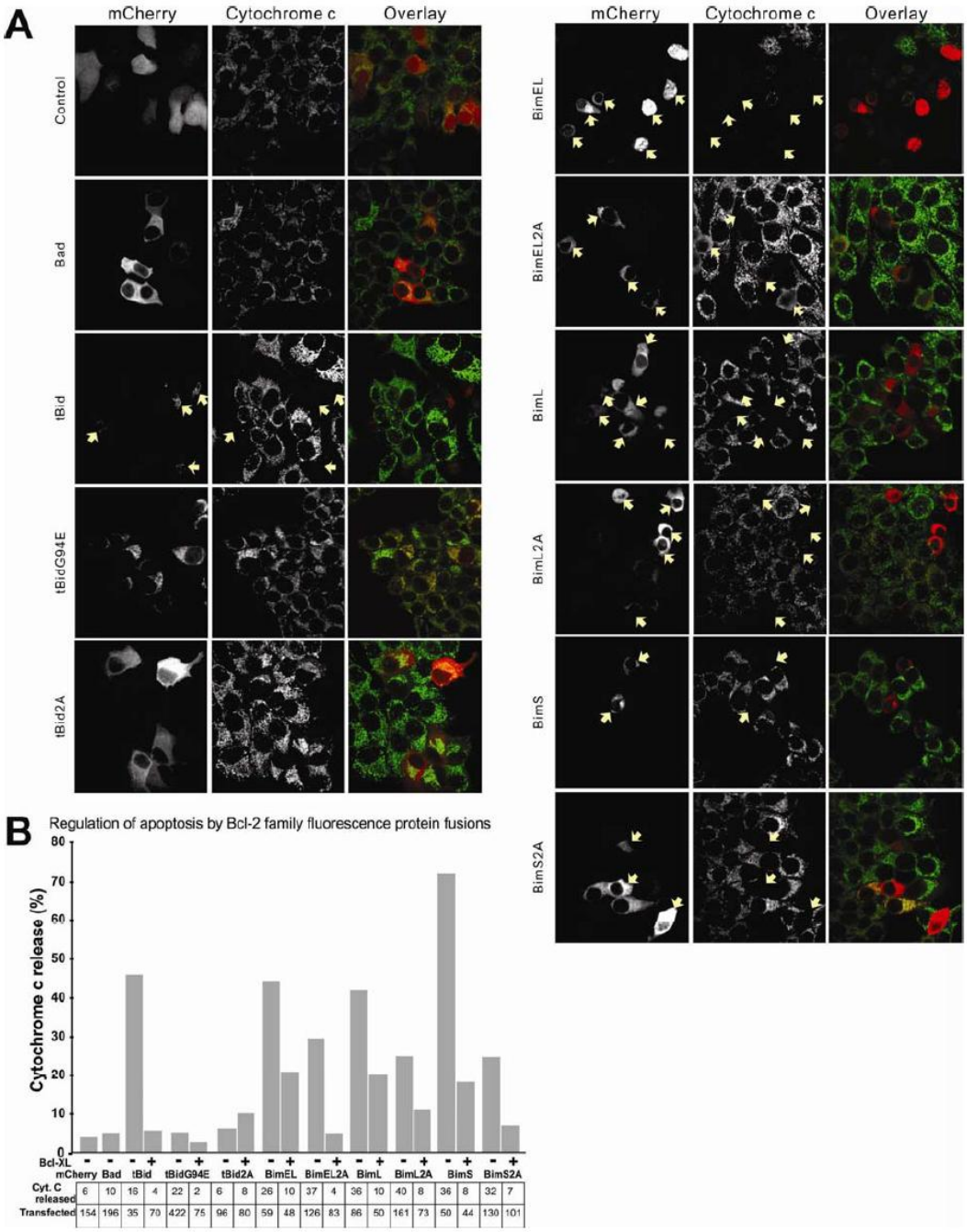

Figure 5.1 Expression of mCherry-BH3 proteins triggers cytochrome c release that is inhibited by Bcl-XL. Legend see next page.

MCF-7 cells and Bcl-XL expressing MCF-7 cells were seeded on coverslips. The next day, the cells were transfected with plasmids encoding mCherry (vector), or mCherry fused to the BH3 protein indicated to the left of the panels. The cells were washed twice in PBS and stained with antibody against cytochrome c. Nuclei were stained with 5 μM DRAQ5 for 30 minutes at room temperature (images not shown). (**A**) Sample images of MCF-7 cells expressing mCherry-BH3 proteins (red in overlay) immunostained for cytochrome c (green in overlay). Some cells expressing mCherry-BH3 protein and showing cytochrome c release are indicated with arrows. tBidG94E is a well characterized inactive mutant of tBid used as a negative control (Lutter, Perkins, & Wang, 2001). (**B**) Quantification of cytochrome c release by mCherry-BH3 proteins and inhibition by Bcl-XL. The inactive tBid mutants tBidG94E and tBid2A (E. F. Lee, et al., 2008) exhibited negligible cytochrome c releasing activity. However, the 2A mutants of all three Bim isoforms retained partial Bcl-XL inhibitable pro-apoptotic activity.

The results we obtained show clearly that mCherry-BH3 fusion proteins trigger cytochrome c release with variable potency, and the expression of Bcl-XL in those cells inhibits the pro-apoptotic activity.

This relatively simple form of automated image analysis allowed me to apply a uniform set of objective criteria to the images, greatly facilitating comparison of the effects of the different BH3 proteins. It also illustrates the power of the approach and suggested that multiparametric image analysis might be useful to quantify the endoplasmic reticulum-specific form of cell death in estrogen deprived breast cancer cells described in Chapter 4. However, since we do not know the distinguishing features of this type of cell death, we decided to see if machine learning techniques could identify features of cells stained with relatively non-specific dyes that would distinguish apoptosis, autophagy and endoplasmic reticulum stress. For these experiments a large number of cellular features (e.g. texture, intensity and morphology features) were collected to provide the information for the classification. A useful marker would distinguish more than one type of cell response. By using drugs at a dose and time point that induce well characterized physiological responses, the images obtained were used both to train classifiers and to test the hypothesis that features associated with non-specific membrane dye can be used to identify different physiological responses in MCF-

7 cells. The known data comprises at least two phenotypes which are used to train the supervised clustering algorithm. By using the supervised clustering method namely Support Vector Machines (SVM), we generated classes for every unknown object in the data set by taking a random selection of some of the wells of untreated cells as the negative control and of the highest dose of the drug as the positive control for that drug to train the classifier. Our goal was to use these templates to ask whether estrogen deprivation induced cell death resembled any of these known cellular responses (Figure 5.1).

We chose the fluorescent dye NAO as a candidate to analyze the three cellular responses. Due to its preferential binding to CL, NAO stains the mitochondrial membrane most intensely (Rodriguez, et al., 2008). Since mitochondria are altered in several forms of cellular responses (Hetz, 2007; Hoye, et al., 2008; Kroemer, et al., 1998), NAO may be a good general probe for cell death analysis.

To test its performance as a cell death marker, we compared NAO staining with the other conventional image based methods after eliciting apoptosis by a standard technique. Several previously established image-based methods were used to quantify cell death in MCF-7 breast cancer cells 24 h post-treatment with TNF-α and cycloheximide (referred to here as TNF-α treatment) (Figure 5.2). Annexin V binding measures the externalization of PS that occurs during apoptosis when cells no longer retain plasma membrane lipid asymmetry. PI staining measures loss in the integrity of the plasma membrane early in necrosis but late during apoptosis (Figure 5.2A). TMRE is a cell-permeant, cationic, red-orange fluorescent dye sequestered by active mitochondria and used to quantify mitochondrial membrane potential (Scaduto & Grotyohann, 1999) (Figure 5.2B). Caspase activation, a hallmark of apoptosis was measured using a Cerulean and Venus FRET-based caspase-reporter (Figure 5.2Ci) and fluorescence lifetime imaging (Figure 5.2Cii). Cleavage of the sensor at the caspase-3/caspase-7 site DEVD separates the donor (monomeric Cerulean, mCer) from the acceptor (enhanced

YFP, eYFP) abolishing FRET and increasing the fluorescence lifetime of the donor. Nuclear condensation and cell counts were derived from DRAQ5 stained cells.

DRAQ5 staining images were used to identify the cell nuclei and cytoplasmic borders in order to quantify the corresponding nuclei and cytoplasmic features for each cell stained with NAO and DRAQ5. As shown in Figure 5.2D, NAO mainly stains the mitochondrial membrane, and the difference in staining is apparent between untreated and TNF-α treated cells. Many features including texture, shape and size of the cytoplasm and nuclei were recorded, and all were processed by supervised clustering with a support vector machine (SVM). The Z-factor is a robust measure of the quality of an assay and is commonly used to assess assays (Zhang, Chung, & Oldenburg, 1999). We quantified Z-factors and P values for a range of conventional measures of cell death including those shown in Figure 5.2 A-D as well as our multiparametric classification approaches trained on untreated cells and the highest dose of TNF-α treated cells as negative and positive controls, respectively. Among all the assays only the changes in membrane integrity (PI positivity) was not significant at $P<0.01$ level. The highest performing conventional assay was TMRE with a Z-factor of 0.57. Other measures of apoptosis such as cell count, nuclear condensation (i.e. nuclear area) were poor assays with Z-factor of less than zero in this assay format. In contrast, NAO-SVM (Z-factor 0.91) outperformed conventional image based apoptosis assays that focused on single aspects of apoptosis (Figure 5.2E). Since the Z-factor is reflective of both the assay signal dynamic range and data variation associated with signal measurements, it is suitable for assay quality assessment (Zhang, et al., 1999). Thus our result suggests the approach using multiparametric analysis of images of cells stained with NAO is superior to other image based techniques.

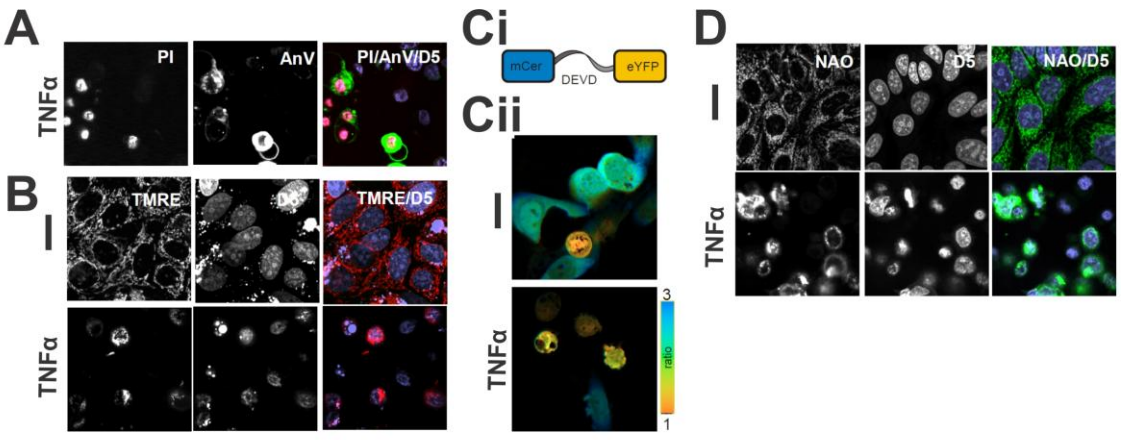

E

Apoptosis readout	Z'	p-val
NAO-SVM	0.91	$2X\ 10^{-7}$
TMRE +ve	0.57	$3X\ 10^{-10}$
Caspase-3+ve	0.34	$3X\ 10^{-6}$
AnnV +ve	0.01	0.004
Cell Count	-0.3	$1X\ 10^{-4}$
PI +ve	-4	0.3
Nuclear area	-27	0.001

Figure 5.2 Comparison of conventional biochemical assays for apoptosis in MCF-7 cells.

Sample images of untreated control cells or cells treated with either 33 ng/mL TNF-α/10 μg/mL cycloheximide or 400 nM TG for 24 hours. Cells were stained with either (**A**) PI; AnnexinV-AF488 and DRQA5 (D5); (**B**) TMRE and DRAQ5; (**C**) expressing CFP-DEVD-EYFP caspase reporter; or (**D**) stained with NAO and DRAQ5. (**E**) The Z-factor and P value of conventional apoptosis assays and NAO-SVM were shown.

To further compare NAO staining with PARP cleavage induced by pathways of apoptosis, we treated cells with the well characterized extrinsic apoptosis inducer TNF-α, or the intrinsic apoptosis inducers staurosporine (STS) and ActD (Figure 5.3). The results indicate that TNF-α causes PARP cleavage at the lowest dose tested (Figure 5.3A). In responses to STS and ActD treatments, PARP expression is up-regulated consistent with previous reports (Oliver, Menissier-de Murcia, & de Murcia, 1999). STS treatment causes PARP cleavage at 0.32 μM and ActD treatment leads to PARP cleavage at 0.02 μM (Figure 5.3A and B). We used the highest concentration of each treatment for the

positive-training sets and derived EC50 values for the response (Figure 5.3C). As Figure 5.3A shows, the dose response curve of TNF-α treatment was generated with the detection limit of 2.33 ng/mL when 300 ng/mL TNF-α treated cells were applied as positive training set. Similarly when we used 20 μM STS treated cells as positive training set, the classifier also generated dose response curves for STS induced apoptosis with the detection limit of 0.64 μM (Figure 5.3C). When using 10 μM ActD treated cells as positive training set, the classifier also generated dose response curves for ActD induced apoptosis with the detection limit of 0.02 μM (Figure 5.3C). Although the detection limit of the NAO staining based multiparametric image analysis approach is not as low as PARP cleavage, its robustness is apparent as it detects responses at both the low and high doses. Therefore, this approach is an excellent tool for primary screens of small molecule libraries. For our purposes, it is also useful to measure the specific form of cell death caused by estrogen deprivation.

To test if changes in NAO staining can detect other cellular responses (endoplasmic reticulum stress and autophagy), cells were treated with increasing concentrations of the endoplasmic reticulum stress inducer TN (Dorner, Wasley, & Kaufman, 1992), and the autophagy inducer TAM (Bursch, et al., 2000). The expression of endoplasmic reticulum chaperones and PARP in treated cells were measured, and the percentage of cells classified positive based on an NAO staining pattern generated by supervised clustering was quantified for each treatment. TN caused the increase of GRP78 (shown by KDEL blot) (Munro & Pelham, 1987) at the dose of 0.76 μM, but only caused PARP cleavage at substantially higher doses (25 μM, Figure 5.4A and B). We used the 200 μM TN treated cells as the positive training set for endoplasmic reticulum stress and observed that dose dependent curve was generated starting at 3.12 μM (Figure 5.4C). This result suggests the NAO staining features is a robust measure of endoplasmic reticulum stress.

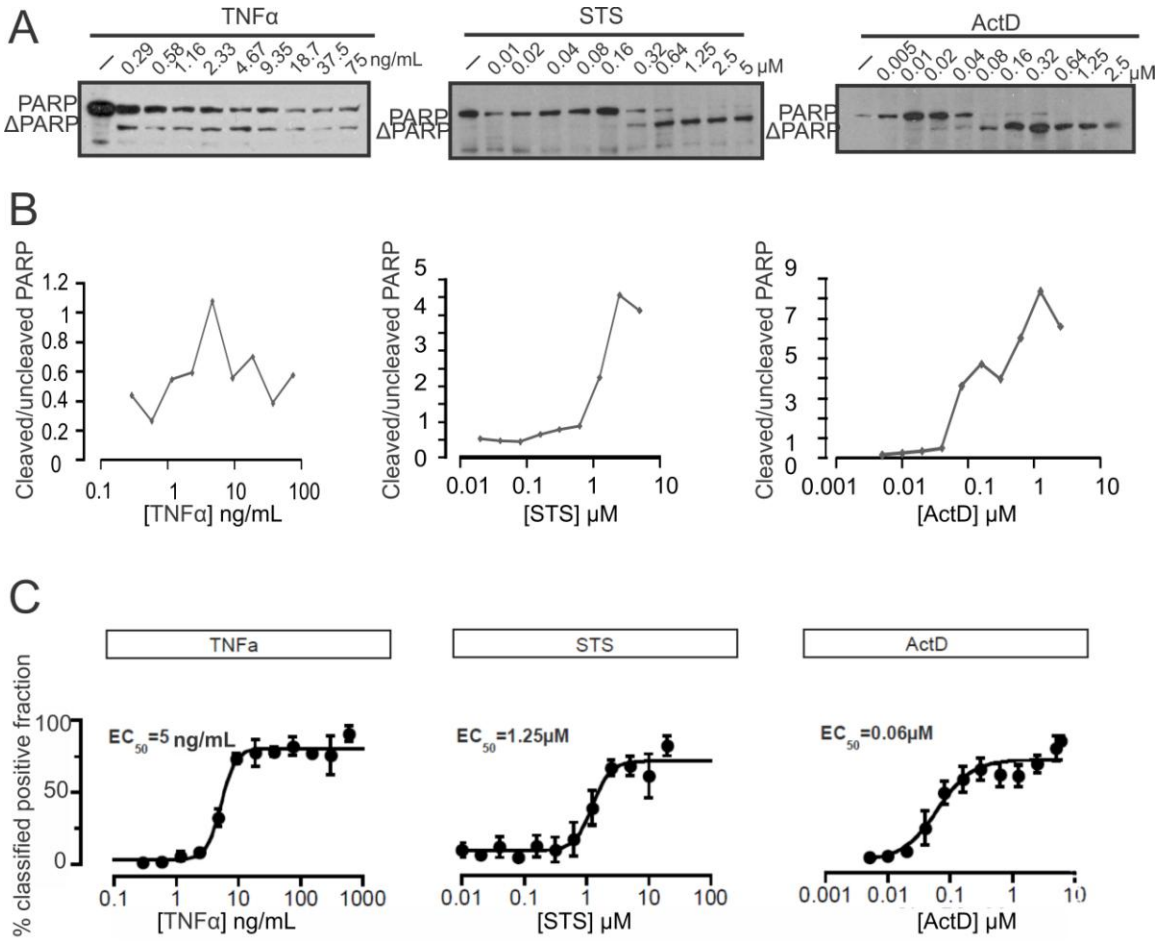

Figure 5.3 Quantification of apoptosis based on multiparametric analysis of cells stained with NAO.

MCF-7 cells were treated with DMSO control (−), or increasing doses of TNF-α, STS and ActD. The treated cells were analyzed by immunoblotting against PARP (**A**). Note: Since the high doses of all the five treatments caused extensive cell death and protein degradation, insufficient cells were obtained for lysates (with missing PARP data) for the following conditions: 150 ng/mL and 300 ng/mL for TNF-α; 10 μM and 20 μM for STS; 5 μM and 10 μM for ActD. (**B**) Densitometry was performed using Image J for the PARP blots shown in Panel A. The ratio of cleaved PARP to uncleaved PARP for each concentration was calculated and plotted. (**C**) The treated cells were stained with NAO and then analyzed with multiparametric approach to generate the dose response curve. Images were acquired at 40x magnification (0.7 NA) and data was extracted from 400 cells per well (on average) and 8 wells per concentration. DMSO controls and the highest dose of each treatment were used as negative and positive training datasets, respectively.

In comparison, the diagnostic 89 kDa fragment of PARP due to caspase-7 cleavage was not detected after TAM treatment, although full-length PARP was clearly degraded at TAM doses as low as 2.34 μM (Figure 5.4A, right panel). This dose of TAM causes an increase of LC3 (Figure 5.4A). However, even when we used 75 μM TAM treated cells as a positive training set for autophagy, no cells were classified as positive based upon NAO staining below this dose despite the positive results with the diagnostic LC3 assay .This suggests that a more robust cell content marker with a richer staining pattern of cellular membranes might be needed for the autophagy detection in the future studies.

More importantly, a 3-way analysis was performed by training the classifier with the three training sets including untreated cells, TN treated cells and TNF-α treated cells (Figure 5.4D). As a result, TN treated cells can be divided into those that have features that classify them as untreated fraction (no response), or TN treated (endoplasmic reticulum stress) or TNF-α treated fraction (apoptosis) (Figure 5.4D). Significantly in all these cells treated identically (with TN) the proportion of cells undergoing endoplasmic reticulum stress (TN pattern) or apoptosis (TNF-α pattern) is comparable to the corresponding GRP78 expression and PARP cleavage profile measured after the same TN treatment (Figure 5.4 A-D left panel).

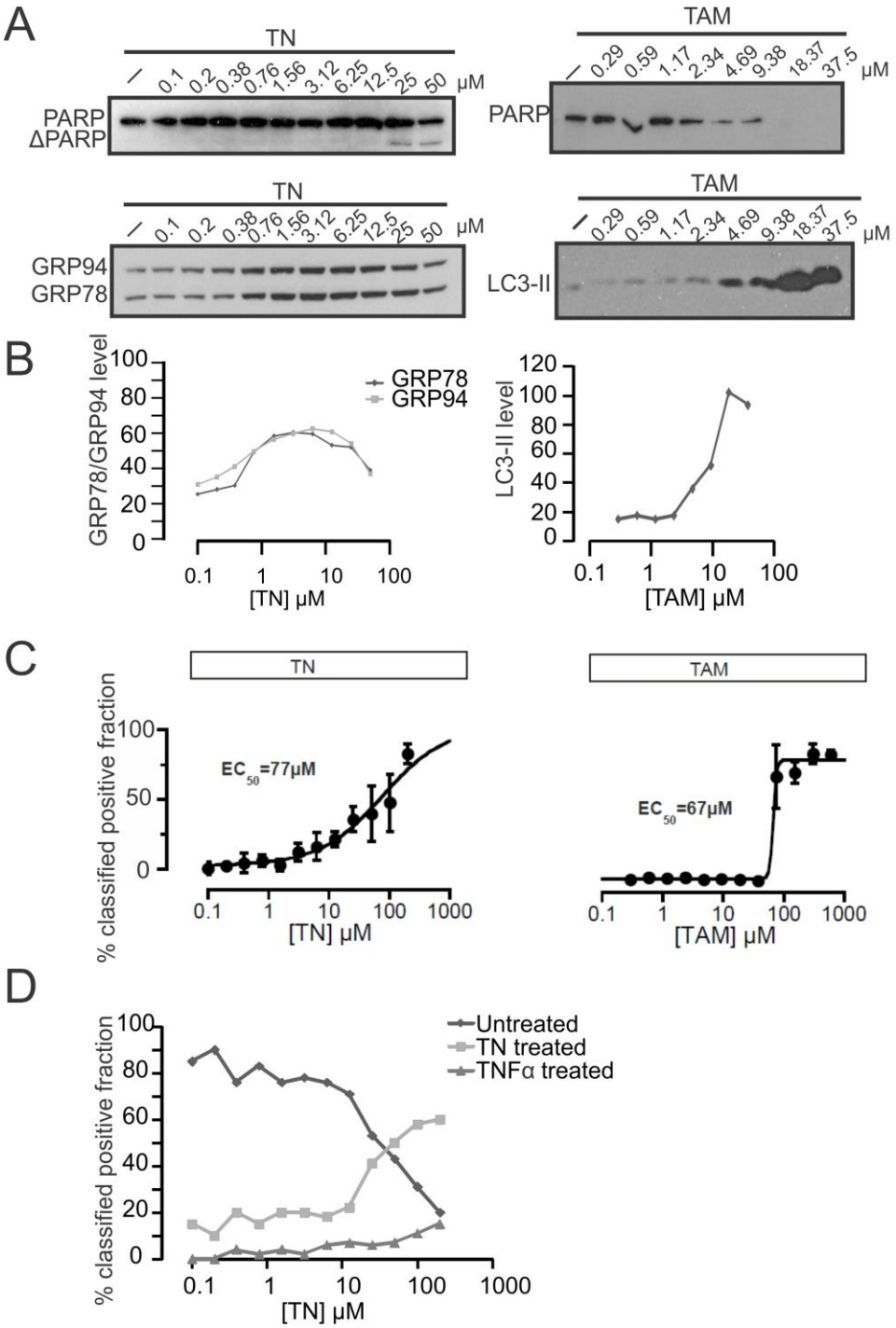

Figure 5.4 Endoplasmic reticulum stress but not autophagy can be quantified based on multiparametric analysis of cells stained with NAO. Legend see next page.

(**A**) In the left panel, MCF-7 cells were treated with DMSO control (−) and increasing doses of TN. The treated cells were either analyzed by immunoblotting against PARP (upper blot) and KDEL (lower blot) or stained with NAO and then analyzed with multiparametric approach to generate the dose response curve. In the right panel, MCF-7 cells were treated with DMSO control (−) and increasing doses of TAM. The treated cells were analyzed by immunoblotting against PARP (upper blot) and LC3 (lower blot). Note: Since the high doses of all the five treatments caused extensive cell death and protein degradation, insufficient cells were obtained for lysates (with missing PARP data) for the following conditions: 100 μM and 200 μM for TN; 75 μM, 150 μM, 300 μM and 600 μM for TAM). (**B**) Densitometry was performed using Image J for the KDEL and LC3 blots shown in Panel A. (**C**) The treated cells were stained with NAO and then analyzed with multiparametric approach to generate the dose response curve. Images were acquired at 40x magnification (0.7 NA) and data was extracted from 400 cells per well (on average) and 8 wells per concentration. DMSO controls and the highest dose of each treatment were used as negative and positive training datasets, respectively. (**D**) A 3-way analysis of TN treated cells by training the classifier with DMSO control cells (untreated control), 200 μM TN treated cells (TN treated) and 300 ng/mL TNF-α treated cells (TNF-α treated).

5.4 Discussion

A cell is often considered dead in vitro when it loses plasma-membrane integrity. However, a cell can be committed to dying long before this point is reached. Initiation of cell death processes is associated with a wide range of measurable changes within the cell. Such responses are typically highly context dependent, varying with cell type and biological environment. Therefore, it is critical to identify the unique characteristics that can be used to define different types of cellular responses for mechanism studies.

Conventional markers in the past vary from DNA, RNA, protein molecules to fluorescent reporters which allow end-point detection or real-time detection. The main drawbacks of the conventional biomarkers are listed as below. First the discovery and validation of a marker of a specific form of cell death requires the full characterization of the phenotype from basic research. Such markers are generally not useful to study unknown phenotypes. For instance, live reporters of caspases and MOMP are only informative if the cell is dying by apoptosis. Secondly, they are mostly single event-based. For example, PARP cleavage can only detect apoptosis which activates effector

caspase-3 or caspase-7 that result in the cleavage of PARP at a defined site to generate a fragment that can be conveniently monitored with the PARP antibody. Thus caspase independent cell death will be non-detectable by PARP cleavage.

The new molecular technologies have allowed us to move from a linear, single event-based concept of cell death to a greater understanding of the alterations in the entire cellular context (Spencer & Sorger, 2011).

Because of the variety of fluorescent dyes, dye selection can influence the sensitivity and accuracy of classification. Why did we choose NAO? First of all, due to its highly specific interaction with CL it highlights CL-enriched membranes of eukaryotic cells (Mileykovskaya & Dowhan, 2009). CL is a phospholipid found uniquely in the inner membrane of mitochondria and at the contact sites between the inner and outer membranes, representing 13-15% of total mitochondrial phospholipids (Rodriguez, et al., 2008). Since the mitochondria regulate multiple forms of cell death (Hoye, et al., 2008), all these properties are reflected in features we extracted from the images of cells stained with NAO and thus the latter can be direct or indirect measure of cell death. Second, it is a fairly inexpensive fluorescent dye, allowing future application in high throughput and high content screening.

The multiparametric image analysis approach based upon the images of cells stained with NAO was proved to be superior to other image based techniques as shown in Figure 5.2. It not only can measure extrinsic and intrinsic apoptosis (Figure 5.3C), but also can measure endoplasmic reticulum stress (Figure 5.4C). More importantly, it could distinguish and quantitatively distinguish three separate cellular responses within one set of sample (Figure 5.4D).

Therefore, this approach has potential applications in drug discovery and mechanistic analysis. By choosing the training sets, this approach is easily applicable to primary screening during the drug discovery stage. For example, an apoptosis inducer screening can be set up using TNF-α treated cells as positive training set. Similarly endoplasmic reticulum stressor screen would use TN treated cells as a positive training

set. In the post-discovery stage, this approach might assist in identifying the mechanisms of interesting hits obtained from the drug screen by using the cellular response classification.

Furthermore, drug off-target effects can also be detected by this approach. We can illustrate this by using a screen using kinase inhibitors (drugs) or shRNA targeting kinases as an example. A kinase inhibitor would affect its target in the treated population rapidly, but may also have multiple targets. By contrast, the time required for antisense transcript expression, protein turnover etc. with genetic knockdown, the phenotype would be more specific but would occur more slowly, thereby providing the cells time to adapt. By comparing the information extracted from NAO staining images of cells treated with kinase inhibitor with the cells treated with multiple shRNA/siRNA against the same kinase, information can be gained concerning the specificity of kinase inhibitor. Taken together these advantages suggest that this approach has broad application in the field of drug discovery, such as developing screening platforms, post-screening studies (e.g. probe the unknown mechanism of interesting hits) and measuring the off-target effect in combination with library screening.

As shown in Chapter 4, estrogen deprivation induces a novel form of cell death in breast cancer cells which can be prevented by Bcl-2 localized at the endoplasmic reticulum instead of Bcl-2 localized at the mitochondria, not caused by endoplasmic reticulum stress, autophagy or Bap31 cleavage. Since NAO staining based image analysis approach can analyze, classify and quantitatively determine multiple cellular responses within the same cellular event, it represents a valuable tool to investigate the unknown response(s) causing the cell death induced by estrogen deprivation.

Chapter 6 : Concluding remarks

In multicellular organisms molecules that transduce signals originating from outside the cell are important determinants of cells fate and behavior. Recent insights have shown that information can also flow in the opposite direction where intracellular stresses can modify this apparatus, and in this thesis I have concentrated on the endoplasmic reticulum as a site where such signaling is mediated, and possibly initiated. As an potential target of such a pathway, the E-cadherin cell adhesion complex is not only critical for the formation of cytoskeleton, but also provides survival signals to prevent cell death (Grossmann, 2002). In response to various stimuli, O-GlcNAc modifications occur on E-cadherin, β-catenin (Zhu, et al., 2001) and plakoglobin (Hatsell, Medina, Merola, Haltiwanger, & Cowin, 2003) suggesting that this type of modification regulates the behavior of the whole complex rather than just one molecule. To begin to analyze this process the work presented in this thesis focused on characterizing the multiple modifications of E-cadherin that occur in response to stress. Results obtained led us to investigate upstream signaling leading to this event, and the involvement of the endoplasmic reticulum triggered a search for a novel cell death pathway that would be specific for this organelle.

O-GlcNAc blocks the trafficking of E-cadherin via preventing its binding to PIPKIγ

There are a variety of substrates which are modified by O-GlcNAc and as a consequence this modification has been used to regulate diverse cellular processes. (Comer & Hart, 2000), especially noted in stress responses (Hart, et al., 2007), proteolytic maturation in cell-cycle regulation (Capotosti, et al., 2011) and pluripotency of embryonic stem cells (Jang, et al., 2012).

We have observed that after the induction of stress response by TG or BFA, newly synthesized E-cadherin molecules are modified by O-GlcNAc in the endoplasmic reticulum. As a result, O-GlcNAcylation blocks exit of E-cadherin precursors from the endoplasmic reticulum and interferes with PIPKIγ binding. Furthermore, we have

identified the second modification as loss of pro-region processing that presumably results from inhibition of proprotein convertases and have shown that this is regulated independently from O-GlcNAcylation. A deletion mutant of E-cadherin (E-cadΔpSer) which removes O-GlcNAc modification maintains the interaction with PIPKIγ and transport of E-cadherin to the plasma membrane during cell stress. Expression of E-cadΔpSer protects cells from stress induced apoptosis, which suggests that inhibited trafficking of E-cadherin to plasma membrane as a consequence of the O-GlcNAc modification promoted cell death.

Growth in CSBS triggered endoplasmic reticulum-specific cell death in breast cancer cells

Since O-GlcNAcylation on E-cadherin occurs in the endoplasmic reticulum, whether this is the site of origin of the signal that initiates this response is important. Endoplasmic reticulum-specific cell death signaling has not (yet) been demonstrated, whereas endoplasmic reticulum involvement in cell death has been investigated for decades. This distinction is critical as the former requires the irreversible commitment to cell death be initiated and mediated by proteins located at the endoplasmic reticulum while the latter only requires that cell death signaling "goes through" the endoplasmic reticulum but is executed at other locations. Cellular events such as the UPR (Bernales, Schuck, & Walter, 2007) and autophagy (Chang, et al., 2010) belong to the latter. In these cases the downstream cell death signaling of endoplasmic reticulum stress leads to initiation of the intrinsic apoptosis pathway requiring MOMP (Hetz, 2007). Similarly, the downstream signaling of autophagic cell death involves the mitochondria as well as the endoplasmic reticulum (Klionsky & Emr, 2000).

Unlike previously reported pathways (classical apoptosis requiring MOMP, UPR, autophagy and Bap31 cleavage), cell death induced by growth in CSBS is protected exclusively by Bcl-2 localized at the endoplasmic reticulum but not at the mitochondria. It is therefore likely that Bcl-2 at the endoplasmic reticulum interacts with organelle-

specific activator(s) to antagonize cell death. And ABT-737 is shown to abolish the protection by Bcl-2 at the endoplasmic reticulum. This suggests the critical binding partner(s) is a BH3-only protein(s) sequestered by Bcl2-cb5 cells. Thus in the absence of Bcl-2 at the endoplasmic reticulum in Neo control cells or Bcl2-ActA cells, this BH3-only protein is free to activate the endoplasmic reticulum-specific cell death.

All biological networks have similar characteristics. In order to provide important functions in normal cells under a variety of conditions and stress factors, as well as to keep the cell alive, these networks must be complex with multiple levels of regulation, fine tuning capabilities, redundancy, and evolvability (Jordan & O'Malley, 2007). Collectively these features allow the cell to adapt to cellular stress, toxins, and potentially hostile environments. Cancer cells exploit these normal functions, which are often altered genetically during oncogenesis to provide them with a survival advantage and the ability to escape the effects of treatment. Although the molecular signaling that underlies the endoplasmic reticulum-specific cell death has yet to be fully elucidated, a detailed understanding of the activities of Bcl-2 on the endoplasmic reticulum represents an important lead for the development of future therapeutic interventions for cancers in which this pathway can be elicited.

The clinical strategy of targeting estrogen receptor-positive breast cancer with a selective estrogen receptor modulator TAM during the last three decades has saved hundreds of thousands of lives and been proved to be the cornerstone for breast cancer treatment (Jordan & O'Malley, 2007; Osborne & Schiff, 2011). However, loss of estrogen receptor expression in the recurrent breast cancer confers resistance to TAM therapy in estrogen receptor-positive patients (Kuukasjarvi, Kononen, Helin, Holli, & Isola, 1996; Naughton, et al., 2007). Therefore, understanding the downstream signaling of estrogen deprivation induced cell death pathway in this thesis may provide important clues to the mechanisms of resistance to endocrine therapy given before or after primary surgery to eradicate distant micrometastases.

BIBLIOGRAPHY

Abe, F., Van Prooyen, N., Ladasky, J. J., & Edidin, M. (2009). Interaction of Bap31 and MHC class I molecules and their traffic out of the endoplasmic reticulum. *J Immunol, 182*(8), 4776-4783.

Aita, V. M., Liang, X. H., Murty, V. V., Pincus, D. L., Yu, W., Cayanis, E., et al. (1999). Cloning and genomic organization of beclin 1, a candidate tumor suppressor gene on chromosome 17q21. *Genomics, 59*(1), 59-65.

Annaert, W. G., Becker, B., Kistner, U., Reth, M., & Jahn, R. (1997). Export of cellubrevin from the endoplasmic reticulum is controlled by BAP31. *J Cell Biol, 139*(6), 1397-1410.

Annis, M. G., Zamzami, N., Zhu, W., Penn, L. Z., Kroemer, G., Leber, B., et al. (2001). Endoplasmic reticulum localized Bcl-2 prevents apoptosis when redistribution of cytochrome c is a late event. *Oncogene, 20*(16), 1939-1952.

Aranovich, A., Liu, Q., Collins, T., Geng, F., Dixit, S., Leber, B., et al. (2012). Differences in the mechanisms of proapoptotic BH3 proteins binding to Bcl-XL and Bcl-2 quantified in live MCF-7 cells. *Mol Cell, 45*(6), 754-763.

Batlle, E., Sancho, E., Franci, C., Dominguez, D., Monfar, M., Baulida, J., et al. (2000). The transcription factor snail is a repressor of E-cadherin gene expression in epithelial tumour cells. *Nat Cell Biol, 2*(2), 84-89.

Baud, V., & Karin, M. (2001). Signal transduction by tumor necrosis factor and its relatives. *Trends Cell Biol, 11*(9), 372-377.

Baylin, S. B., Herman, J. G., Graff, J. R., Vertino, P. M., & Issa, J. P. (1998). Alterations in DNA methylation: a fundamental aspect of neoplasia. *Adv Cancer Res, 72*, 141-196.

Beavon, I. R. (2000). The E-cadherin-catenin complex in tumour metastasis: structure, function and regulation. *Eur J Cancer, 36*(13 Spec No), 1607-1620.

Behrens, J., Lowrick, O., Klein-Hitpass, L., & Birchmeier, W. (1991). The E-cadherin promoter: functional analysis of a G.C-rich region and an epithelial cell-specific palindromic regulatory element. *Proc Natl Acad Sci U S A, 88*(24), 11495-11499.

Behrens, J., Vakaet, L., Friis, R., Winterhager, E., Van Roy, F., Mareel, M. M., et al. (1993). Loss of epithelial differentiation and gain of invasiveness correlates with tyrosine phosphorylation of the E-cadherin/beta-catenin complex in cells transformed with a temperature-sensitive v-SRC gene. *J Cell Biol, 120*(3), 757-766.

Bernales, S., Schuck, S., & Walter, P. (2007). ER-phagy: selective autophagy of the endoplasmic reticulum. *Autophagy, 3*(3), 285-287.

Bertolotti, A., Zhang, Y., Hendershot, L. M., Harding, H. P., & Ron, D. (2000). Dynamic interaction of BiP and ER stress transducers in the unfolded-protein response. *Nat Cell Biol, 2*(6), 326-332.

Berx, G., Becker, K. F., Hofler, H., & van Roy, F. (1998). Mutations of the human E-cadherin (CDH1) gene. *Hum Mutat, 12*(4), 226-237.

Berx, G., Cleton-Jansen, A. M., Strumane, K., de Leeuw, W. J., Nollet, F., van Roy, F., et al. (1996). E-cadherin is inactivated in a majority of invasive human lobular breast cancers by truncation mutations throughout its extracellular domain. *Oncogene, 13*(9), 1919-1925.

Berx, G., Staes, K., van Hengel, J., Molemans, F., Bussemakers, M. J., van Bokhoven, A., et al. (1995). Cloning and characterization of the human invasion suppressor gene E-cadherin (CDH1). *Genomics, 26*(2), 281-289.

Berx, G., & Van Roy, F. (2001). The E-cadherin/catenin complex: an important gatekeeper in breast cancer tumorigenesis and malignant progression. *Breast Cancer Res, 3*(5), 289-293.

Bierkamp, C., Schwarz, H., Huber, O., & Kemler, R. (1999). Desmosomal localization of beta-catenin in the skin of plakoglobin null-mutant mice. *Development, 126*(2), 371-381.

Billen, L. P., Shamas-Din, A., & Andrews, D. W. (2008). Bid: a Bax-like BH3 protein. *Oncogene, 27 Suppl 1*, S93-104.

Bolos, V., Peinado, H., Perez-Moreno, M. A., Fraga, M. F., Esteller, M., & Cano, A. (2003). The transcription factor Slug represses E-cadherin expression and induces epithelial to mesenchymal transitions: a comparison with Snail and E47 repressors. *J Cell Sci, 116*(Pt 3), 499-511.

Booth, C., & Koch, G. L. (1989). Perturbation of cellular calcium induces secretion of luminal ER proteins. *Cell, 59*(4), 729-737.

Breckenridge, D. G., Germain, M., Mathai, J. P., Nguyen, M., & Shore, G. C. (2003). Regulation of apoptosis by endoplasmic reticulum pathways. *Oncogene, 22*(53), 8608-8618.

Breckenridge, D. G., Nguyen, M., Kuppig, S., Reth, M., & Shore, G. C. (2002). The procaspase-8 isoform, procaspase-8L, recruited to the BAP31 complex at the endoplasmic reticulum. *Proc Natl Acad Sci U S A, 99*(7), 4331-4336.

Breckenridge, D. G., Stojanovic, M., Marcellus, R. C., & Shore, G. C. (2003). Caspase cleavage product of BAP31 induces mitochondrial fission through endoplasmic reticulum calcium signals, enhancing cytochrome c release to the cytosol. *J Cell Biol, 160*(7), 1115-1127.

Brostrom, M. A., Prostko, C. R., Gmitter, D., & Brostrom, C. O. (1995). Independent signaling of grp78 gene transcription and phosphorylation of eukaryotic initiator factor 2 alpha by the stressed endoplasmic reticulum. *J Biol Chem, 270*(8), 4127-4132.

Bruncko, M., Oost, T. K., Belli, B. A., Ding, H., Joseph, M. K., Kunzer, A., et al. (2007). Studies leading to potent, dual inhibitors of Bcl-2 and Bcl-xL. *J Med Chem, 50*(4), 641-662.

Bryant, D. M., & Stow, J. L. (2004). The ins and outs of E-cadherin trafficking. *Trends Cell Biol, 14*(8), 427-434.

Bursch, W., Hochegger, K., Torok, L., Marian, B., Ellinger, A., & Hermann, R. S. (2000). Autophagic and apoptotic types of programmed cell death exhibit different fates of cytoskeletal filaments. *J Cell Sci, 113 (Pt 7)*, 1189-1198.

Calfon, M., Zeng, H., Urano, F., Till, J. H., Hubbard, S. R., Harding, H. P., et al. (2002). IRE1 couples endoplasmic reticulum load to secretory capacity by processing the XBP-1 mRNA. *Nature, 415*(6867), 92-96.

Cano, A., Perez-Moreno, M. A., Rodrigo, I., Locascio, A., Blanco, M. J., del Barrio, M. G., et al. (2000). The transcription factor snail controls epithelial-mesenchymal transitions by repressing E-cadherin expression. *Nat Cell Biol, 2*(2), 76-83.

Capdeville, R., Buchdunger, E., Zimmermann, J., & Matter, A. (2002). Glivec (STI571, imatinib), a rationally developed, targeted anticancer drug. *Nat Rev Drug Discov, 1*(7), 493-502.

Capotosti, F., Guernier, S., Lammers, F., Waridel, P., Cai, Y., Jin, J., et al. (2011). O-GlcNAc transferase catalyzes site-specific proteolysis of HCF-1. *Cell, 144*(3), 376-388.

Chang, N. C., Nguyen, M., Bourdon, J., Risse, P. A., Martin, J., Danialou, G., et al. (2012). Bcl-2-associated autophagy regulator Naf-1 required for maintenance of skeletal muscle. *Hum Mol Genet, 21*(10), 2277-2287.

Chang, N. C., Nguyen, M., Germain, M., & Shore, G. C. (2010). Antagonism of Beclin 1-dependent autophagy by BCL-2 at the endoplasmic reticulum requires NAF-1. *EMBO J, 29*(3), 606-618.

Chappell, J., Leitner, J. W., Solomon, S., Golovchenko, I., Goalstone, M. L., & Draznin, B. (2001). Effect of insulin on cell cycle progression in MCF-7 breast cancer cells. Direct and potentiating influence. *J Biol Chem, 276*(41), 38023-38028.

Chen, Q., Gong, B., & Almasan, A. (2000). Distinct stages of cytochrome c release from mitochondria: evidence for a feedback amplification loop linking caspase activation to mitochondrial dysfunction in genotoxic stress induced apoptosis. *Cell Death Differ, 7*(2), 227-233.

Chen, Y. T., Stewart, D. B., & Nelson, W. J. (1999). Coupling assembly of the E-cadherin/beta-catenin complex to efficient endoplasmic reticulum exit and basal-lateral membrane targeting of E-cadherin in polarized MDCK cells. *J Cell Biol, 144*(4), 687-699.

Chinnadurai, G., Vijayalingam, S., & Rashmi, R. (2008). BIK, the founding member of the BH3-only family proteins: mechanisms of cell death and role in cancer and pathogenic processes. *Oncogene, 27 Suppl 1*, S20-29.

Choi, D. W. (1996). Ischemia-induced neuronal apoptosis. *Curr Opin Neurobiol, 6*(5), 667-672.

Comer, F. I., & Hart, G. W. (2000). O-Glycosylation of nuclear and cytosolic proteins. Dynamic interplay between O-GlcNAc and O-phosphate. *J Biol Chem, 275*(38), 29179-29182.

Corso, G., Marrelli, D., Pascale, V., Vindigni, C., & Roviello, F. (2012). Frequency of CDH1 germline mutations in gastric carcinoma coming from high- and low-risk areas: metanalysis and systematic review of the literature. *BMC Cancer, 12*, 8.

Cotman, C. W., & Anderson, A. J. (1995). A potential role for apoptosis in neurodegeneration and Alzheimer's disease. *Mol Neurobiol, 10*(1), 19-45.

Cox, J. S., Chapman, R. E., & Walter, P. (1997). The unfolded protein response coordinates the production of endoplasmic reticulum protein and endoplasmic reticulum membrane. *Mol Biol Cell, 8*(9), 1805-1814.

D'Souza-Schorey, C. (2005). Disassembling adherens junctions: breaking up is hard to do. *Trends Cell Biol, 15*(1), 19-26.

Danial, N. N., & Korsmeyer, S. J. (2004). Cell death: critical control points. *Cell, 116*(2), 205-219.

Daniel, J. M., & Reynolds, A. B. (1997). Tyrosine phosphorylation and cadherin/catenin function. *Bioessays, 19*(10), 883-891.

Daugherty, R. L., & Gottardi, C. J. (2007). Phospho-regulation of Beta-catenin adhesion and signaling functions. *Physiology (Bethesda), 22*, 303-309.

de Medina, P., Silvente-Poirot, S., & Poirot, M. (2009). Tamoxifen and AEBS ligands induced apoptosis and autophagy in breast cancer cells through the stimulation of sterol accumulation. *Autophagy, 5*(7), 1066-1067.

Delva, E., & Kowalczyk, A. P. (2009). Regulation of cadherin trafficking. *Traffic, 10*(3), 259-267.

Denmeade, S. R., & Isaacs, J. T. (2005). The SERCA pump as a therapeutic target: making a "smart bomb" for prostate cancer. *Cancer Biol Ther, 4*(1), 14-22.

Distelhorst, C. W., & Shore, G. C. (2004). Bcl-2 and calcium: controversy beneath the surface. *Oncogene, 23*(16), 2875-2880.

Dixit, V., & Chang, T. M. (1984). In vitro and clinical studies of the removal of cortisol, thyroxine, insulin, and thyroid-stimulating hormone by coated charcoal haemoperfusion. *Life Support Syst, 2*(4), 238-244.

Dorner, A. J., Wasley, L. C., & Kaufman, R. J. (1992). Overexpression of GRP78 mitigates stress induction of glucose regulated proteins and blocks secretion of selective proteins in Chinese hamster ovary cells. *EMBO J, 11*(4), 1563-1571.

Dremina, E. S., Sharov, V. S., Kumar, K., Zaidi, A., Michaelis, E. K., & Schoneich, C. (2004). Anti-apoptotic protein Bcl-2 interacts with and destabilizes the sarcoplasmic/endoplasmic reticulum Ca2+-ATPase (SERCA). *Biochem J, 383*(Pt 2), 361-370.

Elkoreh, G., Blais, V., Beliveau, E., Guillemette, G., & Denault, J. B. (2012). Type 1 inositol-1,4,5-trisphosphate receptor is a late substrate of caspases during apoptosis. *J Cell Biochem, 113*(8), 2775-2784.

Enari, M., Sakahira, H., Yokoyama, H., Okawa, K., Iwamatsu, A., & Nagata, S. (1998). A caspase-activated DNase that degrades DNA during apoptosis, and its inhibitor ICAD. *Nature, 391*(6662), 43-50.

Feige, J. J., & Scheffler, I. E. (1987). Analysis of the protein glycosylation defect of a temperature-sensitive cell cycle mutant by the use of mutant cells overexpressing the human epidermal growth factor receptor after transfection of the gene. *J Cell Physiol, 133*(3), 461-470.

Fiebig, A. A., Zhu, W., Hollerbach, C., Leber, B., & Andrews, D. W. (2006). Bcl-XL is qualitatively different from and ten times more effective than Bcl-2 when expressed in a breast cancer cell line. *BMC Cancer, 6*, 213.

Fulda, S., & Debatin, K. M. (2006). Extrinsic versus intrinsic apoptosis pathways in anticancer chemotherapy. *Oncogene, 25*(34), 4798-4811.

Galluzzi, L., Aaronson, S. A., Abrams, J., Alnemri, E. S., Andrews, D. W., Baehrecke, E. H., et al. (2009). Guidelines for the use and interpretation of assays for monitoring cell death in higher eukaryotes. *Cell Death Differ, 16*(8), 1093-1107.

Gambetta, M. C., Oktaba, K., & Muller, J. (2009). Essential role of the glycosyltransferase sxc/Ogt in polycomb repression. *Science, 325*(5936), 93-96.

Geng, F., Shi, B. Z., Yuan, Y. F., & Wu, X. Z. (2004). The expression of core fucosylated E-cadherin in cancer cells and lung cancer patients: prognostic implications. *Cell Res, 14*(5), 423-433.

Gerl, R., & Vaux, D. L. (2005). Apoptosis in the development and treatment of cancer. *Carcinogenesis, 26*(2), 263-270.

Gilmore, A. P., Owens, T. W., Foster, F. M., & Lindsay, J. (2009). How adhesion signals reach a mitochondrial conclusion--ECM regulation of apoptosis. *Curr Opin Cell Biol, 21*(5), 654-661.

Gloster, T. M., Zandberg, W. F., Heinonen, J. E., Shen, D. L., Deng, L., & Vocadlo, D. J. (2011). Hijacking a biosynthetic pathway yields a glycosyltransferase inhibitor within cells. *Nat Chem Biol, 7*(3), 174-181.

Gobeil, S., Boucher, C. C., Nadeau, D., & Poirier, G. G. (2001). Characterization of the necrotic cleavage of poly(ADP-ribose) polymerase (PARP-1): implication of lysosomal proteases. *Cell Death Differ, 8*(6), 588-594.

Gottardi, C. J., Wong, E., & Gumbiner, B. M. (2001). E-cadherin suppresses cellular transformation by inhibiting beta-catenin signaling in an adhesion-independent manner. *J Cell Biol, 153*(5), 1049-1060.

Graff, J. R., Gabrielson, E., Fujii, H., Baylin, S. B., & Herman, J. G. (2000). Methylation patterns of the E-cadherin 5' CpG island are unstable and reflect the dynamic, heterogeneous loss of E-cadherin expression during metastatic progression. *J Biol Chem, 275*(4), 2727-2732.

Graziano, F., Humar, B., & Guilford, P. (2003). The role of the E-cadherin gene (CDH1) in diffuse gastric cancer susceptibility: from the laboratory to clinical practice. *Ann Oncol, 14*(12), 1705-1713.

Green, D. R., & Reed, J. C. (1998). Mitochondria and apoptosis. *Science, 281*(5381), 1309-1312.

Griffiths, G. J., Dubrez, L., Morgan, C. P., Jones, N. A., Whitehouse, J., Corfe, B. M., et al. (1999). Cell damage-induced conformational changes of the pro-apoptotic protein Bak in vivo precede the onset of apoptosis. *J Cell Biol, 144*(5), 903-914.

Grimm, S. (2012). The ER-mitochondria interface: the social network of cell death. *Biochim Biophys Acta, 1823*(2), 327-334.

Grossmann, J. (2002). Molecular mechanisms of "detachment-induced apoptosis--Anoikis". *Apoptosis, 7*(3), 247-260.

Gumbiner, B. M. (2000). Regulation of cadherin adhesive activity. *J Cell Biol, 148*(3), 399-404.

Gumbiner, B. M. (2005). Regulation of cadherin-mediated adhesion in morphogenesis. *Nat Rev Mol Cell Biol, 6*(8), 622-634.

Hallenberger, S., Bosch, V., Angliker, H., Shaw, E., Klenk, H. D., & Garten, W. (1992). Inhibition of furin-mediated cleavage activation of HIV-1 glycoprotein gp160. *Nature, 360*(6402), 358-361.

Hanahan, D., & Weinberg, R. A. (2000). The hallmarks of cancer. *Cell, 100*(1), 57-70.

Hanson, C. J., Bootman, M. D., Distelhorst, C. W., Wojcikiewicz, R. J., & Roderick, H. L. (2008). Bcl-2 suppresses Ca2+ release through inositol 1,4,5-trisphosphate receptors and inhibits Ca2+ uptake by mitochondria without affecting ER calcium store content. *Cell Calcium, 44*(3), 324-338.

Hanson, C. J., Bootman, M. D., & Roderick, H. L. (2004). Cell signalling: IP3 receptors channel calcium into cell death. *Curr Biol, 14*(21), R933-935.

Harding, H. P., Zhang, Y., & Ron, D. (1999). Protein translation and folding are coupled by an endoplasmic-reticulum-resident kinase. *Nature, 397*(6716), 271-274.

Hart, G. W., Housley, M. P., & Slawson, C. (2007). Cycling of O-linked beta-N-acetylglucosamine on nucleocytoplasmic proteins. *Nature, 446*(7139), 1017-1022.

Hatsell, S., Medina, L., Merola, J., Haltiwanger, R., & Cowin, P. (2003). Plakoglobin is O-glycosylated close to the N-terminal destruction box. *J Biol Chem, 278*(39), 37745-37752.

Haze, K., Yoshida, H., Yanagi, H., Yura, T., & Mori, K. (1999). Mammalian transcription factor ATF6 is synthesized as a transmembrane protein and activated by proteolysis in response to endoplasmic reticulum stress. *Mol Biol Cell, 10*(11), 3787-3799.

He, H., Lam, M., McCormick, T. S., & Distelhorst, C. W. (1997). Maintenance of calcium homeostasis in the endoplasmic reticulum by Bcl-2. *J Cell Biol, 138*(6), 1219-1228.

Heath-Engel, H. M., Chang, N. C., & Shore, G. C. (2008). The endoplasmic reticulum in apoptosis and autophagy: role of the BCL-2 protein family. *Oncogene, 27*(50), 6419-6433.

Heath-Engel, H. M., Wang, B., & Shore, G. C. (2012). Bcl2 at the endoplasmic reticulum protects against a Bax/Bak-independent paraptosis-like cell death pathway initiated via p20Bap31. *Biochim Biophys Acta, 1823*(2), 335-347.

Hetz, C. A. (2007). ER stress signaling and the BCL-2 family of proteins: from adaptation to irreversible cellular damage. *Antioxid Redox Signal, 9*(12), 2345-2355.

Hirota, J., Furuichi, T., & Mikoshiba, K. (1999). Inositol 1,4,5-trisphosphate receptor type 1 is a substrate for caspase-3 and is cleaved during apoptosis in a caspase-3-dependent manner. *J Biol Chem, 274*(48), 34433-34437.

Hoye, A. T., Davoren, J. E., Wipf, P., Fink, M. P., & Kagan, V. E. (2008). Targeting mitochondria. *Acc Chem Res, 41*(1), 87-97.

Huber, A. H., & Weis, W. I. (2001). The structure of the beta-catenin/E-cadherin complex and the molecular basis of diverse ligand recognition by beta-catenin. *Cell, 105*(3), 391-402.

Huber, M. A., Kraut, N., & Beug, H. (2005). Molecular requirements for epithelial-mesenchymal transition during tumor progression. *Curr Opin Cell Biol, 17*(5), 548-558.

Hur, J., Chesnes, J., Coser, K. R., Lee, R. S., Geck, P., Isselbacher, K. J., et al. (2004). The Bik BH3-only protein is induced in estrogen-starved and antiestrogen-exposed breast cancer cells and provokes apoptosis. *Proc Natl Acad Sci U S A, 101*(8), 2351-2356.

Jamsa, E., Simonen, M., & Makarow, M. (1994). Selective retention of secretory proteins in the yeast endoplasmic reticulum by treatment of cells with a reducing agent. *Yeast, 10*(3), 355-370.

Jang, H., Kim, T. W., Yoon, S., Choi, S. Y., Kang, T. W., Kim, S. Y., et al. (2012). O-GlcNAc regulates pluripotency and reprogramming by directly acting on core components of the pluripotency network. *Cell Stem Cell, 11*(1), 62-74.

Janicke, R. U., Sprengart, M. L., Wati, M. R., & Porter, A. G. (1998). Caspase-3 is required for DNA fragmentation and morphological changes associated with apoptosis. *J Biol Chem, 273*(16), 9357-9360.

Jeanes, A., Gottardi, C. J., & Yap, A. S. (2008). Cadherins and cancer: how does cadherin dysfunction promote tumor progression? *Oncogene, 27*(55), 6920-6929.

Jimbo, A., Fujita, E., Kouroku, Y., Ohnishi, J., Inohara, N., Kuida, K., et al. (2003). ER stress induces caspase-8 activation, stimulating cytochrome c release and caspase-9 activation. *Exp Cell Res, 283*(2), 156-166.

Jones, P. A. (1996). DNA methylation errors and cancer. *Cancer Res, 56*(11), 2463-2467.

Jordan, V. C., & O'Malley, B. W. (2007). Selective estrogen-receptor modulators and antihormonal resistance in breast cancer. *J Clin Oncol, 25*(36), 5815-5824.

Julenius, K., Molgaard, A., Gupta, R., & Brunak, S. (2005). Prediction, conservation analysis, and structural characterization of mammalian mucin-type O-glycosylation sites. *Glycobiology, 15*(2), 153-164.

Kabeya, Y., Mizushima, N., Yamamoto, A., Oshitani-Okamoto, S., Ohsumi, Y., & Yoshimori, T. (2004). LC3, GABARAP and GATE16 localize to autophagosomal membrane depending on form-II formation. *J Cell Sci, 117*(Pt 13), 2805-2812.

Kanno, Y., Sasaki, Y., Shiba, Y., Yoshida-Noro, C., & Takeichi, M. (1984). Monoclonal antibody ECCD-1 inhibits intercellular communication in teratocarcinoma PCC3 cells. *Exp Cell Res, 152*(1), 270-274.

Kerr, J. F., Wyllie, A. H., & Currie, A. R. (1972). Apoptosis: a basic biological phenomenon with wide-ranging implications in tissue kinetics. *Br J Cancer, 26*(4), 239-257.

Klinge, C. M. (2001). Estrogen receptor interaction with estrogen response elements. *Nucleic Acids Res, 29*(14), 2905-2919.

Klionsky, D. J., Abeliovich, H., Agostinis, P., Agrawal, D. K., Aliev, G., Askew, D. S., et al. (2008). Guidelines for the use and interpretation of assays for monitoring autophagy in higher eukaryotes. *Autophagy, 4*(2), 151-175.

Klionsky, D. J., & Emr, S. D. (2000). Autophagy as a regulated pathway of cellular degradation. *Science, 290*(5497), 1717-1721.

Knoblauch, R., & Garabedian, M. J. (1999). Role for Hsp90-associated cochaperone p23 in estrogen receptor signal transduction. *Mol Cell Biol, 19*(5), 3748-3759.

Kreppel, L. K., & Hart, G. W. (1999). Regulation of a cytosolic and nuclear O-GlcNAc transferase. Role of the tetratricopeptide repeats. *J Biol Chem, 274*(45), 32015-32022.

Kroemer, G. (1999). Mitochondrial control of apoptosis: an overview. *Biochem Soc Symp, 66*, 1-15.

Kroemer, G., Dallaporta, B., & Resche-Rigon, M. (1998). The mitochondrial death/life regulator in apoptosis and necrosis. *Annu Rev Physiol, 60*, 619-642.

Kroemer, G., Marino, G., & Levine, B. (2010). Autophagy and the integrated stress response. *Mol Cell, 40*(2), 280-293.

Ku, N. O., Toivola, D. M., Strnad, P., & Omary, M. B. (2010). Cytoskeletal keratin glycosylation protects epithelial tissue from injury. *Nat Cell Biol, 12*(9), 876-885.

Kundu, M., & Thompson, C. B. (2005). Macroautophagy versus mitochondrial autophagy: a question of fate? *Cell Death Differ, 12 Suppl 2*, 1484-1489.

Kuo, T. H., Kim, H. R., Zhu, L., Yu, Y., Lin, H. M., & Tsang, W. (1998). Modulation of endoplasmic reticulum calcium pump by Bcl-2. *Oncogene, 17*(15), 1903-1910.

Kuukasjarvi, T., Kononen, J., Helin, H., Holli, K., & Isola, J. (1996). Loss of estrogen receptor in recurrent breast cancer is associated with poor response to endocrine therapy. *J Clin Oncol, 14*(9), 2584-2589.

Lalier, L., Cartron, P. F., Juin, P., Nedelkina, S., Manon, S., Bechinger, B., et al. (2007). Bax activation and mitochondrial insertion during apoptosis. *Apoptosis, 12*(5), 887-896.

Laur, O. Y., Klingelhofer, J., Troyanovsky, R. B., & Troyanovsky, S. M. (2002). Both the dimerization and immunochemical properties of E-cadherin EC1 domain depend on Trp(156) residue. *Arch Biochem Biophys, 400*(1), 141-147.

Leber, B., & Andrews, D. W. (2010). Closing in on the link between apoptosis and autophagy. *F1000 Biol Rep, 2*, 88.

Leber, B., Geng, F., Kale, J., & Andrews, D. W. (2010). Drugs targeting Bcl-2 family members as an emerging strategy in cancer. *Expert Rev Mol Med, 12*, e28.

Leber, B., Lin, J., & Andrews, D. W. (2007). Embedded together: the life and death consequences of interaction of the Bcl-2 family with membranes. *Apoptosis, 12*(5), 897-911.

Lee, A. V., Cui, X., & Oesterreich, S. (2001). Cross-talk among estrogen receptor, epidermal growth factor, and insulin-like growth factor signaling in breast cancer. *Clin Cancer Res, 7*(12 Suppl), 4429s-4435s; discussion 4411s-4412s.

Lee, E. F., Czabotar, P. E., van Delft, M. F., Michalak, E. M., Boyle, M. J., Willis, S. N., et al. (2008). A novel BH3 ligand that selectively targets Mcl-1 reveals that apoptosis can proceed without Mcl-1 degradation. *J Cell Biol, 180*(2), 341-355.

Levine, B., Sinha, S., & Kroemer, G. (2008). Bcl-2 family members: dual regulators of apoptosis and autophagy. *Autophagy, 4*(5), 600-606.

Li, H., Zhu, H., Xu, C. J., & Yuan, J. (1998). Cleavage of BID by caspase 8 mediates the mitochondrial damage in the Fas pathway of apoptosis. *Cell, 94*(4), 491-501.

Li, S., Zhao, Y., He, X., Kim, T. H., Kuharsky, D. K., Rabinowich, H., et al. (2002). Relief of extrinsic pathway inhibition by the Bid-dependent mitochondrial release of Smac in Fas-mediated hepatocyte apoptosis. *J Biol Chem, 277*(30), 26912-26920.

Lickert, H., Bauer, A., Kemler, R., & Stappert, J. (2000). Casein kinase II phosphorylation of E-cadherin increases E-cadherin/beta-catenin interaction and strengthens cell-cell adhesion. *J Biol Chem, 275*(7), 5090-5095.

Lilien, J., & Balsamo, J. (2005). The regulation of cadherin-mediated adhesion by tyrosine phosphorylation/dephosphorylation of beta-catenin. *Curr Opin Cell Biol, 17*(5), 459-465.

Ling, K., Bairstow, S. F., Carbonara, C., Turbin, D. A., Huntsman, D. G., & Anderson, R. A. (2007). Type I gamma phosphatidylinositol phosphate kinase modulates adherens junction and E-cadherin trafficking via a direct interaction with mu 1B adaptin. *J Cell Biol, 176*(3), 343-353.

Ling, K., Doughman, R. L., Firestone, A. J., Bunce, M. W., & Anderson, R. A. (2002). Type I gamma phosphatidylinositol phosphate kinase targets and regulates focal adhesions. *Nature, 420*(6911), 89-93.

Ling, K., Schill, N. J., Wagoner, M. P., Sun, Y., & Anderson, R. A. (2006). Movin' on up: the role of PtdIns(4,5)P(2) in cell migration. *Trends Cell Biol, 16*(6), 276-284.

Littlewood, T. D., & Bennett, M. R. (2003). Apoptotic cell death in atherosclerosis. *Curr Opin Lipidol, 14*(5), 469-475.

Liwosz, A., Lei, T., & Kukuruzinska, M. A. (2006). N-glycosylation affects the molecular organization and stability of E-cadherin junctions. *J Biol Chem, 281*(32), 23138-23149.

Lock, J. G., & Stow, J. L. (2005). Rab11 in recycling endosomes regulates the sorting and basolateral transport of E-cadherin. *Mol Biol Cell, 16*(4), 1744-1755.

Lombaerts, M., van Wezel, T., Philippo, K., Dierssen, J. W., Zimmerman, R. M., Oosting, J., et al. (2006). E-cadherin transcriptional downregulation by promoter methylation but not mutation is related to epithelial-to-mesenchymal transition in breast cancer cell lines. *Br J Cancer, 94*(5), 661-671.

Lum, J. J., Bauer, D. E., Kong, M., Harris, M. H., Li, C., Lindsten, T., et al. (2005). Growth factor regulation of autophagy and cell survival in the absence of apoptosis. *Cell, 120*(2), 237-248.

Luo, X., Budihardjo, I., Zou, H., Slaughter, C., & Wang, X. (1998). Bid, a Bcl2 interacting protein, mediates cytochrome c release from mitochondria in response to activation of cell surface death receptors. *Cell, 94*(4), 481-490.

Lutter, M., Perkins, G. A., & Wang, X. (2001). The pro-apoptotic Bcl-2 family member tBid localizes to mitochondrial contact sites. *BMC Cell Biol, 2*, 22.

Lytton, J., Westlin, M., & Hanley, M. R. (1991). Thapsigargin inhibits the sarcoplasmic or endoplasmic reticulum Ca-ATPase family of calcium pumps. *J Biol Chem, 266*(26), 17067-17071.

Ma, L., Young, J., Prabhala, H., Pan, E., Mestdagh, P., Muth, D., et al. (2010). miR-9, a MYC/MYCN-activated microRNA, regulates E-cadherin and cancer metastasis. *Nat Cell Biol, 12*(3), 247-256.

Maiuri, M. C., Criollo, A., Tasdemir, E., Vicencio, J. M., Tajeddine, N., Hickman, J. A., et al. (2007). BH3-only proteins and BH3 mimetics induce autophagy by competitively disrupting the interaction between Beclin 1 and Bcl-2/Bcl-X(L). *Autophagy, 3*(4), 374-376.

Maiuri, M. C., Zalckvar, E., Kimchi, A., & Kroemer, G. (2007). Self-eating and self-killing: crosstalk between autophagy and apoptosis. *Nat Rev Mol Cell Biol, 8*(9), 741-752.

Maley, F., Trimble, R. B., Tarentino, A. L., & Plummer, T. H., Jr. (1989). Characterization of glycoproteins and their associated oligosaccharides through the use of endoglycosidases. *Anal Biochem, 180*(2), 195-204.

Massarweh, S., Osborne, C. K., Creighton, C. J., Qin, L., Tsimelzon, A., Huang, S., et al. (2008). Tamoxifen resistance in breast tumors is driven by growth factor receptor signaling with repression of classic estrogen receptor genomic function. *Cancer Res, 68*(3), 826-833.

Mileykovskaya, E., & Dowhan, W. (2009). Cardiolipin membrane domains in prokaryotes and eukaryotes. *Biochim Biophys Acta, 1788*(10), 2084-2091.

Mosesson, Y., Mills, G. B., & Yarden, Y. (2008). Derailed endocytosis: an emerging feature of cancer. *Nat Rev Cancer, 8*(11), 835-850.

Munro, S., & Pelham, H. R. (1987). A C-terminal signal prevents secretion of luminal ER proteins. *Cell, 48*(5), 899-907.

Muzio, M., Stockwell, B. R., Stennicke, H. R., Salvesen, G. S., & Dixit, V. M. (1998). An induced proximity model for caspase-8 activation. *J Biol Chem, 273*(5), 2926-2930.

Naughton, C., MacLeod, K., Kuske, B., Clarke, R., Cameron, D. A., & Langdon, S. P. (2007). Progressive loss of estrogen receptor alpha cofactor recruitment in endocrine resistance. *Mol Endocrinol, 21*(11), 2615-2626.

Nelson, W. J. (2008). Regulation of cell-cell adhesion by the cadherin-catenin complex. *Biochem Soc Trans, 36*(Pt 2), 149-155.

Ng, F. W., Nguyen, M., Kwan, T., Branton, P. E., Nicholson, D. W., Cromlish, J. A., et al. (1997). p28 Bap31, a Bcl-2/Bcl-XL- and procaspase-8-associated protein in the endoplasmic reticulum. *J Cell Biol, 139*(2), 327-338.

Nguyen, M., Breckenridge, D. G., Ducret, A., & Shore, G. C. (2000). Caspase-resistant BAP31 inhibits fas-mediated apoptotic membrane fragmentation and release of cytochrome c from mitochondria. *Mol Cell Biol, 20*(18), 6731-6740.

Nwosu, C. C., Seipert, R. R., Strum, J. S., Hua, S. S., An, H. J., Zivkovic, A. M., et al. (2011). Simultaneous and extensive site-specific N- and O-glycosylation analysis in protein mixtures. *J Proteome Res, 10*(5), 2612-2624.

Oakes, S. A., Lin, S. S., & Bassik, M. C. (2006). The control of endoplasmic reticulum-initiated apoptosis by the BCL-2 family of proteins. *Curr Mol Med, 6*(1), 99-109.

Oda, H., & Takeichi, M. (2011). Evolution: structural and functional diversity of cadherin at the adherens junction. *J Cell Biol, 193*(7), 1137-1146.

Oliver, F. J., Menissier-de Murcia, J., & de Murcia, G. (1999). Poly(ADP-ribose) polymerase in the cellular response to DNA damage, apoptosis, and disease. *Am J Hum Genet, 64*(5), 1282-1288.

Oltersdorf, T., Elmore, S. W., Shoemaker, A. R., Armstrong, R. C., Augeri, D. J., Belli, B. A., et al. (2005). An inhibitor of Bcl-2 family proteins induces regression of solid tumours. *Nature, 435*(7042), 677-681.

Osborne, C. K., & Schiff, R. (2011). Mechanisms of endocrine resistance in breast cancer. *Annu Rev Med, 62*, 233-247.

Overholtzer, M., Mailleux, A. A., Mouneimne, G., Normand, G., Schnitt, S. J., King, R. W., et al. (2007). A nonapoptotic cell death process, entosis, that occurs by cell-in-cell invasion. *Cell, 131*(5), 966-979.

Ozawa, M., & Kemler, R. (1990). Correct proteolytic cleavage is required for the cell adhesive function of uvomorulin. *J Cell Biol, 111*(4), 1645-1650.

Pagano, R. E., & Takeichi, M. (1977). Adhesion of phospholipid vesicles to Chinese hamster fibroblasts. Role of cell surface proteins. *J Cell Biol, 74*(2), 531-546.

Pattarozzi, A., Gatti, M., Barbieri, F., Wurth, R., Porcile, C., Lunardi, G., et al. (2008). 17beta-estradiol promotes breast cancer cell proliferation-inducing stromal cell-derived factor-1-mediated epidermal growth factor receptor transactivation: reversal by gefitinib pretreatment. *Mol Pharmacol, 73*(1), 191-202.

Pattingre, S., Tassa, A., Qu, X., Garuti, R., Liang, X. H., Mizushima, N., et al. (2005). Bcl-2 antiapoptotic proteins inhibit Beclin 1-dependent autophagy. *Cell, 122*(6), 927-939.

Pearce, S. T., & Jordan, V. C. (2004). The biological role of estrogen receptors alpha and beta in cancer. *Crit Rev Oncol Hematol, 50*(1), 3-22.

Peifer, M., & Yap, A. S. (2003). Traffic control: p120-catenin acts as a gatekeeper to control the fate of classical cadherins in mammalian cells. *J Cell Biol, 163*(3), 437-440.

Peng, X., Cuff, L. E., Lawton, C. D., & DeMali, K. A. (2010). Vinculin regulates cell-surface E-cadherin expression by binding to beta-catenin. *J Cell Sci, 123*(Pt 4), 567-577.

Perillo, B., Sasso, A., Abbondanza, C., & Palumbo, G. (2000). 17beta-estradiol inhibits apoptosis in MCF-7 cells, inducing bcl-2 expression via two estrogen-responsive elements present in the coding sequence. *Mol Cell Biol, 20*(8), 2890-2901.

Pinho, S. S., Seruca, R., Gartner, F., Yamaguchi, Y., Gu, J., Taniguchi, N., et al. (2011). Modulation of E-cadherin function and dysfunction by N-glycosylation. *Cell Mol Life Sci, 68*(6), 1011-1020.

Posthaus, H., Dubois, C. M., Laprise, M. H., Grondin, F., Suter, M. M., & Muller, E. (1998). Proprotein cleavage of E-cadherin by furin in baculovirus over-expression system: potential role of other convertases in mammalian cells. *FEBS Lett, 438*(3), 306-310.

Qu, L., Huang, S., Baltzis, D., Rivas-Estilla, A. M., Pluquet, O., Hatzoglou, M., et al. (2004). Endoplasmic reticulum stress induces p53 cytoplasmic localization and prevents p53-dependent apoptosis by a pathway involving glycogen synthase kinase-3beta. *Genes Dev, 18*(3), 261-277.

Ringwald, M., Baribault, H., Schmidt, C., & Kemler, R. (1991). The structure of the gene coding for the mouse cell adhesion molecule uvomorulin. *Nucleic Acids Res, 19*(23), 6533-6539.

Rodriguez, M. E., Azizuddin, K., Zhang, P., Chiu, S. M., Lam, M., Kenney, M. E., et al. (2008). Targeting of mitochondria by 10-N-alkyl acridine orange analogues: role of alkyl chain length in determining cellular uptake and localization. *Mitochondrion, 8*(3), 237-246.

Rong, Y., & Distelhorst, C. W. (2008). Bcl-2 protein family members: versatile regulators of calcium signaling in cell survival and apoptosis. *Annu Rev Physiol, 70*, 73-91.

Rosivatz, E., Becker, I., Specht, K., Fricke, E., Luber, B., Busch, R., et al. (2002). Differential expression of the epithelial-mesenchymal transition regulators snail, SIP1, and twist in gastric cancer. *Am J Pathol, 161*(5), 1881-1891.

Saelens, X., Festjens, N., Vande Walle, L., van Gurp, M., van Loo, G., & Vandenabeele, P. (2004). Toxic proteins released from mitochondria in cell death. *Oncogene, 23*(16), 2861-2874.

Savagner, P. (2001). Leaving the neighborhood: molecular mechanisms involved during epithelial-mesenchymal transition. *Bioessays, 23*(10), 912-923.

Scaduto, R. C., Jr., & Grotyohann, L. W. (1999). Measurement of mitochondrial membrane potential using fluorescent rhodamine derivatives. *Biophys J, 76*(1 Pt 1), 469-477.

Scaffidi, C., Fulda, S., Srinivasan, A., Friesen, C., Li, F., Tomaselli, K. J., et al. (1998). Two CD95 (APO-1/Fas) signaling pathways. *Embo J, 17*(6), 1675-1687.

Schiff, R., Massarweh, S. A., Shou, J., Bharwani, L., Mohsin, S. K., & Osborne, C. K. (2004). Cross-talk between estrogen receptor and growth factor pathways as a molecular target for overcoming endocrine resistance. *Clin Cancer Res, 10*(1 Pt 2), 331S-336S.

Schrader, K. A., Masciari, S., Boyd, N., Salamanca, C., Senz, J., Saunders, D. N., et al. (2011). Germline mutations in CDH1 are infrequent in women with early-onset or familial lobular breast cancers. *J Med Genet, 48*(1), 64-68.

Schuck, S., Prinz, W. A., Thorn, K. S., Voss, C., & Walter, P. (2009). Membrane expansion alleviates endoplasmic reticulum stress independently of the unfolded protein response. *J Cell Biol, 187*(4), 525-536.

Shamas-Din, A., Brahmbhatt, H., Leber, B., & Andrews, D. W. (2011). BH3-only proteins: Orchestrators of apoptosis. *Biochim Biophys Acta, 1813*(4), 508-520.

Shapiro, L., Fannon, A. M., Kwong, P. D., Thompson, A., Lehmann, M. S., Grubel, G., et al. (1995). Structural basis of cell-cell adhesion by cadherins. *Nature, 374*(6520), 327-337.

Shen, X., Ellis, R. E., Lee, K., Liu, C. Y., Yang, K., Solomon, A., et al. (2001). Complementary signaling pathways regulate the unfolded protein response and are required for C. elegans development. *Cell, 107*(7), 893-903.

Shimohama, S. (2000). Apoptosis in Alzheimer's disease--an update. *Apoptosis, 5*(1), 9-16.

Smith, C. L., & O'Malley, B. W. (2004). Coregulator function: a key to understanding tissue specificity of selective receptor modulators. *Endocr Rev, 25*(1), 45-71.

Spellman, M. W. (1990). Carbohydrate characterization of recombinant glycoproteins of pharmaceutical interest. *Anal Chem, 62*(17), 1714-1722.

Spencer, S. L., & Sorger, P. K. (2011). Measuring and modeling apoptosis in single cells. *Cell, 144*(6), 926-939.

Stappert, J., & Kemler, R. (1994). A short core region of E-cadherin is essential for catenin binding and is highly phosphorylated. *Cell Adhes Commun, 2*(4), 319-327.

Stephens, L. R., Hughes, K. T., & Irvine, R. F. (1991). Pathway of phosphatidylinositol(3,4,5)-trisphosphate synthesis in activated neutrophils. *Nature, 351*(6321), 33-39.

Su, N., & Kilberg, M. S. (2008). C/EBP homology protein (CHOP) interacts with activating transcription factor 4 (ATF4) and negatively regulates the stress-dependent induction of the asparagine synthetase gene. *J Biol Chem, 283*(50), 35106-35117.

Sun, Y., Turbin, D. A., Ling, K., Thapa, N., Leung, S., Huntsman, D. G., et al. (2010). Type I gamma phosphatidylinositol phosphate kinase modulates invasion and proliferation and its expression correlates with poor prognosis in breast cancer. *Breast Cancer Res, 12*(1), R6.

Szegezdi, E., Logue, S. E., Gorman, A. M., & Samali, A. (2006). Mediators of endoplasmic reticulum stress-induced apoptosis. *EMBO Rep, 7*(9), 880-885.

Takeichi, M. (2007). The cadherin superfamily in neuronal connections and interactions. *Nat Rev Neurosci, 8*(1), 11-20.

Tamura, G., Yin, J., Wang, S., Fleisher, A. S., Zou, T., Abraham, J. M., et al. (2000). E-Cadherin gene promoter hypermethylation in primary human gastric carcinomas. *J Natl Cancer Inst, 92*(7), 569-573.

Teixeira, C., Reed, J. C., & Pratt, M. A. (1995). Estrogen promotes chemotherapeutic drug resistance by a mechanism involving Bcl-2 proto-oncogene expression in human breast cancer cells. *Cancer Res, 55*(17), 3902-3907.

Troyanovsky, R. B., Chitaev, N. A., & Troyanovsky, S. M. (1996). Cadherin binding sites of plakoglobin: localization, specificity and role in targeting to adhering junctions. *J Cell Sci, 109 (Pt 13)*, 3069-3078.

Tsujimoto, Y., Finger, L. R., Yunis, J., Nowell, P. C., & Croce, C. M. (1984). Cloning of the chromosome breakpoint of neoplastic B cells with the t(14;18) chromosome translocation. *Science, 226*(4678), 1097-1099.

Tsujimoto, Y., & Shimizu, S. (2007). Role of the mitochondrial membrane permeability transition in cell death. *Apoptosis, 12*(5), 835-840.

Twiddy, D., Cohen, G. M., Macfarlane, M., & Cain, K. (2006). Caspase-7 is directly activated by the approximately 700-kDa apoptosome complex and is released as a stable XIAP-caspase-7 approximately 200-kDa complex. *J Biol Chem, 281*(7), 3876-3888.

Umayahara, Y., Kawamori, R., Watada, H., Imano, E., Iwama, N., Morishima, T., et al. (1994). Estrogen regulation of the insulin-like growth factor I gene transcription involves an AP-1 enhancer. *J Biol Chem, 269*(23), 16433-16442.

van Loo, G., Saelens, X., van Gurp, M., MacFarlane, M., Martin, S. J., & Vandenabeele, P. (2002). The role of mitochondrial factors in apoptosis: a Russian roulette with more than one bullet. *Cell Death Differ, 9*(10), 1031-1042.

van Roy, F., & Berx, G. (2008). The cell-cell adhesion molecule E-cadherin. *Cell Mol Life Sci, 65*(23), 3756-3788.

Vosseller, K., Wells, L., & Hart, G. W. (2001). Nucleocytoplasmic O-glycosylation: O-GlcNAc and functional proteomics. *Biochimie, 83*(7), 575-581.

Wakana, Y., Takai, S., Nakajima, K., Tani, K., Yamamoto, A., Watson, P., et al. (2008). Bap31 is an itinerant protein that moves between the peripheral endoplasmic reticulum (ER) and a juxtanuclear compartment related to ER-associated Degradation. *Mol Biol Cell, 19*(5), 1825-1836.

Wang, B., Nguyen, M., Breckenridge, D. G., Stojanovic, M., Clemons, P. A., Kuppig, S., et al. (2003). Uncleaved BAP31 in association with A4 protein at the endoplasmic reticulum is an inhibitor of Fas-initiated release of cytochrome c from mitochondria. *J Biol Chem, 278*(16), 14461-14468.

Wang, H. L., Akinci, I. O., Baker, C. M., Urich, D., Bellmeyer, A., Jain, M., et al. (2007). The intrinsic apoptotic pathway is required for lipopolysaccharide-induced lung endothelial cell death. *J Immunol, 179*(3), 1834-1841.

Wang, L., Du, F., & Wang, X. (2008). TNF-alpha induces two distinct caspase-8 activation pathways. *Cell, 133*(4), 693-703.

Wang, X., Olberding, K. E., White, C., & Li, C. (2011). Bcl-2 proteins regulate ER membrane permeability to luminal proteins during ER stress-induced apoptosis. *Cell Death Differ, 18*(1), 38-47.

Wang, Y., & Qin, Z. H. (2010). Molecular and cellular mechanisms of excitotoxic neuronal death. *Apoptosis, 15*(11), 1382-1402.

Wei, M. C., Zong, W. X., Cheng, E. H., Lindsten, T., Panoutsakopoulou, V., Ross, A. J., et al. (2001). Proapoptotic BAX and BAK: a requisite gateway to mitochondrial dysfunction and death. *Science, 292*(5517), 727-730.

Wells, L., & Hart, G. W. (2003). O-GlcNAc turns twenty: functional implications for post-translational modification of nuclear and cytosolic proteins with a sugar. *FEBS Lett, 546*(1), 154-158.

Welshons, W. V., Grady, L. H., Engler, K. S., & Judy, B. M. (1992). Control of proliferation of MCF-7 breast cancer cells in a commercial preparation of charcoal-stripped adult bovine serum. *Breast Cancer Res Treat, 23*(1-2), 97-104.

White, E. (2007). Entosis: it's a cell-eat-cell world. *Cell, 131*(5), 840-842.

Wlodkowic, D., Skommer, J., & Darzynkiewicz, Z. (2008). SYTO probes in the cytometry of tumor cell death. *Cytometry A, 73*(6), 496-507.

Wu, S., Hu, Y., Wang, J. L., Chatterjee, M., Shi, Y., & Kaufman, R. J. (2002). Ultraviolet light inhibits translation through activation of the unfolded protein response kinase PERK in the lumen of the endoplasmic reticulum. *J Biol Chem, 277*(20), 18077-18083.

Wyllie, A. H., Kerr, J. F., & Currie, A. R. (1980). Cell death: the significance of apoptosis. *Int Rev Cytol, 68*, 251-306.

Yap, A. S., Crampton, M. S., & Hardin, J. (2007). Making and breaking contacts: the cellular biology of cadherin regulation. *Curr Opin Cell Biol, 19*(5), 508-514.

Yin, X. M., Wang, K., Gross, A., Zhao, Y., Zinkel, S., Klocke, B., et al. (1999). Bid-deficient mice are resistant to Fas-induced hepatocellular apoptosis. *Nature, 400*(6747), 886-891.

Yoshida, H. (2007). Unconventional splicing of XBP-1 mRNA in the unfolded protein response. *Antioxid Redox Signal, 9*(12), 2323-2333.

Youle, R. J., & Strasser, A. (2008). The BCL-2 protein family: opposing activities that mediate cell death. *Nat Rev Mol Cell Biol, 9*(1), 47-59.

Zhang, J. H., Chung, T. D., & Oldenburg, K. R. (1999). A Simple Statistical Parameter for Use in Evaluation and Validation of High Throughput Screening Assays. *J Biomol Screen, 4*(2), 67-73.

Zhu, W., Cowie, A., Wasfy, G. W., Penn, L. Z., Leber, B., & Andrews, D. W. (1996). Bcl-2 mutants with restricted subcellular location reveal spatially distinct pathways for apoptosis in different cell types. *EMBO J, 15*(16), 4130-4141.

Zhu, W., Leber, B., & Andrews, D. W. (2001). Cytoplasmic O-glycosylation prevents cell surface transport of E-cadherin during apoptosis. *EMBO J, 20*(21), 5999-6007.

Zhurinsky, J., Shtutman, M., & Ben-Ze'ev, A. (2000). Plakoglobin and beta-catenin: protein interactions, regulation and biological roles. *J Cell Sci, 113 (Pt 18)*, 3127-3139.

Zong, W. X., Lindsten, T., Ross, A. J., MacGregor, G. R., & Thompson, C. B. (2001). BH3-only proteins that bind pro-survival Bcl-2 family members fail to induce apoptosis in the absence of Bax and Bak. *Genes Dev, 15*(12), 1481-1486.

Zou, D., Yoon, H. S., Perez, D., Weeks, R. J., Guilford, P., & Humar, B. (2009). Epigenetic silencing in non-neoplastic epithelia identifies E-cadherin (CDH1) as a target for chemoprevention of lobular neoplasia. *J Pathol*, *218*(2), 265-272.